Effective removal of ammonia from the drinking water system: A case study at Magalies Water

ME Mugwili

orcid.org/0000-0001-8266-1299

Dissertation accepted in fulfilment of the requirements for the degree *Master of Engineering in Chemical Engineering* at the North-West University

Supervisor: Prof F Waanders

Co-supervisor: Dr V Masindi

Co-supervisor: Prof Elvis Fosso-Kankeu

Graduation: May-June 2023

Student number: 36845590

Declarations

I, **Muyahavho Enemiah Mugwili**, declare that my thesis entitled: **Effective removal of ammonia from the drinking water system: A case study at Magalies Water,** which I herewith submit to the North-West University (NWU), is my own work in execution and design unless specifically indicated to the contrary in the text. Sources used are indicated and duly acknowledged by complete references. In addition, the thesis has not been submitted to any or other institution for examination. The thesis is being submitted for the degree of Master of Engineering in Chemical Engineering to the University of North-West University (NWU).

Signature of Student ____________ Student No. 36845590

Signed at Wallmannsthal WTW Date 11 August 2022

Acknowledgements

First and foremost, I would like to acknowledge and express my sincere gratitude to my supervisors, **Prof Frans Waanders, Dr Vhahangwele Masindi, and Prof Elvis Fosso-Kankeu,** who made this work possible. Their continuous support, guidance, patience and enthusiasm throughout this study have enabled me to complete the expected outputs of this project. I would also like to thank **North-West University**, Water Pollution Monitoring and Remediation Initiatives Research Group, **Council for Scientific and Industrial Research (CSIR)**, the **University of South Africa (UNISA)**, Institute for Nanotechnology and Water Sustainability (iNanoWS), College of Science Engineering and Technology (CSET) and the Department of Environmental Sciences for their insightful comments, inputs, support and encouragement throughout the study. Further, I would like to acknowledge **Christelle Woudberg** for editing this dissertation.

I would also like to give special thanks to the **Magalies Water Board, Scientific Services, Production and Human Resource Department** staff for their support and funding of this project. In particular, I would like to thank Miss **Phinda Rikhotso, my research assistant,** who was always available regardless, assisting with grace and gratitude.

More importantly, I would like to thank my mother, **Mavis Mugwili,** for her continuous support during this period. Your prayers kept me going even in difficult times, strengthening my faith and eventually allowing me to complete this study. To my late father, **William Mugwili**, I will always be an example to my siblings as I had promised; completing this study will be extra motivation for always striving to be the best one can be. My daughter, **Vhulenda Mugwili,** thank you for your love and understanding throughout this period.

Finally, I would like to show my appreciation to God. Thank you for blessing me daily, giving me guidance and strength to preserver in successfully completing this research. My trust and belief in you will never waiver.

Publications and other research outputs

Research publications

Mugwili, ME., Waanders, FB., Masindi, V., Fosso-Kankeu, E. 2022. Advances and challenges on the removal of ammonia from aqueous environments: An update. Science of The Total Environment**, <u>Paper under review</u>**.

Mugwili, ME., Waanders, FB., Masindi, V., Fosso-Kankeu, E. 2022. Effective removal of ammonia from aqueous solution using a combination of precipitation and breakpoint chlorination. Journal of Water Process Engineering**, <u>Paper under review</u>**.

Mugwili, ME., Waanders, FB., Masindi, V., Fosso-Kankeu, E. 2022. Techno-economic analysis of the removal of ammonia from the aqueous environment using the integration of struvite synthesis and breakpoint chlorination: A pilot study. Process Safety and Environmental Protection**, <u>Paper under review</u>**.

Conference publications and presentations

Mugwili, ME., Waanders, FB., Masindi, V., Fosso-Kankeu, E. Removal of ammonia from river water using breakpoint chlorination. 17th JOHANNESBURG Int'l Conference on Science, Engineering, Technology & Waste Management (SETWM-19) Nov. 16-17, 2020 Johannesburg (S.A.)***. http://doi.org/10.17758/EARES1O***

Mugwili, ME., Waanders, FB., Masindi, V., Fosso-Kankeu, E. Effective removal of ammonia from Surface Water using a combination of precipitation and breakpoint chlorination. WISA 2022 Biennial Conference and Exhibition. Sep. 28-30, 2022. Sandton (S.A). **Abstract accepted for oral presentation.**

Mugwili, ME., Waanders, FB., Masindi, V., Fosso-Kankeu, E. A hybrid approach for the removal of ammonia from aqueous solution using an integration of struvite precipitation and breakpoint chlorination. 1st International Conference on Sustainable Chemical and Environmental Engineering. 31^{st} Aug- 04^{th} Sep 2022. Rythymno, Crete. (Greece). **Abstract accepted for oral presentation.**

Table of contents

List of Figures

List of tables

List of Abbreviation

AOB	Ammonia oxidising Bacteria
BAF	Biological Air Filters
BNR	Biological Nutrients Removal
Ca	Calcium
CAPEX	Capital Expenditure
COD	Chemical Oxygen Demand
DBPs	Disinfection By-products
DMAI	Dimethylammonium Iodide
DMAP	Dimethlylamimopyridine
DWA	Department of Water Affairs
DWTP	Drinking Water Treatment Plants
EAOP	Electrochemical Advanced Oxidation Process
E. COLI	Escherichia Coli
ED	Electrodialysis
Fe	Iron
HTH	High Test Hypochlorite
LMIC	Low- and Middle-Income Countries
LPH	Litres Per Hour
MAP	Magnesium Ammonia Phosphate
MF	Microfiltration
Mg	Magnesium
Mn	Manganese
MPP	Magnesium Potassium Phosphate
MSP	Magnesium Sodium Phosphate
NF	Nanofiltration
NH3	Ammonia
NOM	Natural Organic Matter
NTU	Nephelometric Turbidity Unity
OFAAT	One Factor at A Time
PAC	Powder Activated Carbon
RO	Reverse Osmosis
THMs	Trihalomethanes
SABS	South African Bureau of Standards

SANS	South African National Standards
TPC	Total Plate Count
UF	Ultrafiltration
UV	Ultraviolet
US: EPA	United States Environmental Protection Agency
WHO	World Health Organisation
WSA	Water Services Authority
WSP	Water Services Provider
WTP	Water Treatment Plant
WWTWs	Wastewater Treatment Works
2MIB	2-Methlysoborneol

Abstract

Access to clean drinking water and sanitation is recognised as a human right and imperative to holistic functioning of life and interlocking nitty-gritties. In recent years, the quality of surface water in low- and middle-income countries (LMICs) has deteriorated significantly, primarily attributed to upstream activities. Specifically, municipal wastewater treatment processes, agricultural practices, and industrial activities are the main contributors to catchment problems, mainly due to the discharge of effluents rich in nutrients, including ammonia, organic matter, metals, and microbial load. Introducing those contaminants negatively affects the water quality of the catchment, resulting in myriads of challenges such as oxygen depletion, eutrophication, algal bloom, and hyacinth blankets in aqueous environments. In addition to operational challenges associated with nutrient-rich surface water, the efficiency of conventional drinking water treatment systems regarding the removal of ammonia and metals is relatively low, leading to final water with the potential to cause health and aesthetic challenges, impacting the human right to access drinking water. Worryingly, incorporating different technologies into drinking water systems will require structural amendments, which will increase the capital expenditure (CAPEX) and operational expenditure (OPEX), while the environmental impacts limit the capabilities of other technologies. As such, water service providers are searching for cost-effective, safe, and environmentally friendly technologies compatible with existing water treatment systems, hence the purpose of this study. The present study was conceptualised to assess the synergistic potential of integrating struvite synthesis and breakpoint chlorination for the removal of ammonia from drinking water. Specifically, this study is stratified into two step-wise approaches, i.e., batch laboratory (i) and pilot studies (ii) and two treatment steps that comprise struvite precipitation and breakpoint chlorination.

In the first study, batch laboratory experiments were conducted to fulfil the goals of this study. Low magnesium and phosphate concentrations in surface water necessitated augmentation of low-cost calcined magnesite as magnesium source, while potassium dihydrogen phosphate provided the phosphate for precipitation with surface water ammonia. Operational parameters comprises the effect of chemical species dosage (magnesium and phosphate), mixing speed, and contact time. State-of-the-art analytical instruments were used to underpin the fate of chemical species. The chemical compositions of the samples were ascertained in an ISO-accredited laboratory following standard methods. Specifically, the laboratory is at Magalies Water Board Laboratory (ISO/IEC 17025:2017 accredited) in Brits, North West, South Africa. Optimum conditions were observed to be 110 mg/L of Mg and P dosage (concentration), 150 rpm mixing speed, 60 minutes contact time and 120 minutes sedimentation. Under these

conditions, the pH increased from 6.7 to ≥ 9.6, while the turbidity was reduced from 9.1 to ≤ 1.3 NTU. Approximately 97 of manganese and 99% of iron were removed with ammonia attenuated from 7.60 to ≤ 2.84 mg/L (62.63%). Lastly, in stage 1, the antimicrobial effects on *E. coli* and total coliform attained ≥ 99% removal efficiency, respectively, while the removal efficiency of TPC was ≥ 87%. The resultant sludge was observed to comprise struvite from XRD and FTIR results, confirming ammonia's fate post-treatment. Product water from this reactor was taken to another stage of water treatment that comprised breakpoint chlorination. In particular, the breakpoint chlorination experiments were conducted using calcium hypochlorite as the chlorine source. Experiments were conducted at an ammonia weight (Cl_2:NH_3) ratio of 8:1, 200 rpm of mixing speed, and 30 minutes of contact time. Under these conditions, ammonia and total plate count (TPC) removal attained ≥ 99% from aqueous environments. The synergistic and complementary effects of integrating struvite synthesis (precipitation) and breakpoint chlorination completely removed contaminants from drinking water. Albeit there was the formation of trivial disinfection byproducts, mostly chloroform, post the breakpoint chlorination, their levels were below WHO and SANS 241 drinking water standards.

Finally, in the second study, the upscaling of the laboratory system into a pilot study was pursued, and cost analysis (OPEX) was also performed. The pilot plant had a capacity of 1000 liters (1 m^3) per run (LPR), and optimum laboratory assays were adopted here. Interestingly, results obtained on the pilot scale were similar to those obtained from laboratory assays. Specifically, in Stage 1 of the treatment process, the pH increased from 8.2 to 10.2 while ≥ 99% removal efficacy for manganese and iron was registered. *E. coli* and coliform reduction was ≥ 99%, while TPC reduction was 91%. Ammonia was reduced from 6.73 mg/L to 2.40 mg/L-N (64.33 %). Furthermore, in Stage 2, i.e., breakpoint chlorination, ammonia was reduced from 2.40 mg/L to ≤ 0.009 mg/L-N after the interaction of water with chlorine, whilst the TPC was reduced from 2340 CFU/1mL to 4 CFU/1mL. The cost evaluation, i.e., OPEX, amounted to **R4.85/kl ($0.31/m^3)** hence comparing favourably to similar studies. Moreover, replacing pure chemicals with chemicals such as waste phosphoric acid can potentially lead to cost savings of **R2.58/kl (0.16/m^3).** As expected, the hybrid process removed contaminants from surface water, yielding product water compliant with WHO and SANS 241 standards and specifications, respectively. Overall, the integration of struvite precipitation and breakpoint chlorination demonstrated synergistic effects toward surface water treatment to the required standard. However, future research should focus on integrating powdered activated carbon into the studied process to remove potential DBPs.

Keywords: Surface water**;** ammonia; eutrophication; methemoglobinemia; Struvite Synthesis; breakpoint chlorination; cost analysis (OPEX); and Laboratory and pilot studies.

Chapter one

Introduction

1.1 Background information

The ever-growing discharge of nutrient-rich effluents into receiving aqueous ecosystems and ecological compartments notoriously perpetuates the deterioration of the quality of the receiving waterbody. Specifically, the enrichment of surface water with nutrients mainly occurs due to the discharge of poorly treated effluent into receiving streams, affecting its quality. In compounding to this problem are the ageing infrastructure, influent water that exceeds the design capacity, rapid population growth, and reduced rainfall patterns that hamper the performance of wastewater treatment systems (Pastor et al., 2008, Mavhungu et al., 2019). In addition, illegal disposals of garbage, agricultural waste, and leakages from industries and landfills also contribute to the pollution of surface water bodies (Abu Hasan et al., 2020). These challenges are primarily experienced in low and middle-income countries (LMICs) (Sharma et al., 2021).

In South Africa, municipal wastewater effluent is the main culprit in the enrichment of receiving waterbodies with nutrients and other contaminants. Wastewater effluents generally comprise organic, inorganic, and microbial constituents that need to be removed during the wastewater treatment processes, albeit with the aforementioned technical challenges. Amongst those pollutants, ammonia has been identified as a pollutant of grave concern, primarily due to its notorious and worrying toxicological effects. In addition, the overabundance of ammonia in surface water eventually leads to eutrophication (Warmadewanthi et al., 2020, Devi and Dalai, 2021), which harms aquatic life hence exasperating the depletion of oxygen, algal bloom, and infestation of waterbodies with blue-green algae and covering of waterbodies with hyacinth. According to stringent regulatory frameworks, $\geq$ 1.5 mg/L of ammonia in drinking water can impart taste and smell problems. In addition, such concentration increases disinfectant demand, i.e., chlorine demand, whilst providing nutrients for microbial community hence their prolific growth. Furthermore, the potential oxidation of ammonia forms nitrate and nitrite as by-products. Exposure to elevated nitrite levels in drinking water may result in methemoglobinemia, or blue-baby syndrome, which is caused by the inability of the blood to carry and deliver enough oxygen to the body (WHO, 2017).

Traditionally, ammonia is primarily managed, treated, and removed in wastewater treatment works (WWTWs). The most effective technology for ammonia removal was incorporated into the WWTWs, through the use of biological nutrients treatment (BNR) and phytoremediation (Ekama, 2011, Mook et al., 2012, Karri et al., 2018). Other technologies that have been used on an industrial scale to redress elevated levels of ammonia are membrane filtration, ion exchange, chlorination (breakpoint chlorination), stripping, adsorption, and chemical precipitation (struvite synthesis) (Tünay et al., 1997, Zhang et al., 2018, Ryskie et al., 2020). These technologies, however, have their disadvantages and advantages. Filtration and ion exchange technologies are energy-dependent and generate brine, posing secondary pollution. Furthermore, the fouling of the membrane affects the production rates and increases the treatment costs (Eskicioglu et al., 2018, Adam et al., 2019, Hube et al., 2020). Stripping of ammonia requires higher pH and temperature hence leading to scaling of packing towers (Guštin and Marinšek-Logar, 2011, Kinidi et al., 2018), while advanced electrochemical oxidation can result in the formation of nitrates and nitrites as by-products (Wang et al., 2014, Xiao et al., 2016). Lastly, as much as it is a popular technology, BNR is affected by lower temperatures, but heating the substrate is the primary modality in WWTWs (Abu Hasan et al., 2014). Furthermore, the evolving and emerging technologies require structural amendments and modifications for them to be incorporated into existing WWTWs, which will further increase the capital expenditure (CAPEX) of the technology.

To date, breakpoint chlorination is the most promising technology for removing ammonia from aqueous environments (Stefán et al., 2019, Sharma et al., 2021). This technology has been widely used for the removal of ammonia, and according to Pressley et al. (1972), the effective ammonia to chlorine weight ratio of 7.6:1 proved to be the most effective stoichiometry. Furthermore, higher concentrations of ammonia in raw water inflate the exorbitant demand for feed chlorine hence increasing the operational cost along with the potential formation of disinfectant by-products (THMs), mainly when used in raw water with natural organic matter (NOMs) (Sharma et al., 2021). On the other hand, the struvite technology has also been successfully applied to remove ammonia from wastewater (Mavhungu et al., 2021). Recent studies have reported on chemical precipitation with struvite yielding higher ammonia (±≥75%) and manganese (100%) removal from municipal wastewater, urine, and landfill leachates (Wang et al., 2017, Karri et al., 2018, Mavhungu et al., 2020).

However, struvite precipitation has not been used in drinking water systems primarily due to phosphate deficiency. Considering the deficiencies of the two technologies and leveraging their strength, the employment of struvite synthesis and breakpoint chlorination could yield an effective, cheap option for removing ammonia from drinking water. Furthermore, these technologies' integration and application in drinking water treatment have not been explored. As such, this is the first study in the design and execution to explore the use of struvite synthesis (precipitation) and breakpoint chlorination for the removal of ammonia. Stage one will be the pre-treatment step toward the removal of ammonia, and stage two is the polishing step towards the removal of ammonia. Finally, this technological modality will eliminate the weaknesses of individual technologies while enhancing performance, yielding synergy, and reducing operational costs. Findings from this study will go a long way in curtailing the eco-toxicological effects of ammonia in drinking water, specifically for developing countries and further afield.

1.2 Problem statement

Raw water improvement plans have been initiated by the Department of Water Affairs (DWA), enforcing municipalities to comply with South African municipality discharge limits, i.e., general, and special limits. However, delays in upgrading and maintaining wastewater treatment work led to continuous enrichment of nutrients in water catchments, increasing the contaminant level in the receiving catchment streams. Specifically, raw water in South Africa, our case study, comprises high levels of contaminants, i.e., ammonia (±6 mg/L), manganese (±100 µg/L), *E. coli* (±167 counts/100mL), total coliform (±2420 counts/100mL) and circum-neutral pH (±6.6). A drinking water treatment plant can effortlessly reduce the microbial load with chlorine without significant hassles. However, the presence of ammonia and manganese is already impacting the treatment system negatively due to exorbitant chlorine demand. Specifically, ammonia is reacting with chlorine forming chloramine, at times hampering the oxidation of manganese, resulting in product water (final water) with a metallic taste and an increase in the number of complaints regarding staining of laundry post-end-use. In addition, failure to break down the ammonia to required drinking water levels of 1,5 mg/L N (WHO, 2011, SABS, 2015) has led to oxidation of ammonia in the distribution, resulting in the formation of nitrite with levels exceeding ≥ 0.9 mg/L, posing an immediate health challenge of methemoglobinemia, especially if infants consume the water (WHO, 2017). Elevated ammonia levels in raw water have led to the temporary shutdown of drinking water systems in the northern side of Hammanskraal, Pretoria, Tshwane Metropolitan Municipality, Republic of South Africa (Etheridge, 2019).

The phenomenon of periodic drinking water treatment system shutdowns was reported by Abu Hasan et al. (2014), and the leading cause was the inabilities of conventional treatment systems (aeration, coagulation and flocculation, sedimentation, filtration, and chlorination processes) to treat water with elevated levels of ammonia and manganese. These shutdowns consequently led to water shortages in the human population and industries. Supply of safe drinking water is a human right, as such drinking water treatment plants have resorted to excessive chlorine dosages to avert ammonia issues, leading to increment in operational cost, with noticeable observation in the formation of carcinogenic disinfection by-products. In addition, the ineffectiveness of drinking water treatment plants (DWTP) regarding elevated levels of ammonia and occasional manganese levels has at times resulted in the discharge of water with manganese which oxidises in the distribution systems creating aesthetic challenges leading to the consumer losing confidence in the quality of produced water.

Several treatment technologies have been explored to remove ammonia and other contaminants (Guštin and Marinšek-Logar, 2011). However, some of these technologies are premature and were only investigated on a laboratory scale (Adam et al., 2019). Mainly, the treatment technologies will either require system upgrades or will not be economically viable due to the low to medium range ammonia concentration, which reduces the beneficiation aspect of the recovery of ammonia (Guštin and Marinšek-Logar, 2011). Breakpoint chlorination can effectively de-ammonise water. However, ammonia removal is achieved at the expense of extremely high chlorine dosages which excessively increases operational costs. Furthermore, higher chlorine dosages can potentially form carcinogenic disinfection by-products (THMs).

Further, occasional increases in raw water manganese coupled with elevated ammonia levels hinder the application of breakpoint chlorination due to exorbitant chlorine demand. Similarly, struvite synthesis technology has also been explored in wastewater, urine and landfill leachates. This technology has yielded higher ammonia and manganese removal rates (Shu et al., 2019, Chen et al., 2022). Albeit, this technology is yet to be explored in drinking water systems. As such, this study aims at integrating precipitation and breakpoint chlorination to complete the de-ammonification process. Specifically, struvite and breakpoint technologies have been successfully applied to remove ammonia from aqueous solution (Mavhungu et al., 2019, Mavhungu et al., 2021, Chen et al., 2022), with breakpoint chlorination used in countries like Hungary and India to break down ammonium to nitrogen gas (Stefán et al., 2019, Sharma et al., 2021). However, the integration of these two technologies and their application in removing ammonia and other contaminants from drinking water has not been explored. This will then be the first study in the design and execution to explore the use of struvite and breakpoint chlorination.

1.3 Aim and objectives

1.3.1 Aim of the study

The overall aim of this study was to evaluate the effectiveness of integrating struvite synthesis and breakpoint chlorination for the removal of ammonia from an aqueous solution.

1.3.2 Specific objectives

To achieve the main aim of this study, the following specific objectives will be pursued:

- To investigate raw water's physicochemical and microbial properties at the Wallmannsthal water treatment plant (WTP).
- To determine conditions suitable for removing ammonia and other contaminants from Wallmannsthal WTP raw and point out the underpinning chemistry.
- To characterise the feed and product sludge during the synthesis of struvite using activated magnesite.
- To perform a cost analysis of the chemicals used in the developed technology denoting the proposed system's viability.
- To compare the quality of product water with different water quality regulatory frameworks.

1.4 Significance of the study

Wastewater treatment systems, i.e., upstream from the catchment, are discharging effluent that fails to comply with stringent regulatory standards (DWA, 1999). This led to significant increases in levels of ammonia, manganese, bacteria and natural organic matter, which resulted in a high raw water treatability index exceeding 80 times the limit (Masindi, 2020). Such levels put a strain on drinking water treatment systems, especially in the case of ammonia, as drinking water systems are not designed to handle such elevated concentration influxes. The expectancy of drinking water to yield potable water, fit for consumption, remains valid, regardless of the change in raw water quality. To achieve the expected yields, drinking water plants maximise their efficiency by increasing the operational cost because of the higher chemical dosages needed. The higher chemical dosages pose a health risk, especially for chlorine with the resultant formation of by-products. Worse still, the presence of both manganese and ammonia reduces the efficacy of breakpoint chlorination technology resulting in water quality with potential myriads of health, aesthetic, and operational challenges. Surface water deterioration is expected to continue, with plant shutdowns seemingly being the common solution (Abu Hasan et al., 2014, Etheridge, 2019). A shutdown eventually leads to water shortages, which impacts the human right to supply clean drinking water, consequently leading to unrest. To ensure the continuous supply of potable water, research studies are being conducted on drinking water systems to develop an economically and environmentally friendly technology that can be integrated into existing systems.

The current study focused on integrating struvite precipitation and breakpoint chlorination to achieve complete de-ammonification of the surface water. Struvite precipitation has already been proven to be an environmentally and economically viable technology with a higher percentile ammonia recovery in various aqueous solutions (landfill leachate, wastewater, etc.). Furthermore, some benefits associated with the technology include the increase in surface water pH, oxidation of manganese, and act as a coagulant aid, thus making it ideal for integration in drinking water treatment, as it will potentially reduce operational costs in drinking water systems due to product water with reduced chlorine demand, coagulant dosage, and no need for pH correction with lime. Previous studies have reported on the beneficiation of struvite as a slow-release fertiliser, which can be applied in neutral and acidic soils (Rahman et al., 2014, Mavhungu et al., 2020), and the same benefit is envisaged in the sludge to be generated from this study. Breakpoint chlorination will then be the polishing step on the pre-treated product water, ensuring that the produced water complies with drinking water regulations.

1.5 Hypothesis

The integration of struvite synthesis and breakpoint chlorination in a stage-wise fashion will effectively remove ammonia from the aqueous solution to the required limits, as stipulated in different water quality regulatory frameworks.

1.6 Thesis Layout

To respond to identified objectives and the problem of the study, this document comprises five (5) chapters and they include:

Chapter 1: Introduction

This section discusses the background and gives direction to the path followed in this study. Current problems facing surface water treatments are outlined, and a potential solution to the challenges is also presented. Issues include the recent enrichment of surface water with nutrients from non-compliant sewage effluent, its effect on drinking water treatment works, and the overall effect on final water quality. Thereafter, the study's problem statement, objectives, hypothesis, and significance are presented.

Chapter 2: Literature Review

This section discusses the existing body of knowledge to highlight the source of ammonia in surface water and its impact on the environment and drinking water treatment plants. Furthermore, available treatment technologies are extensively reviewed, critiquing their potential application in drinking water plants and their challenges. Legal requirements on water quality are also discussed in this chapter. In addition, eco-toxicology impacts may arise due to increased ammonia levels in surface water.

Chapter 3: Integration of struvite and breakpoint chlorination: Laboratory study

This section determines optimal conditions for a multi-stage ammonia removal process that combines struvite precipitation and breakpoint chlorination. In the first stage, one factor a time

(OFAT) method, optimising the different factors (mixing duration, Mg and P dosages, mixing speed and feed dosage), was applied. The chlorine to ammonia ratio was also optimised in the second stage to decompose ammonia fully. The raw water treated is eventually treated at the optimal condition and final water results are reported. In addition, the section also discusses the chemistry of the resultant sludge and the fate of the chemical species in surface water and feed material before and after the treatment process. Findings from this study were used in the pilot study (subsequent stage).

Chapter 4: Integration of struvite and breakpoint chlorination: Pilot study

This section deals with raw water treatment in a 1000 $L.h^{-1}$ pilot plant. As aforementioned, this study adopted optimal conditions from laboratory studies. After which, an in-depth cost analysis is conducted and reported. In addition, the section also discusses the fate of chemicals in the resultant sludge and surface water, specifically focusing on the feed material before and after the treatment process.

Chapter 5: General conclusions and recommendations

In this section, the outcomes of the results in light of the crafted objectives are discussed, and the thesis is succinctly concluded. This will be based on the findings discussed in the previous chapters. Thenceforth, the dissertation meticulously distils sectional conclusions based on its findings to it. Finally, recommendations are presented, and this will specifically focus on future research avenues. This will also look at the knowledge gained from this novel research and its discoveries.

References

Abu Hasan, H., Muhammad, M. H. & Ismail, N. I. 2020. A review of biological drinking water treatment technologies for contaminants removal from polluted water resources. Journal of Water Process Engineering, 33, 101035.

Abu Hasan, H., Sheikh Abdullah, S. R., Kamarudin, S. K., Tan Kofli, N. & Anuar, N. 2014. Kinetic evaluation of simultaneous COD, ammonia and manganese removal from drinking water using a biological aerated filter system. Separation and Purification Technology, 130, 56-64.

Adam, M. R., Othman, M. H. D., Abu Samah, R., Puteh, M. H., Ismail, A. F., Mustafa, A., A. Rahman, M. & Jaafar, J. 2019. Current trends and future prospects of ammonia removal in wastewater: A comprehensive review on adsorptive membrane development. Separation and Purification Technology, 213, 114-132.

Chen, Y., Long, J., Chen, S., Xie, Y., Xu, Z., Ning, Z., Zhang, G., Xiao, T., Yu, M., Ke, Y., Peng, L. & Li, H. 2022. Multi-step purification of electrolytic manganese residue leachate using hydroxide sedimentation, struvite precipitation, chlorination and coagulation: Advanced removal of manganese, ammonium, and phosphate. Science of The Total Environment, 805, 150237.

Devi, P. & Dalai, A. K. 2021. Implications of breakpoint chlorination on chloramines decay and disinfection by-products formation in brine solution. Desalination, 504, 114961.

DWA 1999. Discharge limits and conditions set out in the National Water Act. Government Gazette No. 20526.

Ekama, G. A. 2011. 4.14 - Biological Nutrient Removal A2 - Wilderer, Peter. Treatise on Water Science. Oxford: Elsevier.

Eskicioglu, C., Galvagno, G. & Cimon, C. 2018. Approaches and processes for ammonia removal from side-streams of municipal effluent treatment plants. Bioresource Technology, 268, 797-810.

Etheridge, J. 2019. Water in Hammanskraal not fit for human consumption - SAHRC [Online]. News 24. [Accessed 23/12/2019 2019].

Guštin, S. & Marinšek-Logar, R. 2011. Effect of pH, temperature and air flow rate on the continuous ammonia stripping of the anaerobic digestion effluent. Process Safety and Environmental Protection, 89, 61-66.

Han, M., Zhao, Z.-W., Gao, W. & Cui, F.-Y. 2013. Study on the factors affecting simultaneous removal of ammonia and manganese by pilot-scale biological aerated filter (BAF) for drinking water pre-treatment. Bioresource Technology, 145, 17-24.

Hube, S., Eskafi, M., Hrafnkelsdóttir, K. F., Bjarnadóttir, B., Bjarnadóttir, M. Á., Axelsdóttir, S. & Wu, B. 2020. Direct membrane filtration for wastewater treatment and resource recovery: A review. Science of The Total Environment, 710**,** 136375.

Karri, R. R., Sahu, J. N. & Chimmiri, V. 2018. Critical review of abatement of ammonia from wastewater. Journal of Molecular Liquids, 261**,** 21-31.

Kinidi, L., Tan, I. a. W., Abdul Wahab, N., Tamrin, K., Nolasco-Hipolito, C. & Salleh, S. 2018. Recent Development in Ammonia Stripping Process for Industrial Wastewater Treatment. International Journal of Chemical Engineering, 2018**,** 1-14.

Masindi, V. 2020. Dataset on physicochemical and microbial properties of raw water in four drinking water treatment plants based in South Africa. Data in Brief, 31**,** 105822.

Mavhungu, A., Foteinis, S., Mbaya, R., Masindi, V., Kortidis, I., Mpenyana-Monyatsi, L. & Chatzisymeon, E. 2021. Environmental sustainability of municipal wastewater treatment through struvite precipitation: Influence of operational parameters. Journal of Cleaner Production, 285**,** 124856.

Mavhungu, A., Masindi, V., Foteinis, S., Mbaya, R., Tekere, M., Kortidis, I. & Chatzisymeon, E. 2020. Advocating circular economy in wastewater treatment: Struvite formation and drinking water reclamation from real municipal effluents. Journal of Environmental Chemical Engineering, 8**,** 103957.

Mavhungu, A., Mbaya, R., Masindi, V., Foteinis, S., Muedi, K. L., Kortidis, I. & Chatzisymeon, E. 2019. Wastewater treatment valorisation by simultaneously removing and recovering phosphate and ammonia from municipal effluents using a mechano-thermo activated magnesite technology. Journal of Environmental Management, 250**,** 109493.

Mook, W. T., Chakrabarti, M. H., Aroua, M. K., Khan, G. M. A., Ali, B. S., Islam, M. S. & Abu Hassan, M. A. 2012. Removal of total ammonia nitrogen (TAN), nitrate and total organic carbon (TOC) from aquaculture wastewater using electrochemical technology: A review. Desalination, 285**,** 1-13.

Pastor, L., Mangin, D., Barat, R. & Seco, A. 2008. A pilot-scale study of struvite precipitation in a stirred tank reactor: Conditions influencing the process. Bioresource Technology, 99**,** 6285-6291.

Pressley, T. A., Bishop, D. F. & Roan, S. G. 1972. Ammonia-nitrogen removal by breakpoint chlorination. Environmental Science & Technology, 6**,** 622-628.

Rahman, M. M., Salleh, M. a. M., Rashid, U., Ahsan, A., Hossain, M. M. & Ra, C. S. 2014. Production of slow release crystal fertilizer from wastewaters through struvite crystallization – A review. Arabian Journal of Chemistry, 7**,** 139-155.

Ryskie, S., Gonzalez-Merchan, C., Neculita, C. M. & Genty, T. 2020. Efficiency of ozone microbubbles for ammonia removal from mine effluents. Minerals Engineering, 145**,** 106071.

SABS 2015. South African National Standard (SANS 241-1:2015) Drinking Water. Part 1: Microbiological, Physical, Aesthetic and Chemical Determinands. In: (SABS), S. D. O. T. S. A. B. O. S. (ed.). Pretoria, South Africa.

Sharma, N., Mohapatra, S., Padhye, L. P. & Mukherji, S. 2021. Role of precursors in the formation of trihalomethanes during chlorination of drinking water and wastewater effluents from a metropolitan region in western India. Journal of Water Process Engineering, 40**,** 101928.

Shu, J., Wu, H., Chen, M., Peng, H., Li, B., Liu, R., Liu, Z., Wang, B., Huang, T. & Hu, Z. 2019. Fractional removal of manganese and ammonia nitrogen from electrolytic metal manganese residue leachate using carbonate and struvite precipitation. Water Research, 153**,** 229-238.

Stefán, D., Erdélyi, N., Izsák, B., Záray, G. & Vargha, M. 2019. Formation of chlorination by-products in drinking water treatment plants using breakpoint chlorination. Microchemical Journal, 149**,** 104008.

Tünay, O., Kabdasli, I., Orhon, D. & Kolçak, S. 1997. Ammonia removal by magnesium ammonium phosphate precipitation in industrial wastewaters. Water Science and Technology, 36**,** 225-228.

Wang, H., Wang, X., Xia, P., Song, J., Ma, R., Jing, H., Zhang, Z., Cheng, X. & Zhao, J. 2017. Eco-friendly synthesis of self-existed magnesium oxide supported nanorod-like palygorskite for enhanced and simultaneous recovery of nutrients from simulated wastewater through adsorption and in-situ struvite formation. Applied Clay Science, 135**,** 418-426.

Wang, H., Zhang, X., Su, Y., Yu, H., Chen, S., Quan, X. & Yang, F. 2014. Photoelectrocatalytic oxidation of aqueous ammonia using TiO2 nanotube arrays. Applied Surface Science, 311**,** 851-857.

Warmadewanthi, Rodlia, A., Ikhlas, N., Pandebesie, E. S., Bagastyo, A. Y. & Herumurti, W. 2020. The Effect of Mixing Rate on Struvite Recovery from The Fertilizer Industry. IOP Conference Series: Earth and Environmental Science, 506**,** 012013.

WHO 2011. Guidelines for drinking-water quality. 4th ed ed. Geneva: World Health Organization.

WHO 2017. Guidelines for drinking-water quality: fourth edition incorporating first addendum, Geneva, World Health Organization.

Xiao, S., Wan, D., Zhang, K., Qu, H. & Peng, J. 2016. Enhanced photoelectrocatalytic degradation of ammonia by in situ photoelectrogenerated active chlorine on TiO2 nanotube electrodes. Journal of Environmental Sciences, 50**,** 103-108.

Zhang, C., He, D., Ma, J. & Waite, T. D. 2018. Active chlorine mediated ammonia oxidation revisited: Reaction mechanism, kinetic modelling and implications. Water Research, 145, 220-230.

CHAPTER TWO

Literature review

This chapter provides a review of relevant topics and highlights sources of ammonia in surface water and its impact on the environment and drinking water treatment plants (DWTP). In addition, the numerous treatment technologies are extensively reviewed, critiquing, and emphasising the viability of their potential application in drinking water plants and the challenges thereof.

Abstract

Ammonia is a compound that prevails in various spheres of the environment. If not properly managed, this compound could pose severe ecological stresses, pressure, and toxicity to different receiving environments. The notorious footprints of ammonia could be traced to anoxic conditions, an infestation of aquatic ecosystems, hyperactivity, convulsion, and methaemoglobin, popularly known as "the blue baby syndrome". In this review, the latest updates regarding the advancements and challenges in the removal of ammonia from aqueous solutions, i.e., river and wastewater, are briefly elucidated in light of future perspectives. Viable routes and ideal hotspots, i.e., wastewater and drinking water, for ammonia removal under the cost-effective lens have been unpacked. Key technologies for ammonia removal are bioremediation, oxidation, adsorption, filtration, and ion exchange. This review has shown that biological nutrient removal, struvite precipitation, and breakpoint chlorination have been noted as emerging and promising for the removal of ammonia from aqueous environments. Finally, the future perspective, avenues of exploitation and areas that deserve in-depth exploration are duly underscored.

Keywords: Ammonia, toxicological effects, removal technologies, drinking water, and wastewater.

2.1 Introduction

Ammonia is a major pollutant contaminating surface water and commonly exists in the non-ionised NH_3 or ionised NH_4 form (Adam et al., 2019). The compound, made up of hydrogen, nitrogen, and ammonia, is colourless and in gas form; it has a strong smell, and its solubility in water is very high. According to the WHO (World Health Organisation), the natural concentration in groundwater is 0.2 mg/L, higher values in natural water can be as much as three mg/L and is mainly due to strata that is rich in humic substance or iron or forests, while surface water averages 12 mg/L globally. Ammonia levels exceeding geogenic levels indicate faecal pollution (WHO, 2011). Furthermore, levels exceeding the natural concentrations have been reported to disrupt aquatic ecosystems leading to oxygen depletion and excessive plant growth. Chlorinating water with 0.2 mg/l ammonia might give water an acceptable taste and odour (WHO, 2017). Additionally, Adam et al. (2019) reported that the toxicity of non-ionised ammonia is due to its uncharged form and solubility in an aqueous solution. Human activities, metabolic, agricultural, and industrial processes and disinfection processes are primarily the origins of ammonia (Booker et al., 1996, Huang et al., 2016b, Shoda et al., 2019). Ammonia concentration in industrial and municipal wastewater ranges between 5-1000 mg/L and 10-200 mg/L, respectively (Adam et al., 2019). Ammonia in industrial wastewater is primarily from chemical fertilisers, cooking, pharmaceutical, petrol refining, coal gasification, and catalyst factories, while in municipal wastewater, ammonia is mainly attributed to faecal excretion (Ansari et al., 2017, Huang et al., 2018, Vareda et al., 2019).

Ammonia removal processes are primarily in wastewater treatment works. However, with the current failure to meet discharge limits, catchments are polluted with ammonia from agricultural, industrial, natural and domestic activities (Abel-Denee et al., 2018, Chuang et al., 2019). Enriching surface water sources and catchment with nutrients and ammonia results in eutrophication, leading to oxygen depletion in water, resulting in toxicity effects on aquatic life (Loganathan et al., 2013, Zhang et al., 2015a, Huang et al., 2018). Furthermore, ammonia can affect the neurological condition of aquatic animals due to its poisonous effect, which may result in hyperactivity and seizure among fishes, affecting their balance (Bernardi et al., 2018). Eventually, eutrophication will promote the growth of algae in surface water and can also increase plant life.

Water being a scarce commodity that must be preserved, the contaminated surface water sources are already impacting the DWTP system. The WHO regards ammonia as an aesthetic determinant, with a concentration threshold for taste and smell at 1.5 mg/L and 35 mg/L N, respectively, under alkaline conditions (WHO, 2011). The United States Environmental Protection Agency US: EPA (2019) reported on the health risk associated with ammonia and stated that human health-related risks associated with ammonia intake/consumption are very low. However, the challenge with ammonia is the potential for nitrification in the distribution system resulting in nitrite, which poses an acute health risk to humans post-consumption (Ekama, 2011, Liu et al., 2017, Ruiz-Beviá and Fernández-Torres, 2019, Yun et al., 2019). Furthermore, the presence of ammonia harms manganese removal as ammonia reacts with chlorine to form chloramine. Manganese will stain laundry and give the water a metallic taste if not removed from the water. The consumer also loses confidence in the water produced as a result of the aesthetic colour indicative in the water, even if it does not pose a health risk (Department of Water Affairs and Forestry, 1996).

Many researchers have reported different technologies incorporated to eliminate ammonia in wastewater. In comparison, the focus in the research community has also shifted to treatment technologies that can be introduced in drinking water treatment to effectively remove ammonia and ensure that the effluent from drinking water treatment systems is acceptable to the South African Drinking Water standards of 2015 (SABS, 2015). The SANS 241 standard limits for ammonia, nitrite and nitrate are 1.5 mg/L, 0.9 mg/L and 11 mg/L, respectively, and the Water Service Providers (WSP) and Water Services Authority (WSA) are required to adhere to these limits to ensure that water is safe for consumption. There are no review studies comparing treatment technologies that can be introduced into the drinking water system to eliminate the growing ammonia threat. This paper will review existing technologies like air tripping, membrane filtration, biological air filtration, adsorption and ion exchange, membrane filtration, advanced electrochemical oxidation, photocatalytic oxidation, and chemical precipitation, with the primary focus being the feasibility of introducing the technologies in conventional drinking water treatment system with emphasizes placed on cost, removal efficiency and simplicity in application processes.

2.2 Ecological impacts of ammonia

The ammonia level in water is not toxic to humans and is considered an aesthetic determinant. It, however, has a toxic effect on the aquatic life, as it increases the nutrient contents in the water, which in turn promotes the growth of algae - known as eutrophication. Two forms of ammonia can be found in water: unionised and ionised, depending on the pH and temperature of the solution. The unionised ammonia form is toxic to aquatic organisms. A pH of six and below promotes the formation of non-toxic ammonia, with the ratio of ammonia to ammonia being 1 to 3000. However, an increase in pH to levels exceeding 8 reduces the ammonium to ammonia ratio to 1 to 30. Warm water will contain more toxic ammonia than cooler water. An unionised ammonia concentration level of 0.02 mg/L (48-hour LC_{50}) is reportedly deadly to certain aquatic specimens. Many studies have reported that the presence of unionised ammonia in water can negatively affect freshwater invertebrates with a 48-hour LC_{50} of 0.66 mg/L for *Daphnia Magna*.

2.3 Toxicological and epidemiological challenges

SANS 241:2015 classifies ammonia as an aesthetic health determinant. In particular, a concentration of ammonia exceeding 0.2 mg/L in drinking water gives taste and odour. Furthermore, it also negatively affects the disinfection efficiency with 68% chlorine that is reacting with the ammonia (WHO, 2011). Elevated ammonia levels from the water source interfere with manganese oxidation in treatment systems as the ammonia reacts with chlorine, reducing the oxidation levels. Failure to oxidise manganese will give the treated water a mouldy, earthy taste. A catalytic action in the distribution system might also lead to drinking water containing nitrite when the raw water source is contaminated with ammonia. Concentrations of nitrite in water exceeding the SANS 241:2015 limit (0.9 mg/L) have been reported to potentially impact the red blood cells by binding with haemoglobin, thus, leading to blood failing to carry oxygen resulting in a health condition known as methemoglobinemia (blue baby syndrome). Furthermore, ammonia in surface water reacts with chlorine leading to chloramine, which gives water an acceptable taste and smell.

2.4 Treatment Technologies Approaches

In this section, the technologies used to remove ammonia in both water and wastewater are being unpacked.

2.4.1 Break Point Chlorination

Breakpoint chlorination is the most used technology to oxidise ammonia to nitrogen, and hydrogen gas and free chlorine are released, as shown in **Equation 2.4**. The technology is available in both drinking water and wastewater treatment plants. A breakpoint is defined as the point where ammonia is decomposed completely to zero levels, leading to the availability of free chlorine. Water sources typically contain microbial communities (*E. coli*, total coliform, and other heterotrophs), which can cause harm to end users and chlorination is primarily used to deactivate the microbial community in the water, ensuring that the water is suitable for consumption. Capodaglio et al. (2015) reported that breakpoint chlorination technology could be regarded as a technique that further enhances the effluent water quality in a system with limited effectiveness in treating water with high ammonia-nitrogen levels. Breakpoint chlorination involves the oxidation of available ammonia to nitrogen gas, free chlorine (residual chlorine) release, being the dominant chlorine species present (US: EPA, 2019). This methodology has been used for decades to disinfect water and in controlling the odour and taste of the water (Takó, 2012). The first part of breakpoint chlorination involves the addition of chlorine in the water with the ammonia present, after which an initial increase of the residual chlorine level is observed. In the second part, continuous chlorination leads to the reduction in the chlorine residual levels, in conjunction with the ammonia concentration in water until the residual chlorine starts to increase, leading to the practical decomposition of the ammonia to nitrogen gas (Capodaglio et al., 2015, Adam et al., 2019). Many studies reported a stoichiometric weight ratio of 7.6:1 of Cl_2:NH_3 as suitable for complete oxidation of ammonia to nitrogen gas, provided that ammonia is the only dominant demand in the water (Capodaglio et al., 2015). However, studies have shown that the theoretical ratio is accurate only in synthetic water. Higher ratios were reported when the technology was applied to natural water sources with constituents such as natural organic matter (NOM). Pressley et al. (1972) predicted that with chlorine to ammonia (Cl_2:NH_3) weight ratio of 8:1 in a system with ammonia, the chlorine demand would be able to remove ammonia as nitrogen. Takó (2012) reported on a study conducted by Laky et al. (2010), who decomposed ammonia to nitrogen at a Cl_2:NH_3 ratio of 8.6:1. Specifically, Takó (2012) argued that if the water contains natural organic matter (NOM) and iron (Fe), the chlorine demand will increase leading to a higher chlorine dosage to decompose ammonia.

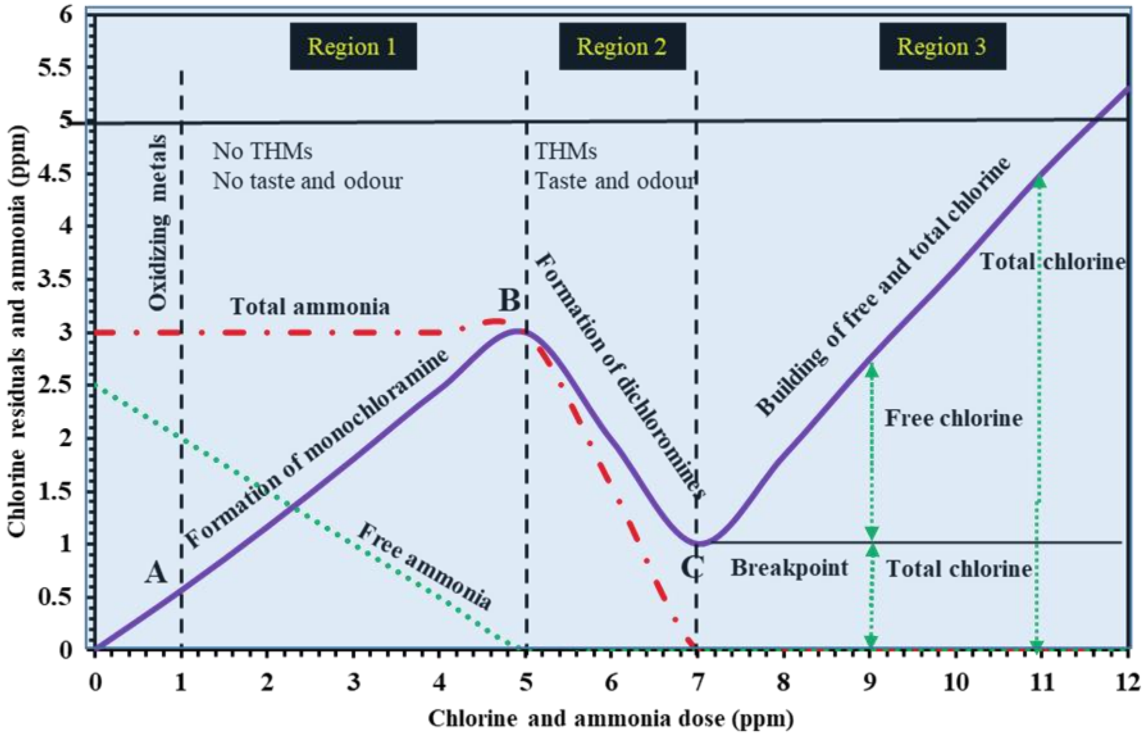

Figure 2.1: An illustration of the breakpoint chlorination curve [Adopted from Capodaglio et al. (2015)].

Figure 2.1 gives a graphical representation of the breakpoint chlorination curve. The initial reaction, after chlorine dosing, involves the formation of monochloramine when chlorine reacts with ammonia **(Equation 2.1).** Continuing with the chlorine dosage will increase dichloramine **(Equation 2.2)** and eventually lead to tri-chloramine formation and the residual chlorine required **(Equation 2.3).** Tri-chloramine is unstable and decomposes into nitrogen gas. Breakpoint chlorination reactions are depicted as follows: (Capodaglio et al., 2015; Pressley et al., 1972; Takó, 2012):

$\mathrm{NH_3 + HOCl \rightarrow NH_2Cl + H_2O}$ (Monochloramine) (2.1)

$\mathrm{NH_2Cl + HOCl \rightarrow NHCl_2 + H_2O}$ (Dichloramine) (2.2)

$\mathrm{NHCl_2 + HOCl \rightarrow NCl_3 + H_2O}$ (Nitrogen trichloride) (2.3)

Capodaglio et al. (2015) summarised the breakpoint chlorination equation as follows:

$\mathrm{NH_4^+ + 1.5\ HOCl \rightarrow 0.5N_2 \uparrow + 1.5\ H_2O + 2.5\ H^+ + 1.5\ Cl^-}$ (2.4)

Drinking water ammonium concentrations range from as low as 0.5 mg/L to 8 mg/L and implementing a stoichiometric ratio of 7.6:1 of Cl_2:NH_3 as suggested by Pressley et al. (1972), will require an over chlorine dosage above 60 mg/L to break down the ammonium to nitrogen gas, but leading to increased operational costs. Extremely high chlorine dosages will potentially form problematic disinfection by-products (DPBs*)* with raw water sources contaminated with ammonia and natural organic matter (NOM). The halogenated DBPs have been reported to express toxicity toward humans (Zhang et al., 2015).

2.4.2 Biological Nutrient Removal (BNR)

Biological nutrient removal (BNR) is a frequently applied technology to decompose ammonia in aqueous municipal wastewater. This methodology employs nitrification and denitrification processes. Nitrification involves the transformation of aqueous ammonia to nitrite **(Equation 2.5)** and nitrate **(Equation 2.6).** The formed nitrate then converts to nitrogen gas under an anoxic environment, known as denitrification (Bock, 2016). The biological decomposing of ammonia occurs due to the availability of microorganisms. Two main microorganisms, ammonia oxidising archaea (AOA) and ammonia oxidising bacteria (AOB), are responsible for the oxidation of aqueous ammonia to nitrite. Nitrobacter (Nitrite oxidising bacteria (NOB)) and nitrospira are responsible for nitrite oxidation to nitrate. The formed nitrate is decomposed into nitrogen in the anaerobic zone without oxygen.

$\mathrm{NH_4^+ + 1.5O_2 \rightarrow NO_2^- + 2H^+ + H_2O}$ (2.5)

$\mathrm{2NO_2^- + O_2 \rightarrow 2NO_3^-}$ (2.6)

Nitrifying bacteria are chemoautotrophs and rely on the availability of carbon dioxide as a source of food and are reported to utilise ammonia as a nitrogen source for cellular synthesis as depicted by **Equations 2.7** and **2.8** below:

$$4CO_2 + HCO_3^- + NH_4^+ + H_2O \rightarrow C_5H_7NO_2 + 5O_2 \qquad (2.7)$$

$$2NO_3^- + 10e^- + 12H^+ \rightarrow N_2 + 6H_2O \qquad (2.8)$$

BNR technology is usually applied to municipal wastewater and non-toxic industrial waste waters. This technology can be applied in suspended growth processes such as the activated sludge process, which involves anoxic, anaerobic, and aerobic stages. Different reactors suitable for BNR are available, including plug flow, batch sequencing and complete mix reactors. This technology can be applied in attached growth process filtering systems such as trickling filters (TF) and biological aerated filters (BAF). BNR is primarily applied in municipal wastewater treatment systems. However, the challenges ranging from population growth and breakdown of mechanical equipment in wastewater treatment systems have led to the discharge of effluents rich in nutrients being discharged into the water stream, leading to surface water contamination with ammonia. The aim is to remedy the surface water rich in ammonia impacting the drinking water system.

Research is focusing on the introduction of BNR in drinking water systems. In China, aerated biological filters (BAF) have already been introduced in DWTP by constructing a bioreactor and submerging biofilms to remove ammonia. Results from the studies indicated that the technology relied on seasonal climatic conditions. BAF is applied in wastewater treatment works (WWTWs). However, this technology has shown a higher efficiency in removing ammonia from surface water polluted with nutrients during warmer temperatures (Liu et al., 2017). Oxygen is key in the ammonium breakdown process. BAFs are aerated to provide oxygen to enable the growth of aerobic microorganisms and to further assist in decimating and rehabilitating pollutants (Abu Hasan et al., 2014). The design of the BAF can be in the form of a rectangle, square, or shaped like a column, and the influent configuration can either be up-flow or down-flow. Aeration provides oxygen for biofilm growth and hence increases the efficacy of BAF. Abu Hasan et al. (2014) further elaborated that ammonia oxidising requires higher aeration intensity. Backwashing in the BAF system is included to minimise excessive biomass and remove the biofilm that might clog the filter media. A previous study has reported filter run times ranging from 14 to 15 days for efficient operation of the BAF system (Abu Hasan et al., 2014). Bio-film carriers in the BAF system include floating types such as polypropylene and polyethene media, while submerged carriers include lava, zeolite, pebbles, and ceramic. The BAF method does not require additional chemicals, and no hazardous chemicals are formed. Due to the BAF requiring the introduction of microorganisms to decompose ammonia, Abu Hasan et al. (2014) reported that the technology is more reliable and efficient when used in conjunction with a disinfection process and even proposed that it should be implemented before post-chlorination.

Microorganisms used to decompose the ammonia in a BNR can cause acute health challenges to end users, and bacteria must be deactivated before distribution. This can be achieved by post-disinfection with chlorine. Activated sewage sludge can be used as a bacterial source to remove ammonia and manganese. It is important to determine the bacterial kinetic parameters to maximise the potential to remove ammonia in the water. Han et al. (2013) also stated that no study was piloted that focused on the growth kinetics of bacteria when removing chemical oxygen demand (COD), ammonia, and manganese simultaneously.

BNR ammonia removal efficacy can be influenced by the rate of aeration, organic loading, and hydraulic retention. A study conducted by Abu Hasan et al. (2014) revealed that contamination of surface water with high COD, ammonia and manganese would require higher aeration rates to remove the contaminants efficiently. If the condition becomes anoxic, removal efficiency is hampered, and the system will fail to perform. Abu Hasan et al. (2014) conducted lab-scale experiments that showed 92 – 94 % ammonia removal efficiency. Han et al. (2013) conducted experimental studies using an aerated biological filter with a lava-based column to remove ammonia and manganese simultaneously. In the study, decomposition of ammonia and manganese was due to oxidising ammonia bacteria (AOB), nitrite oxidising bacteria (NOB) and manganese oxidising bacteria (MOB) and achieved 84% and 86.1% ammonia and manganese removal efficiency within a temperature range of 6-32°C. The duration of the studies was 200 days, and the authors found that increasing the hydraulic loading from $7.12\mathrm{m}^3\ /(\mathrm{m}^2\mathrm{h})$ to $10.69\mathrm{m}^3/(\mathrm{m}^2\mathrm{h})$ reduced the removal efficiency of ammonia and manganese to 75.3% and 73.75%, respectively. The higher removal efficiency was achieved when the hydraulic loading rates ranged between $3.56\mathrm{m}^3\ /(\mathrm{m}^2\mathrm{h})$ to $7.12\mathrm{m}^3/(\mathrm{m}^2\mathrm{h})$ with 89% removal efficiency yielded for both ammonia and manganese. Furthermore, BAF was efficient in removing both taste and odour compounds, geosmin and 2-methylisorboneol (2MIB), yielding geosmin and 2MIB removal efficiency of 82% and 84%, respectively. Studies involving simultaneous removal of ammonium and manganese, including factors influencing removal performance, are limited. Abu Hasan et al. (2014) reported on a study conducted by Hasan et al. (2012) where both manganese and ammonia using BAF were removed. However, the microbial matter used was from wastewater sludge. In conclusion, the risk posed by introducing heavy metals in drinking water constituted in waste-activated sludge was also noted (Puyen et al., 2012). Furthermore, a lower temperature was found to limit the effectiveness of the oxidising ammonia bacteria leading to a lower ammonia removal efficiency. Liu et al. (2017) conducted a pilot study for four years using lava based-BAF system. In their study, the authors achieved a higher ammonia removal efficiency of 92.62% in summer when temperatures ranged between 18.6 to 32.9°C, while the removal efficiency reduced to 77.52% in winter with lower temperatures ranging from 5.1 to 8°C. Additionally, the study showed that temperature affected the nitrite removal rate with 98% nitrate removal in warmer temperatures. Lower temperatures promoted the accumulation of nitrite concentrations. In the study, lower temperatures resulted in effluent nitrite levels (0.212 mg/L N) exceeding the influent (0.122mg/L) concentration because of accumulation. Even with the accumulation, the nitrite levels were still lower than the drinking water standard regulation. Primary AOB for decomposing ammonia in summer and winter were the psychrophilic and mesophilic AOBs, respectively. In this technology (BNR), a lower temperature negatively affects the nitrification process leading to failure to remove ammonia. As such, a biological air filter (BAF) has proven to be a practical technology which can be applied in warmer temperatures to decompose ammonia from surface water. The challenge associated with BAF in drinking water plants is the low efficiency during winter periods where ammonia in the surface water is higher due to lower rainfall levels, which can neutralise the nutrients from wastewater treatment plans. Furthermore, the introduction of BAF will require new process designs involving the construction of specialised filters leading to increased cost, and the use of a bacterial community will pose a higher risk to safety during the subsequent processing if the post disinfection fails (Li et al., 2011).

2.4.3 Air/Steam Stripping Ammonia Removal

Ammonia stripping is another process that has shown greater efficiency in removing ammonia in media such as landfill leachates, pig slurry and wastewater effluents contaminated with ammonia, such as that from the production of fertilisers (Guštin and Marinšek-Logar, 2011), where a mass transfer process was used (Kinidi et al., 2018). The ammonia stripping process requires an aqueous media condition change to convert ammonia ions to ammonia gas, which can be stripped from the liquid phase using air (Guštin and Marinšek-Logar, 2011). The advantages of the stripping process are the simplicity of the process and the cost-effectiveness of the method when used in wastewater plants. The air or steam stripping process is a cost-effective method that applies a desorption process to remove ammonia in the wastewater (Adam et al., 2019). Ammonia gas is tripped out of the aqueous stream by contacting wastewater with air. Two packed towers are put in operation to remove the ammonia, which allows for transferring the volatile ammonia found in aqueous media to gas. Ammonia in water is found either as an ammonium ion or ammonia gas, and the form depends on the solution's pH (Adam et al., 2019). The stripping technology relies on the conversion of ammonium to ammonia gas, and conversion can be attained with the addition of lime to increase the pH to >10, which promotes shifting of the chemical equilibrium to the right and, as a result, promotes the release of ammonia gas as depicted by **Equation 2.9** (Capodaglio et al., 2015).

$$NH_4^+ + OH^- \leftrightarrow NH_3 \uparrow + H_2O \qquad (2.9)$$

The equilibrium state is reliant on both the temperature and pH concerning the reaction ionization constant (K_{eq}):

$$K_{eq} = \frac{(NH_4^+)(OH^-)}{NH_3} = 1.8 * 10^{-5} \text{ @ } 25°C \qquad (2.10)$$

Capodaglio et al., 2015 have found the optimum pH for air stripping ranging between 10.8 - 11.5, where hydrated lime (calcium carbonate) was the preferred chemical to adjust the pH of the wastewater before ammonia stripping(Guštin and Marinšek-Logar, 2011, Capodaglio et al., 2015, Adam et al., 2019). Lime dosage is primarily used to increase the pH before the stripping process. However, carbonation can be incorporated after the process, neutralising the water. The generated calcium carbonate from lime addition can potentially serve as a coagulant for particulate matter in wastewater.

The ammonia stripping occurs in the packed stripping towers, which can either be crossflow or counter-current flow. The ammonia gas formed after pH adjustments is then removed from the stripping towers by air and discharged into the atmosphere (Adam et al., 2019). In a study conducted by O'Farrell et al. (1972), 90% of ammonia from a secondary effluent was removed. Kinidi et al. (2018) reported on a study that was done by Raboni et al. (2013) to determine the efficiency of the ammonia stripping technique for remediation of groundwater that the stripping process managed to remove 95 % of the ammonia from an initial concentration of 199 mg/L to 22.5 mg/L. The experimental setup included a heater which increased the water temperature to 38 °C, and the experiment was conducted at a pH of 11, with different flocculants added for coagulation and flocculation.

Discharging of the leading ammonia gas formed into the atmosphere might have a negative impact and result in pollution of the surrounding air with pungent gas, thus, most stripping towers are coupled with adsorption towers for capturing the released ammonia. Ammonia adsorption in towers occurs after the addition of sulphuric acid, leading to the formation of ammonia sulphate, which can be used as a fertiliser. With the system dependent on high lime dosages, calcium carbonate scaling on the stripping towers is known to form and can reduce the stripping potential; thus, frequent chemical cleaning is required. The air stripping process is efficient in high pH conditions. The air stripping technology is energy-dependent and increases operational costs. Capodaglio et al. (2015) reported that the steam stripping process is similar to air stripping, with the major difference being that steam stripping requires higher temperatures (above 95 °C).

Furthermore, steam stripping requires a higher energy input to heat and increase the temperature, and thus it is applicable when ammonia recovery is economically beneficial (Capodaglio et al., 2015). Bonmatí and Flotats (2003) undertook a study where 99% ammonia as nitrogen gas was removed in a batch stripping column operated at a pH of 11.5 and temperature of 353 K within 3hrs. Laureni et al. (2013) successfully used air stripping and absorption to remove ammonia in pig slurry. The by-product of this process was ammonia sulphate, a marketable agricultural product as fertiliser. The stripping technology is effective on wastewater with ammonia concentrations ranging from 10 – 100 mg/L (Guštin and Marinšek-Logar, 2011). Furthermore, the stripping process is temperature dependent, and stripping is redundant in freezing conditions and fails to remove nitrite or organic nitrogen. Guštin and Marinšek-Logar (2011) reported that an ammonia removal efficiency was insignificant when the pH exceeded 10.5 as it no longer affects the ionization balance but will, however, result in increased production of sludge and high alkalinity due to the high lime dosage to increase the pH, finally resulting in increased treatment and maintenance costs.

2.4.4 Removal of Ammonia by Chemical Precipitation (Struvite)

Chemical precipitation is utilised to remove ammonia as a solid phase. Ammonia in water is in a soluble state, and thus struvite ($MgNH_4PO_4.6H_2O$) can recover ammonia by a crystallisation process. This technology has been applied mostly in water with a high ammonia concentration (Yan and Shih, 2016).

Struvite is a white insoluble crystalline compound forming when the collective concentrations of magnesium, ammonia and phosphate in solution are higher than their solubility limit of 23 mg per 100 mL (Huang et al., 2014, Huang et al., 2015). Struvite consists of PO_4^{3-} (tetrahedral), $Mg^{2+}.6H_2O$ (octahedral), and NH_4^+ (tetrahedral) groups, connected by hexa-hydrogen bonds (Huang et al., 2014). Factors promoting the formation of struvite include ionic compositions, temperature, pH and ion-specific characteristics (Rahman et al., 2014). The white crystalline substance of MAP can form at equimolar molar concentrations of 1:1:1 for magnesium, ammonia, and phosphorus, respectively (Galbraith et al., 2014). The chemical reaction for struvite formation is depicted by **Equation 2.11**.

$$\mathrm{NH_4^+ + Mg^+ + HPO_4^{2-} + 6H_2O \rightarrow NH_4MgPO_4 + 6H_2O} \tag{2.11}$$

Struvite can be used as a fertiliser and compares favourably with mineral phosphates based on a broad range of varying pH levels (Mehta and Batstone, 2013), and its availability can curtail the pressure mounted on dwindling deposits of phosphate rock as a source of phosphate for the production of fertilisers. Hexa-hydrous struvite crystallisation is primarily a thermodynamically unstable process which stabilises through nucleation (either primary or secondary), followed by the development of crystals (Mehta and Batstone, 2013). The first stage of crystal formation involves the nucleation of seed crystals (Bock, 2016) and is dependent on the saturation state of the solution. If the solution is supersaturated, the nucleation process transpires within the bulk solution (Rahman et al., 2014) and is referred to as homogeneous nucleation. The supersaturation environment provides conditions where the high ion activities can overcome the thermodynamic uncertainty of the phase transformation from liquid to solid. When the saturation ratios are low, other impurities in the water, such as colloidal material, act as a catalyst for nucleation reaction leading to the formation of crystals onto the solid impurities present in the water. Specifically, struvite formation occurs in stages, of which the first stage is to overcome the induction period by super-saturation, leading to the formation of principal crystal nuclei (primary nucleation), followed by the formation of nuclei because of the presence of other struvite crystals, leading to crystal growth where the crystal boundaries and magnitude with which the crystal size is distributed (Rahman et al., 2014, Bock, 2016). The induction time is inversely proportional to super-saturation, where the induction period is a period between the realisation of super-saturation conditions and the formation and noticeable appearance of crystal nuclei.

Furthermore, the struvite growth rate is affected by pH, super-saturation, temperature, mixing rate and the existence of foreign ions in the aqueous solution (Mehta and Batstone, 2013). The pH range between 8.5 - 9.5 ensures the highest crystal growth rates (Hu et al., 2020). The formed struvite is heavy and settles out of the aqueous solution, resulting in the removal of ammonia nitrogen from contaminated water (Adam et al., 2019).

2.4.4.1 Chemical reagents used for the formation of struvite and removal of ammonia

Struvite formation is an equimolar-driven process whereby precise ratios of chemical compositions are required. According to literature (Adam et al., 2019), adding $MgCl_2 \cdot 6H_2O$ and $Na_2HPO_4 \cdot 12H_2O$ provides the most efficient chemical combination to remove ammonia in water. However, this combination produces the highest salt concentration, as depicted by **Equation 2.12**:

$$\mathrm{MgCl_2.6H_2O + Na_2HPO_4.12H_2O + NH_4 \rightarrow MgNH_4PO_4\,.6H_2O + 2NaCl} \tag{2.12}$$

From the equation, the speculative molar relation of $Mg^{2+}: NH_4^+: PO_4^{3-}$ to achieve the highest ammonia removal was found to be 1.15:1:1 (Adam et al., 2019). Struvite is a recognized slow-release fertiliser suitable for crops planted in soils low in pH (Ronteltap et al., 2010). Research has primarily been focused on determining the efficiency of struvite precipitation to maximise ammonia removal.

Table 2.1 shows varying ammonia removal rates from different types of wastewater using different chemical reagents. From **Table 2.1**, the highest ammonia removal rate was 99.6% complex wastewater using magnesium chloride as a magnesium source (Chai et al., 2017). In Chai et al. (2017) studies, Na_2HPO_4 was used as a phosphate source, and the higher removal rates confirm the findings of Adam et al. (2019). More prevalently, Mg-based materials are used for the synthesis of struvite. This is further proof that struvite formation is dependent on ionic composition, as reported by Rahman et al. (2014) and Mehta and Batstone (2013) in their studies. The cost of chemicals added during the struvite precipitation limits the application of this technology. As such, researchers have evaluated the use of low-cost magnesium sources. Low-cost magnesium sources like calcined magnesite (Mavhungu et al., 2019), dolomite (Xiao et al., 2018), bittern salt (Ye et al., 2011) and low-cost Magnesium oxide (Huang et al., 2014, Astals et al., 2021) have been used successfully to synthesis struvite achieving higher ammonia removal rates from different types of wastewater. Furthermore, decomposing struvite and recycling the by-products have also been evaluated as an option to minimise cost. Huang et al. (2021) used calcium hydroxide to break down struvite forming Mg_3PO_4, $Mg(OH)_2$ and $Ca_3(PO_4)_2$. The by-products were used as magnesium and phosphate sources in the cooking water, achieving 86% ammonia removal. Huang et al. (2015) decomposed struvite with chlorine forming Newberyite ($MgHPO_4$), magnesium and phosphate sources in landfill leachate, yielding 92% ammonia removal.

Table 2.1: Different chemicals added to synthesise struvite from different types of wastewater.

Type of wastewater	Chemicals added	Dosages/ratios (Mg: N:P)	Initial concentration (mg/L)	Mixing rate (rpm)	Removal	References
Municipal wastewater	Calcined magnesite	8.6g	123	300	75%	(Mavhungu et al., 2019)
7- Aminocelphalosporanic acid wastewater	$MgCl_2$+ 85% k_2HPO_4	1:1:1	1128		81.3%	(Li et al., 2012)
Landfill leachate	$MgSO_4$+ Phosphoric acid	2:2.5:1	840	200	45%	(Warmadewanthi et al., 2020)
Swine wastewater	$MgCl_2.6H_2O$ + K_2HPO_4	1:1:1	844		88%	(Ryu and Lee, 2010)
Model wastewater	Calcined dolomite ($MgO/CaCO_3$) + k_2HPO_4	1:1:1.2	2000	200	89.7%	(Chen et al., 2017)
Swine wastewater	Dolomite + sulfuric acid	1.2:1:1	528	400	83%	(Xiao et al., 2018)
Cooking wastewater	Calcium hydroxide decomposed struvite by-products formed by Mg_3PO_4 +$Mg(OH)_2$ +$Ca_3(PO_4)_2$	1.2:1:1	535	200	86%	(Huang et al., 2021)
Landfill leachate	Chlorine decomposed by-product Newberyite ($MgHPO_4$)	1:1.2:1	823	-	92%	(Huang et al., 2015)

Pig slurry	Low-grade MgO + H_3PO_4	-	12500	200	73%	(Astals et al., 2021)
Wastewater	MgO + Waste bone ash recovered P	1:1:1	400	-	72%	(Darwish et al., 2017)
Pre-AnMBR treated abattoir effluent	$MgCl_2$	2:1:1	87	220	66%	(Hakimi et al., 2020)
Swine water from a digester	Bittern salt	1:1:1.06	-	-	29%	(Ye et al., 2011)
Landfill leachate	Low-cost MgO	3:1:1	1980	-	83%	(Huang et al., 2014)
Oil and gas industries produced water	Mg^{2+} + $NaHPO_4$	1.5:1:1.5	596	300	85.9%	(Hu et al., 2020)
Complex wastewater	$MgCl_2$ + Na_2HPO_4	1:1.2:1.5	500	-	99.6%	(Chai et al., 2017)

Most of the wastewater has a low concentration of phosphates and magnesium in the aqueous solution, and the cost of introducing the precipitants in the struvite formation will increase operational costs further. Li et al. (2012) evaluated the effects of varying magnesium sources on the removal of ammonia in water. In the study, MgO removed 40% ammonia in the water while $MgCl_2.6H_2O$ and $MgSO_4$ each achieved 65% ammonia removal as struvite. The low removal efficiency for MgO alone was attributed to its low solubility in water. Calcined magnesite is another source that has 53% MgO and 40% solubility in water (Huang et al., 2015, Romero-Güiza et al., 2015). Mavhungu et al. (2019) achieved 75% ammonia removal by adding 8g/L calcined magnesite from an initial concentration of 123 mg/l **(Table 2.1).** The availability of low-cost magnesium sources, the recycling of struvite by direct pyrolysis and sodium hydrogen pyrogenation and recycling of struvite by-products, and the success rate reported further give confidence in incorporating struvite precipitation technology in existing systems at reduced operational cost.

2.4.4.2 Factors that influence the formation of struvite or removal of ammonia

2.4.4.2.1 Effect of pH

An acidic and basic pH plays a significant part in removing contaminants and detecting the oxidation state of contaminants in aqueous solutions. The pH influences struvite's solubility and thermodynamic properties (Li et al., 2012). In struvite precipitation, the pH of the solution is responsible for determining the ion species and the crystal part Saturation Index (SI) (Song et al., 2015), as shown in **Equation 2.13**:

$$\mathrm{SI} = \log\ (\mathrm{IAP}/\mathrm{k_{sp}}) \tag{2.13}$$

IAP and k_{sp} represent the end product ion activity product and thermodynamic solubility product of the crystal phase. Song et al. (2015) conducted a study using a geochemical programme (PHREEQC) and noticed that the pH increases from 5 to 9, resulting in an increase in SI and logarithmic ion activity of phosphate, magnesium, and ammonia until a pH of 9. The study concluded that the optimum pH of 9 was suitable for struvite crystallisation. Li et al. (2012) also reported an optimum pH of 9 during the synthesis of struvite. The study involved removing ammonia from 7-Aminocephalosporanic Acid Wastewater at an equimolar ratio of $Mg^{2+}: NH_4^+ : PO_4^{3-} (1:1:1)$ using $MgCl_2.6H_2O$ and 85% H_3PO_4 as magnesium and phosphate sources. In the study, struvite was not detected at a pH of 7, pH of 8 gave a minute struvite, while the growth of the struvite improved at a pH of 9, leading to a settlement of sediments. Many researchers have successfully crystallised struvite at varying optimal pH (Mavhungu et al., 2019, Hu et al., 2020). Mehta and Batstone (2013) reported on a study conducted by Abbona and Boistelle (1979), which focused on the influence of pH on struvite crystallisation. In the study, a pH > 8 gave twinned dendritic crystals, while in the pH ranges between 7 and 8 gave a tubular crystal form, and at a lower pH < 6 crystals became elongated and needle-like in shape. It was concluded that the tubular form is more desirable in a engineering process point of view as it is uniform and is less likely to break into smaller fragments. Hu et al. (2020) compared the molar ratios of $Mg^{2+}: NH_4^+ : PO_4^{3-}$ (1.5:1:1.5) against pH and reported that ammonia removal increased with increasing pH from 8-9.5 with a pH of 9.5 yielding 86 % ammonia removal, where the pH is accountable for the dissemination of species such as Mg^{2+}, $MgOH^+$, $MgPO_4^-$, H_3PO_4, $H_2PO_4^-$, HPO_4^{2-}, PO_4^{3-}, NH_3, and NH_4^+ in the solution. Increasing the pH above 9.5 reduced the percentage of ammonia removed due to the conversion of ammonium to ammonia at higher temperatures impacting on the overall purity of the struvite.

2.4.4.2.2 Effect of temperature

Temperature influences the rate of a chemical reaction and its equilibrium state. Kabdaşlı and Tunay (2018) stated that struvite solubility was directly proportional to temperature until a maximum temperature was reached. Struvite crystallisation is known to be a fast and spontaneous reaction. **Equation 2.14** represents the Gibbs free energy and SI for thermodynamic driving force:

$$\triangle G = -(2.303RT/n) * SI \quad (2.14)$$

R is the gas constant T, the temperature, and the number of ions presents within the crystal product formed. Equilibrium in the solution occurs if SI = 0, which then also entails that $\Delta G = 0$. if SI<0, Gibb's energy will be greater than zero ($\Delta G>0$), which represents a solution that is under saturation, meaning that no crystallisation will happen. Furthermore, in a situation when SI>0, the Gibbs energy is then less than zero ($\triangle G<0$), and crystallisation occurs naturally due to the supersaturation conditions present. Ronteltap et al. (2010) reported in the study that the particle size of the struvite increased when the supersaturation condition was reduced. An increase in temperature from 5˚C to 30̊ C led to a reduction in particle size. They concluded that optimal conditions were at a pH of 9 and temperature of 20°C, which resulted in a particle size of 95 µm on an equimolar ratio of $Mg^{2+}: NH_4^+: PO_4^+$ concentrations. The study found that lower temperatures decreased the solubility and increased the supersaturation conditions leading to smaller struvite particle sizes. Furthermore, a temperature approaching 50̊ C leads to the decomposition of struvite, leading to a breakdown of the precipitate (Kabdaşlı and Tunay, 2018).

2.4.4.2.3 Effect of mixing speed and time

Many researchers have conducted struvite precipitation at different mixing rates and hydraulic retention times, achieving satisfactory ammonia removal rates. Mavhungu et al. (2019) achieved 75% ammonia removal from wastewater at a mixing speed rate of 500 rpm using calcined magnesite as a magnesium source. In the study, the contents were allowed to mix for 30 minutes. Ronteltap et al. (2010) compared using a magnetic agitator and two-blade propellers running at a speed of 300 rpm. In the study, the two-blade propeller formed a more extensive particle (92 µm) compared to 45 µm achieved using a magnetic stirrer. The study concluded that the lower turbulence resulted in a slower dissipation of particles, leading to a higher saturation, favourable to nucleation, as compared to particle growth. Wen et al. (2018) evaluated the mixing speed for efficient struvite formation. The authors observed that when the mixing speed was increased from 60 to 180 rpm, the removal rate of phosphate removal increased from 82 % to 93 %.

Furthermore, the authors also reported a reduction in phosphate removal when the mixing speed was increased from 180 - 300 rpm to 300 rpm yielding 67% removal of phosphate. The study has shown that high mixing speeds limit crystal growth leading to crystal breakage. Li et al. (2012) evaluated struvite formation at mixing times ranging from 5 to 60 minutes under an equimolar ratio of $\mathrm{Mg^{2+}}: \mathrm{NH_4^+} : \mathrm{PO_4^{3-}}$ (1:1:1) at 100 rpm mixing speed and a pH of 9. The studies showed that a crystal size of 20 µm was achieved after 10 minutes and the size increased to 75 µm after 60 minutes of stirring.

2.4.4.2.4 Effect of dosage

Drinking water treatment plants (DWTP) use aluminium and ferric-based coagulants to destabilise charges and enable the formation of larger flocs. Al_3^+ and Fe_3^+ ions in solution can inhibit the formation of struvite due to their competition with $\mathrm{Mg^{2+}}$ ions for PO_4^{3-} and the valence and isomorphic capacity could limit the capability of Mg due to the valence difference (Huang et al., 2014, Yan and Shih, 2016). However, a study by Huang et al. (2014) indicated that at a high pH range, the predominant aluminium species was aluminium hydroxide, which cannot interact with the available phosphates, leading to 77% ammonia removal when the pH was higher. $\mathrm{Al^{3+}}$ ions can only interfere when the pH is low by forming aluminium phosphate ($AlPO_4$). The process involves the adsorption of $\mathrm{Al^{3+}}$ ions, followed by incorporation of soluble phosphate by suspended colloids, leading to the formation of aluminium phosphate as presented in **Equation 2.15** (Huang et al., 2014)

$$\mathrm{Al^{3+}} + \mathrm{PO_4^{3-}} \leftrightarrow \mathrm{AlPO_4} \qquad (2.15)$$

Yan and Shih (2016) conducted a study on the impact of ferric ions on struvite formation and concluded that iron inhibits struvite production more on limited dosages than calcium ions. Ferric ions inhibit struvite in the same manner as aluminium ions. Equation 2.16 depicts the adsorption of phosphate ions by ferric ions:

$$Fe^{3+} + PO_4^{3-} \rightarrow FePO_4 \quad (2.16)$$

The structure of struvite has resulted in blockages of pipes in wastewater treatment plants (WWTP), leading to increased maintenance costs if not formed in a centralised place (Yan and Shih, 2016). A study conducted by Shu et al. (2019) compared different precipitation methods, namely carbonate, sulphide, hydroxide and struvite precipitation, on the efficiency of manganese and ammonia removal from electrolytic manganese residue leachate. It was concluded that struvite precipitation was excellent in removing both ammonia and manganese with a removal efficiency of 98 % and 99.9 %, respectively, at a P: N ratio of 1.1:1, with other precipitation methods excellent with manganese removal but only averaging 28 % ammonia removal.

2.4.4.2.5 Effects of co-existing ions

The impact of calcium and sodium on magnesium potassium phosphate (MPP) and MAP struvite was evaluated by Hu et al. (2020). The study used produced water from oil and gas industries with high calcium and sodium ion concentrations. When the sodium concentration was increased, commencing from 0 to 46 g/L, the ammonia removal yield decreased from 92 % to 78 %. The sodium competes with NH_4^+ leading to the formation of magnesium sodium phosphate (MSP, $MgNaPO_4 \cdot 7H_2O$), inhibiting the formation of magnesium ammonia phosphate (MAP). The presence of calcium in the solution, with an initial concentration of calcium (4779 mg/L), yielded only 0.3 – 6 % ammonia removal from the initial concentration. This can be attributed to calcium ions initially reacting with phosphate forming calcium phosphate ($Ca_3(PO_4)_2$) and hydroxyapatite ($Ca_5(PO_4)_3(OH)$) (Hu et al., 2020). The lower solubility constant (K_{sp}) of calcium phosphate (2.0 $\times 10^{-29}$) compared to that of MAP (2.5 $\times 10^{-13}$), which means that the reaction will favour the formation of calcium phosphate precipitation compared to that of MAP, as depicted by **Equations 2.17-2.19** below:

$$Mg^{2+} + Na^{+} + H_nPO_4^{n-3} + 7H_2O \rightarrow MgNaPO_4.7H_2O \downarrow + nH^{+} \quad (2.17)$$

$$Ca^{+} + 3HPO_4^{2-} + H_2O \rightarrow Ca_5(PO_4)_3(OH) \downarrow + 4H^{+} \quad (2.18)$$

$$3Ca^{2+} + 2HPO_4^{2-} \rightarrow Ca_3(PO_4)_2 \downarrow + 2H^{+} \quad (2.19)$$

2.4.5 Membrane Filtration

Membrane filtration has become one of the prominent technologies incorporated in drinking water treatment to remove ammonia. The main challenge associated with the technology is the fouling of the membrane caused by the natural organic matter (NOM) and microbial load when used in large-scale industrial applications. Membrane filtration technology depends on factors such as initial concentration, type of membrane and driving force to remove the contaminants (Cheremisinoff, 2002a). Membranes are made up of ultra-thin layers of partially penetrable materials which remove substances when energy or a force is applied. Membrane treatment, which can be applied in water and wastewater treatment plants, is electro dialysis, microfiltration (MF), ultrafiltration (UF), nanofiltration (NF), and reverse osmosis (RO). A membrane provides a boundary between the different phases (either solid, liquid or gas phase), trapping the contaminants and allowing for clean effluent to pass through them and achieving separation (Adam et al., 2019). In addition, a membrane can be permeable, semi-permeable, unbiased, or charged and can serve as a selective barricade toward the separating solutions. Membrane technologies depend on the passageway of solutes or solvents via a tinny, permeable polymeric film. Microfiltration (MF), ultrafiltration (UF) and nanofiltration (NF) vary due to size and the operating pressure, but all use a sieving mechanism for separation. The different separation ranges of membranes are as follows: 0.1 to 1 µm (MF), 0.005 to 0.1 µm (UF), 0.001 to 0.005 µm (NF), and 0.0001 to 0.001 µm (RO) (Cheremisinoff, 2002a). Membrane filtration technologies effectively remove protozoa, microbial load, particulates, suspended solids, different bacteria and algal concentrations and sediments. Ultra-filtration membranes are more efficient in removing minor colloidal particles and viruses. On the other hand, nanofiltration membrane targets dissolved organic matter. Reverse osmosis integrates a non-porous membrane and is proficient in separating dissolved solids from water molecules in aqueous solutions, which is achieved by membranes made of special polymers capable of permitting water molecules to pass through and simultaneously trapping the other molecules constituted in the water. This is achieved by applying osmotic pressure through the membrane to achieve separation. (Abu Hasan et al., 2014). Both membrane filtration and ultra-filtration have been reported to achieve outstanding removal capacities when dealing with sand, silt, clays, *Giardia lamblia* and *Cryptosporidium* cysts, algae, and some bacterial species. On the other hand, nanofiltration can completely separate the cysts, bacteria, viruses, humic materials, and alkalinity in water. Electro-dialysis (ED) uses ion-exchange membranes for transporting ions from one solution to another when an electrical charge is present. This technology has been applied in industrial waste (Hube et al., 2020). The use of membrane technologies in water treatment has disadvantages which are the high capital and electrical costs, coupled with membranes being prone to fouling, leading to lower filtration rates over time (Cheremisinoff, 2002a). Adam et al. (2019) reported in a study that the fabrication of a mixed-matrix membrane from natural zeolite incorporated into the *PSU* polymer matrix demonstrated a high capacity and high stability towards the removal of ammonia in wastewater yielding 90 % removal from aquaculture water.

2.4.6 Adsorption

Adsorption involves a process where constituents arising from a gas concoction or aqueous solution attach to a solid or liquid surface (Cheremisinoff, 2002b). In this process, physicochemical methods are employed to remove pollutants in aqueous media. The method is a surface and charge-driven phenomenon involving the removal of contaminants/pollutants through physical and chemical bonds, including weak electrostatic forces. A positively charged surface will attract negatively charged substances from the water or vice versa. Different mechanisms such as ion exchange, isomorphous substitutions, pore diffusion, precipitation, and surface binding play a significant role in contaminants attenuation. Different kinds of natural and synthesized adsorbents can be used for contaminant removal and the materials include clays, metals, activated carbon (granular and powdered), and their composites.

The adsorption process depends on the surface area, with a higher surface area yielding a higher adsorption capacity and a smaller surface area resulting in limited adsorption capacity, leading to low adsorption and removal. Natural zeolites are more suitable for ammonia adsorption due to their greater ion exchange potential (Adam et al., 2019). Natural zeolite absorbents include clinoptilolite and mordenite,, which are efficient due to the vast surface areas available to absorb ammonia onto the surface (Karri et al., 2018). Zeolites are defined as crystal-like microporous metal silicates (mainly aluminium silicates) made up of a negatively charged framework with weakly bound transferrable cations (Vocciante et al., 2018). A raw clinoptilolite normally comprises an extensive potassium concentration, making it difficult to exchange with ammonia due to its more significant attraction. Pre-treatment with concentrated sodium or calcium salt is advised before a solution containing ammonia is used. (Alshameri et al., 2014, Bock, 2016, Vocciante et al., 2018). Natural zeolites are cheap, safe, and only release non-toxic transferrable cations (Guaya et al., 2015).

The studies have reported adsorption results, with preference given to natural zeolites with an ammonia uptake capacity ranging from 2 mg/g to 30.6 mg/g (Adam et al., 2019). Huang et al. (2018) reported on different types of adsorbents and found that modified biochar has the highest adsorptive capacity (518.9 mg/g) of carbon-based adsorbents. The same study reported that Na-modified zeolite, prepared with an anion exchange resin using kunama and akadama clay, had 75 mg/g adsorptive capacity and yielded 95 % ammonia removal from municipal wastewater, being the best performing synthetic zeolite. Furthermore, the best polymeric ion exchanger was reported to be K - U – 2 – 8 synthetic zeolite with an adsorptive capability of 74.7 mg/g while Turkish sepiolite was the best natural zeolite with an adsorptive capacity of 49 mg/g.

With surface water quality deteriorating due to enrichment with ammonia, many researchers (Huang et al., 2018, Wongcharee et al., 2020) have started with laboratory scale investigations to introduce adsorption technologies in drinking water treatment plants (DWTP). The authors optimised an absorbent with a polymer using a jar test method to remove ammonia, natural organic matter and disinfection by-products were used in the study. Powder-activated carbon (PAC) has a low ammonia adsorptive capacity. As such, Huang et al. (2018) modified a nanocomposite adsorbent termed Advanced Cellular Zeolite (ACZ), which has the combined capacity of zeolite and powder activated carbon (PAC) in a solitary product, resulting in 76% ammonia removal, 90% dissolved oxygen carbon (DOC*)* removal and 95% reduction in trihalomethane formation potential within 20 min when used concurrently with a coagulant. Xue et al. (2018) investigated the use of powder-activated carbon (PAC) in conjunction with various zeolites such as the Bear River zeolite, mordenite zeolite and zeolite-y to remove ammonia and N-nitrosamine precursors in drinking water treatment plants. The study reported that mordenite zeolite yielded higher ammonia removal rates compared to other zeolites when used in conjunction with coagulation. Ammonia removal was at 67%. Furthermore, this relationship reduced the disinfection by-products dimethylammonium iodide (DMAI) and dimethylaminopyridine (DMAP) by 73% and 40% respectively. In both the studies conducted by Xue et al. (2018) and Wongcharee et al. (2020), the results showed that if a zeolite was used, more ammonia removal was obtained due to the selective ammonia capacity of the media, and the adsorbent PAC was more efficient with reduced concentration of disinfection by-products. Activated carbon has a larger surface area, which promotes the adsorption of organic matter (Cheremisinoff, 2002b). Vocciante et al. (2018) conducted a study which measured the efficiency of sodium (Na) prepared clinoptilolite (Na/HUE) in removing ammonia from groundwater in Italy. The groundwater had a massive presence of competing ions, which exceeded the NH_4^+ ion concentration. In the study, the prepared clinoptilolite had an initial ammonia adsorptive capacity of 24 mg/g. However, the competing ions Na^+ (944 mg/L), Ca^{2+} (177 mg/L), K^+ (41 mg/L) and Mg^{2+} (89 mg/L) reduced the ammonia absorptive capacity to 4 mg/g. Furthermore, a synthetic solution with K^+ (40 mg/L) and NH_4^+ (17 mg/L) resulted in an ammonia adsorptive capacity of 10 mg/g. The study proved that clinoptilolite has a higher affinity to potassium (K^+), as is also reported by other researchers (Guaya et al., 2015) and care must be taken when selecting the ion exchange substance. These findings are supported by a study conducted by Guaya et al. (2015) where the aluminium hydroxide modified zeolite capacity was reduced from 30 mg/g to 26 mg/g due to presence of Na^{+}, Ca^{2+}, K^{+} and Mg^{2+} ions in the synthetic solution. Vocciante et al. (2018) proposed the use of a more expensive synthetic zeolite that is more selective of ammonia to avoid low quality water production, frequent regeneration, and high production of brine when using the natural zeolite with the co-presence of competing ions, particularly potassium.

Factors affecting the adsorption of ammonia using zeolite include pH, temperature, stirring time, initial concentration of ammonia ions and adsorbent used (Arslan and Veli, 2012, Alshameri et al., 2014). Many researchers have reported on different optimum pH values for ammonia adsorption (Arslan and Veli, 2012, Alshameri et al., 2014). Arslan and Veli (2012) conducted a study using Zeolite 13 times to remove ammonia and achieved 90% ammonia removal at a pH ranging from 6 to 8 and selected pH as optimum. In a study conducted by Alshameri et al. (2014), the highest ammonia removal was achieved at a pH of 8. A review conducted by Bock (2016) reported that an optimum pH of 6 is suitable for ammonia removal using adsorption. Higher pH is reported to promote the formation of $NH_{3,}$ which is not reactive in the ion exchange process. Equilibrium concentrations for ammonia in solution are presented in **Equation 2.20**:

$$\mathrm{NH_4^+} \leftrightarrow \mathrm{NH_3} + \mathrm{H^+}\ @\ \mathrm{pH\ of\ 9.25} \qquad (2.20)$$

From **Equation 2.20**, it can be observed that increasing the pH beyond 9.25 shifts the equilibrium towards the right, promoting the formation of unionised ammonia. In both the studies by Alshameri et al. (2014) and Arslan and Veli (2012), the results showed that the adsorbent dosage was directly proportional to the ammonia removal. Increasing the adsorbent dosage increased the ammonia removal yield because of the increase in the surface area. **Table 2.2** summarises the ammonia adsorptive capacity from different natural and modified adsorbents.

Table 2.2: Summary of different natural and modified adsorbents and their ammonia adsorptive capacity in mg/g of the adsorbent.

Adsorbent Name	Initial concentration	Absorbent Dosage (g/L)	Adsorptive Capacity (mg/g)	Percentage Removal (%)	References
Hydrated Aluminium modified Slovakian natural zeolite	25	0.5	30	95	(Guaya et al., 2015)
Yemen clinoptilolite (NZ)	80	1.8	8.29	92	(Alshameri et al., 2014)
Na Modified Yemen clinoptilolite (*SNZ*)	80	1.2	11.8	99	(Alshameri et al., 2014)
Mordenite zeolite	1.19	1	-	67	(Xue et al., 2018)
Na/HUE Clinoptilolite	17	5	24	75	(Vocciante et al., 2018)
Zeolite *X13*	25	0.5	4.8	90	(Arslan and Veli, 2012)
Ph 10 treated Bentonite clay	200	0.5	6.9	64	(Zaini et al., 2021)
Mg-doped biochar/bentonite composite	168.1	7.5	39.9	35.6	(Xi et al., 2022)
Ph 10 treated kaolin	200	0.5	1.087	13	(Zaini et al., 2021)

Aluminium tanned modified bentonite composite), (Al-Ten-bent)	168.8	1	5.85	71	(Cheng et al., 2019)
Rice husk Charcoal	20	2.67	6.6	96.8	(Joseph et al., 2021)
Orange peel bisorbents	1	5	40.84	100	(Dey et al., 2021)

As indicated in **Table 2.2**, the most used natural zeolites are modified with sodium or calcium concentrated salt before use to increase the adsorptive capacity of the zeolite media. However, other adsorbents such as orange peels ((Dey et al., 2021), rice husk charcoal (Joseph et al., 2021), treated with bentonite clay (Cheng et al., 2019, Zaini et al., 2021, Xi et al., 2022) has been used successfully in varying wastewaters yielding desirable ammonia removal rates. Dey et al. (2021) used natural adsorbents and orange peels in contaminated water, achieving a 100% ammonia removal rate. In their study, contaminated water was in contact with orange peels for 90 minutes at mixing rates of 90 rpm, and the adsorbent dosage was 5g/L. Cheng et al. (2019) modified bentonite with aluminium cross-linking and double tannin modification, forming an adsorbent which yielded 71% ammonia removal from wastewater with low temperature. Adsorption technology in drinking water is extensively researched, with success rates well documented. Joseph et al. (2021) used agricultural waste material, rice husk charcoal, as an adsorbent and removed 96.8% ammonia from drinking water sources from an initial concentration of 20 mg/L.

From **Table 2.2**, optimal adsorbent dosage ranges from 500 mg/L upwards depending on raw water quality and the type of adsorbent used for efficient removal of ammonia, even at low concentrations. Such dosages increase the operational cost and production of sludge. Furthermore, the addition of calcium or sodium hydroxide to stabilise the water will impact the adsorptive capacity of the absorbent. The presence of competing ions in the water will lead to a high volume of brim production during the regeneration of zeolite, and this will also reduce the amount of freshwater produced (Vocciante et al., 2018). Regeneration is reported to increase water losses by approximately 20 – 30% of the freshwater used during the regeneration process. The drinking water system industry norm allows for only 5% water losses for a system to be productive. As such, this technology is not viable in the drinking water system.

2.4.7 Ion Exchange

Ion-exchange treatment technologies allow for swapping comparable interchangeable ions between the primary aqueous medium and ions within the ion exchanger (Ding and Sartaj, 2016). The process removes targeted ions in a solution using reversible reactions, which allows for the replacement of dissolved ions with similar charges that are constituted in the ion exchange media while the ions to be removed attach to the ion exchanger (Karri et al., 2018). This process is commonly applied as a water softening technique and has been used to remove calcium and magnesium in hard water. Types of ion exchangers include natural zeolite or synthetically produced organic resins. Natural ion exchangers normally come from the minerals that are crystalline, hydrated, aluminosilicate of alkali, or alkaline earth ions such as

Na, K, Ca and Mg (Adam et al., 2019). Due to the complex nature of many aqueous media, synthetic organic resins can be prepared for particular applications (Cheremisinoff, 2002b). Additionally, advantages that come with synthetic ion exchange include a faster exchange rate and longevity coupled with a higher capacity to exchange ions. This has led to researchers replacing natural zeolite with synthetic ion exchangers (Ding and Sartaj, 2016).

Many researchers have reported natural zeolite, synthetic zeolite and strong acid cation resin as being the most suitable for ammonia removal in aqueous media (Owusu-Agyeman et al., 2015, Adam et al., 2019). Owusu-Agyeman et al. (2015) argued that a strong acid ion exchange resin was the most suitable for ammonia removal due to the highest ammonia exchange capacity compared to other ion exchangers like natural or synthetic zeolites. Ion exchange resins are structured with a high molecular polyelectrolyte which can exchange their ions with similarly charged ions present in the aqueous solution. Resins are structured with a distinctive number of spots to maximise the volume of ions that can be exchanged within a resin.

The technology has been successfully applied in petroleum, chemical industries, and wastewater treatment systems. Benefits of an ion exchange technology include the ability to regenerate the ion exchange resins, which enables the re-use of the resins without affecting the ammonia removal efficiency. Acid and base solutions are used to regenerate cation and anion resins, respectively (Cheremisinoff, 2002b). The ion exchange technology has effectively removed ammonia in a wide temperature range (Karri et al. (2018). They reported that temperature ranges from 0ºC to 35ºC had a negligible effect on the removal of ammonia in both low and high concentrated water solutions. Ion exchange technology removes ammonia by replacing ammonium ion with a sodium ion, as depicted by **Equation 2.21** (Owusu-Agyeman et al., 2015):

$$R\text{-}Na + NH_4^+ \leftrightarrow R\text{-}NH_4 + Na^+ \quad (2.21)$$

As seen from Equation 2.21, ion exchange typically increases sodium concentration in the aqueous solution. Researchers have successfully removed ammonia in an aqueous solution using the ion exchange technique. Ammonia can be in both ionised (NH_4^+) and unionised (NH_3) forms. And ion exchange removes unionised ammonia in an aqueous solution (Abu Hasan et al., 2014) and as such, it is more efficient at a low pH. Ding and Sartaj (2016) evaluated the impact of pH, resin dosage and temperature to remove ammonia using an Amberlite IR120 H industrial-grade strong acid cation exchanger and achieved 84 % ammonia removal at a pH of 6. Çelik et al. (2001) compared the ion exchange capacity of different types of clay and minerals in fixed and fluidised beds. In the study, clinoptilolite was removed between 95% - 98% ammonia in fixed bed columns and between 70% - 85% ammonia in fluidized bed columns.

The most commonly used zeolite is clinoptilolite and has an ion selectivity as depicted in **Equation 2.22** (Bock, 2016):

$$K^{+} > NH4^{+} > Na^{+} > Ca^{2+} > Fe^{2+} > Al^{2+} > Mg^{2+} > Li^{+} \qquad (2.22)$$

Based on the ion's selectivity of natural zeolite, evaluating the potassium concentration in the aqueous solution is imperative because it might impact the ammonia removal efficiency. The presence of high valence ions in water limits this technology to smaller applications. Furthermore, running costs are high due to the need for regeneration of the resins, being important to evaluate the economic benefits when selecting ion exchange resins. Furthermore, ion exchange is efficient at low pH. This will require the addition of an acid to lower the pH of the influent to create optimal conditions for ammonia removal and a base to increase the pH of the effluent to minimise the risk of effluent corroding the distribution line.

2.4.8 Advanced Oxidation Process

2.4.8.1 Electrochemical Oxidation Process

The electrochemical advanced oxidation process (EAOP*)* is another encouraging technology that can remove ammonia in aqueous solutions. The advantage of the EAOP technology is the ability to remove ammonia without adding chemicals, and there is no sludge production. (Rajasekhar et al., 2020). The electrochemical oxidation process introduces an electrical current in water containing ammonia. The technology's success depends on the electrode's composition, current density, hydrogen potential and the concentration of ions in the solution (Bock, 2016).

In this technology, ammonia can be broken down in two ways, direct oxidation in an alkaline solution which converts ammonia into nitrogen and indirect oxidation, which involves active hydroxyl ion radicals (OH^-) and hypochlorite ions in an acidic solution (Yao et al., 2020). Direct anodic oxidation encompasses the adsorption of ammonia into the anode surface and decomposing of the ammonia into nitrogen gas. Since it decomposes ammonia, the technology will require adjustment of the pH to levels that exceed equilibrium pH for NH_4^+/NH_3 to promote the formation of ammonia (NH_3) since it is impossible to oxidise ammonium (NH_4^+) directly at the anode. Indirect oxidation uses active chlorine generated at the anode during electrolysis to oxidise the ammonia to nitrogen gas (Zhang et al., 2018). Zöllig et al. (2015) argued that reaction rates of the EOAP are low and efficient electrodes like platinum are costly, limiting the application of the methodology in the industry. A study reviewed by Zhang et al.

(2018) reported that indirect oxidation was faster and more efficient and will save operational costs, compared to direct oxidation, on the condition that the chloride ion in the wastewater exceeds a concentration of 300 mg/L.

Furthermore, it was reported that the availability of chloride in water encourages the in-situ generation of active chlorine at the anode, which oxidises ammonia to nitrogen gas. Many researchers have reported on the indirect electrochemical ammonia oxidation process (EAOP) using the same mechanism as breakpoint chlorination to break down ammonia. Breakpoint chlorination involves ammonia reacting with chlorine species to form monochloramine and dichloramine until nitrogen gas is released and free residual chlorine starts appearing (Adam et al., 2019). Bock (2016) disputed the breakpoint chlorination after reviewing results from previous studies and reported that the breakdown of ammonia to nitrogen gas ensues during the initial stages of the electrolysis process prior to the attainment of the active chlorine / ammonia mole ratio of 1.5 in electrochemical indirect oxidation of ammonia.

The disadvantage associated with electrochemical oxidation is the possibility of the formation of by-products nitrate, nitrite and chlorate (Zhang et al., 2018), which can cause harm to consumers. Studies by Rajasekhar et al. (2020) and Yao et al. (2020) supported the other studies that showed the formation of by-products. Rajasekhar et al. (2020) investigated ammonia removal efficiency using Ti/Sb-SnO_2/PbO_2 as anode and stainless steel as the cathode on separate wastewater sources and achieved almost 100% ammonia decomposition from the separate wastewaters which had an initial ammonia concentration ranging between 7 and 68 mg/L.. On both occasions, however, the nitrate concentration increased with a decrease in ammonia levels. Yao et al. (2020) compared the efficiency of ammonia removal by electrochemical oxidation in a non-chlorinated synthetic solution and wastewater using a stable titanium lead oxide (Ti/PbO_2) electrode at different pH ranges. In their study, indirect oxidation at pH of 3 and 5, using the current density of 15 mA/cm^2, 95% ammonia was removed as N_2 gas, and 5% was converted to nitrate. Furthermore, ammonia was removed in alkaline conditions (pH 9 and 12). However, only 75% was removed as nitrogen gas, while the remaining ammonia was converted to nitrate and nitrite.

2.4.8.2 Photocatalytic Oxidation of Ammonia

Photocatalyst oxidation is a technology that uses a nano-crystalline anatase form of titanium oxide (TiO_2) to oxidise organic pollutants prompted by light availability. The titanium oxide nanocrystalline anatase has low toxicity and provides a wide band gap equivalent to 3.2 *e*V providing excellent stability when used as a semiconductor (Sirés et al., 2014) Furthermore the material is of low cost, with excellent photochemical stability and also has the benefit of preventing photo corrosion (Sirés et al., 2014, Wang et al., 2014b). The potential to modify TiO_2 with nano-particles such as Au (0), Pb (0), Pt (0) and Ag (0) increases the trapping ability of the metal nanoparticles on the TiO_2, leading to accelerated and efficient separation, the effective parting of the e^- - H^+ couples in the presence of lighting, resulting in higher ammonia decomposition percentages (Ren et al., 2020). Decomposition of ammonia occurs when titanium oxide nanoparticles are exposed to ultraviolet (UV) photons which can provide an energy equivalent to λ < 380 nm allowing for electrons to relocate from the valence band to the conduction band (e^-CB). This will create a positively charged hole (H^+VB) which promotes the occurrence of redox reactions to oxidise ammonia or promote the oxidation of chloride to produce active chlorine, which can oxidise the ammonia (Bock, 2016). A positively charged hole forms when the negative and positively charged electron fails to recombine after separation.

In photocatalytic oxidation of ammonia, the main oxidant is hydroxide radicals (OH) and is formed when, after oxidation of water and breakdown of the produced H_2O_2 in the photocatalytic (Ren et al., 2020) system occurs, as depicted in **Equation 2.23**:

$$\mathrm{H_2O_2 + hv(Ag_2O/P25) \rightarrow\ 2{\cdot}OH} \qquad (2.23)$$

Both the positively generated hole and hydroxide radicals resulting from the reaction amongst the light-produced vacancy and adsorbed water can oxidise the natural organics.

Photocatalytic breakdown of ammonia is influenced by air concentration, pH, photo catalyst type, UV radiation intensity and the initial concentration of ammonia (Altomare and Selli, 2013, Bock, 2016; Yao et al., 2020). These factors are responsible for the final product after oxidation being either nitrogen gas (N_2) or nitrate (NO_3^-) and the overall breakdown of the initial ammonia concentration percentage decomposition (Ren et al., 2020). Increasing the photocatalyst concentration favours the decomposition of ammonia to nitrite and nitrate, as reported in studies conducted by Yao et al. (2020) and Altomare and Selli (2013). In a study conducted by Ren et al. (2020), the photocatalyst was increased from 0.2 to 1 g/L leading to an increase in ammonia decomposition from 39% to 84%. However, the selectivity toward N_2 production gas formation reduced from 14% to 0.1% using Degussa Ag_20/P25TiO_2, while ammonia was primarily oxidised to nitrite and nitrate. Altomare and Selli (2013) discovered that, when the concentration is lower than 1 g/L, incomplete oxidation of ammonia to nitrite/nitrate/nitrogen gas occurs while, on the other hand, a photocatalyst concentration from 1 g/L and above led to total oxidation of ammonia to nitrate. Yao et al. (2020) assessed the impact of pH on the photocatalytic oxidation of ammonia using a modified semiconductor Cu-H_3PW12O40/TiO_2 in the presence of UV light. Their studies found that increasing the pH to 11 reduced the removal of ammonia to 82% with 90% of the decomposed ammonia converted to nitrogen gas.

Additionally, Yao et al. (2020) concluded that a high pH promotes adsorption of ammonia on the surface of the catalyst forfeiting photo produced holes and partaking in photocatalytic reaction regularly. In addition, alkaline solutions produced additional radicals (OH^-), which play an active role in the photo catalysis process. Commonly tested crystal structures are rutile (Bock, 2016). The photo catalytic oxidation can be used at high ammonia concentration as depicted in **Table 2.3**.

Table 2.3: Comparison of photocatalysts and their efficiency in the decomposition of ammonia.

Photo Catalyst	Initial ammonia conc mg/L)	Experimental setup	Percentage Removal Rate **(%)**	References
Cu- $H_3PW12O40/TiO_2$	300	Dosage:1.5g/L, pH:11, hg lamp (125W), 7 hrs	82	(Yao et al., 2020)
Ag_2O/TiO_2 (P25)	100	Dosage: 1 g/L, pH 11.8, Hg lap (300W). 0.368hrs	84	(Ren et al., 2020)
TiO_2-xNx/PdO	25	Dosage:0.4 g/L, pH 10, Xe lamp (300W), 2 hrs	90	(Sun et al., 2015)
TiO_2-CuO/HSC	100	Dosage:0.6 g/L, pH 8, Xe lamp irradiation (300W), 2 hrs	61	(Peng et al., 2019)
P25 TiO2	100	Dosage: 0.1 g/L, pH 10.5, Hg lamp irradiation, 25W	88	(Altomare and Selli, 2013).
RuO_2–IrO_2/Ti	5	0.05g/L, Xenon light irradiation, Wavelength 300 nm	100	(Du et al., 2022)
AC/TiO_2/CeO_2 composite	568	Dosage: 0.5g/L, UV light irradiation, 25W	63.85	(Dalanta and Kusworo, 2022)
TiO_2/perlite catalyst	170	Dosage: 11.7g/L, pH 11, UV light irradiation, 125W	64.3	(Shavisi et al., 2014)
Photocatalytic composite $Ag_{(NP)}$-(g-C_3N_4)/CNT	2	Dosage: 0.5g/L, pH 11, lamp radiation, 180W, 6hrs	88.2	(Sun et al., 2021)

CuO/ZnO	85	Dosage: 5 wt% CuO/ZnO platter, Ph 10.5, Hg Lamp irradiation, 125 W, 3 hrs	77.2	(Shavisi et al., 2016)
Cu/TiO_2	500	pH 10, Xe lamp irradiation, Wavelength 300 nm	-	(Feng et al., 2021)
g-C_3N_4/rGO/TiO_2	50	Dosage: 1g/L, pH 9.5, Xe lamp irradiation, 500W	93.90	(Li et al., 2022)
Atomic single layer graphitic-C_3N_4 (SL g-C_3N_4)	1.5	Xe lamp irradiation (195 Mw*cm^{-2})	80	(Wang et al., 2014a)

Table 2.3 shows that most modified TiO_2 catalysts can achieve higher ammonia decomposition in alkaline solutions (high pH). Li et al. (2022) prepared and employed modified photocatalyst g-C_3N_4/rGO/TiO_2 at a dosage of 1g/L in alkaline conditions (pH 9.5) to remove 93.90% ammonia raw water. While Dalanta and Kusworo (2022) removed 63.85% ammonia from wastewater using composite photocatalyst AC/TiO_2/CeO_2 at a pH of 10.5. A lower pH reduces the decomposition efficiency (Peng et al., 2019). This technology is dependent on the catalyst. Altomare and Selli (2013) investigated the impact of UV without a catalyst. In the study, there was no decomposition of ammonia by irradiation of ammonia solution even with UV light ($1.5 * 10^{-6}$ Einstein $s^{-1}L^{-1}$). Most of the efficient catalyst are titanium based, however Sun et al. (2021) synthesized a photocatalytic composite (Ag(NP)-(g-C3N4)/CNT) and achieved 88.2% aqueous ammonia removal in water. Shavisi et al. (2016) employed photocatalyst composite CuO/ZnO and removed 77.2% ammonia from the solution. The success of photocatalytic oxidation technology in laboratory scale experiments on varying initial ammonia concentrations and types of wastewater has been vastly investigated **(Table 2.3).** Dependence of the photocatalytic oxidation technology on pH, catalyst and energy source will increase operational costs, especially in large-scale treatment systems like drinking water treatment plants.

2.4.8.3 Photo-electrocatalytic Oxidation

The photo-electrocatalytic oxidation method depends on the collaboration between electrochemistry and photocatalysis to increase the efficacy of wastewater remediation. This technology relies on an electrically charged, TiO_2 coated photo anode catalyst to decompose ammonia. In this method, a metallic electrode, which can conduct electricity, is coated using an extremely small film of titanium constructed catalyst, which allows stimulation of the electron group of the titania into the transmission group resulting in the formation of reactive electrons and holes that oxidise ammonia when enough light energy is provided. The rate at which ammonia is oxidised depends on the pH, chloride salts, applied voltage and activity of the photocatalyst (Kropp et al., 2009). A voltage preference can be applied in the middle of the photo-anode and cathode, which has the potential to reduce the rate at which the generated electrons and positively charged hole can recombine when the photo-anode is treated with UV light. The technology prefers the use of UV lamps like UVA (λ = 315 – 400 nm), UVB (λ = 285 – 315 nm), and UVC (λ < 285 nm) lights which can provide efficient power for the treatment of the solutions (Sirés et al., 2014).

Additionally, sunlight (< 280 nm) can be considered an energy source to minimise operational costs. The addition of voltage is known to delay the rate at which charges recombine, promoting higher removal efficiencies in comparison with photocatalytic oxidation on its own

(Selcuk and Anderson, 2005). Rutile and anatase structures are based on the heated temperature of the titania. Titania heated at 500 ^oC produces a rutile structure, and one heated at 300 ^oC forms an anatase structure. Kropp et al. (2009) reported that rutile structures provide a greater catalytic potential than anatase structures.

PEC technology uses electrolytic cells in either agitated chambers or flows reactors, allowing UV light to pass through the aqueous media, reaching the anode with minimal radiation disturbance. (Sirés et al., 2014). Photo anode types are based on titanium oxide coatings, $ZnOBi_2MoO_6$-BDD, with WO3 and BiO_x–TiO_2 also being used (Sirés et al., 2014). The advantage associated with this technology is the high selectivity in transforming ammonia into nitrogen gas (N_2). Kropp et al. (2009) reported that PEC operational philosophy involved the conversion of the available chloride ions to chlorine and hypochlorous acid. The chlorine or hypochlorous acid is then the breakdown of aqueous ammonia into nitrogen gas. Ji et al. (2017) investigated the use of solar-driven photo electrocatalytic chlorine radical ions *(*PEC) by using an observable well-lit WO_3 array plate in an aqueous ammonia solution containing chloride ions. Photo holes below the radiance promoted the conversion of chlorine ions Cl^- to chloride radicals, which were able to transform ammonia to 79 % nitrogen (N_2) and 19 % to Nitrite at a pH of 4. The conversion was compared favourably with that of breakpoint chlorination. Ji et al. (2017) also compared it to the PEC to breakpoint chlorination. They concluded that PEC was a more efficient and economical means to degrade ammonia due to its higher removal efficiency and low operational cost as it does not require the addition of chlorine. Furthermore, the available chlorine will promote the disinfection of microorganisms and manganese oxidation.

Xiao et al. (2016) prepared a titanium oxide (TiO_2) nanotube (TiNT) anodised in a fluorinated organic solution and tested it on a PEC technology using the TiNT as a photocatalyst and Ti wire as an electrode. Their study used a 15 W low-pressure mercury lamp as an energy source, and the applied potential was 0.5 V. The PEC decomposed 22% ammonia by hydroxyl ions without the presence of chloride ions at high pH (10.7). The introduction of 0.05 mol of NaCl resulted in 99% ammonia decomposition due to the in-situ generation of chlorine and hypochlorous acid, which play an active role in the decomposition of ammonia. Xiao et al. (2016) concluded that adding chloride ions makes the technology independent of pH.

The technology is currently incorporated in small-scale pilot systems, and the primary disadvantage is that the technology is still in the research phase and is yet to be scaled up to treat water in systems with a high design capacity volume. Furthermore, scaling of the cathode with calcium carbonate presents a challenge if the system uses calcium hydroxide to stabilise the water. In addition, chloride ions are key in the generation of chlorine for disinfection;

drinking water treatment system has a low chloride concentration, and it will require the addition of salt for the system to be effective. Lastly, the technology will increase electrical cost in powering the electrical charge and UV lamps to activate the catalyst. **Table 2.4** summarises removal efficiencies of different ammonia of ammonia treatment technologies on varying raw water sources.

Table 2.4: Summary of ammonia treatment technologies.

Technology	Efficiency (%)	Advantages	Disadvantages	References
Ion Exchange/ adsorption	75- 99	Reagents can be regenerated and used efficiently.	Costly to regenerate. Increases salt concentration in aqueous solution which might require further treatment. Produced brine increases waste in the water.	(Karri et al., 2018).
Biological Nutrient removal	75 - 95	Commonly used technology. Does not require additional chemicals. Effective ammonium removal.	Anoxic conditions and low temperatures reduce removal efficiency.	(Abu Hasan et al., 2014).
Break-point chlorination	80 - 95	The available technology is efficient and removes ammonia comprehensively. Controls taste and odour. .	Requires 7.6:1 chlorine to ammonia ratios. Requires high chlorine dosages. Forms disinfection by-products with organic matter.	(Adam et al., 2019; Pressley et al., 1972; Takó, 2012).
Air/ Steam Stripping process	90 - 99	Simple effective method effective at high ammonium concentration.	pH-dependent. Energy-dependent. Fouling and scaling on packing towers.	(Bonmatí and Flotats, 2003; Guštin and Marinšek-Logar,

Technology	Efficiency (%)	Advantages	Disadvantages	References
				2011; Kinidi et al., 2018).
Electrochemical advanced oxidation process	60 - 99	Technology does not require chemical addition. No sludge production.	Complicated technology. Dependent on electrode, density, pH and chloride. Can decompose ammonia to nitrite and nitrate.	(Peng et al., 2019; Wang et al., 2014b; Xiao et al., 2016; Yao et al., 2019).
Chemical precipitation	60-90	Efficient in solution with high ammonium concentration. Simple technology. Product can be used as a slow-release fertiliser.	Dependent on pH, ion concentration and mixing rates. Produces sludge which can scale the pipeline.	(Mavhungu et al., 2019; Yan and Shih, 2016).
Filtration Technologies	80-99	Efficient removal method. Removes cysts, bacteria, viruses, and natural organic matter.	High capital cost. Membrane fouling decreases filtration over time. Energy and pressure dependent.	(Adam et al., 2019; Eskicioglu et al., 2018; Hube et al., 2020).

2.5 Overview of the review, status quo analysis, and future perspectives

Concerning this review, it can be noted that the contamination of surface water with effluent rich in ammonia is a challenge that is affecting Water Services Providers (WSP). A conventional drinking water process which involves oxidation, coagulation and flocculation, sedimentation, filtration, and disinfection is not suitable to deal with the ever-increasing deterioration of the incoming surface water. The ammonia levels on the surface water have at times increased to 8 mg/L, leading to a high chlorine demand at the 'drinking water treatment plant (DWTW). This is mainly attributed to the reaction of chlorine with ammonia to form chloramine. Furthermore, high ammonia levels that are not removed at the WTW final product water can oxidise in the distribution system, leading to nitrite and nitrate formation. Drinking water with nitrite and nitrate has the potential to impact the blood cells leading to blue baby syndrome (Methemoglobinemia), coupled with the fact that water with ammonia impacts the oxidation of manganese, leading to final treated water that is turbid, in addition to having colour and a metallic taste. The supply of quality drinking water is a legal requirement imposed by the Department of Water and Sanitation (DWS), and it is the responsibility of the WSP to ensure that the end product complies with the South African Drinking Water Standards of 2015 (SANS 241:2015-2). Traditionally, ammonia is primarily removed in a wastewater treatment system (WWTS) by a biological nutrient removal approach, which involves the oxidation of ammonia with oxygen. To catalyse this stage, the process is facilitated by oxidising ammonia bacteria and denitrifying bacteria under anaerobic and anoxic conditions. The ammonia is broken down into N_2 gas and eventually gets released into the atmosphere.

However, with an ever-increasing population, the failure of municipal treatment systems results in the discharge of nutrient-rich water, which ultimately leads to eutrophication and algal bloom in dams and catchment areas, including other receiving aquatic ecosystems. As such, the WSPs are looking at research for cost-effective treatment systems that can be introduced as an addition to drinking water treatment systems to deal with the ammonia challenges. To the author's knowledge, the breakpoint chlorination technique is the available treatment technique that is readily available in DWTP. However, with stoichiometric ratios of 7.6:1 Cl_2:NH_3 to oxidise the ammonia, 60 mg/L of chlorine is required, and this will excessively increase the production cost and possibly result in the formation of disinfection by-products from their reaction with natural organic matter. Introducing biological air filters has also been investigated primarily on a laboratory scale. However, this methodology will involve the introduction of microorganisms (pathogenic bacteria) into the drinking water system. Failure of the chlorine system will contaminate the distribution system with acute microbial organisms like E. coli, and Cryptosporidium, which is detrimental to the health of the consumers. Furthermore, the efficiency of the bacteria is low during winter seasons when the ammonia levels are more concentrated due to low temperatures. The air stripping process will require high energy to supply air and high pH to strip the ammonia in the water, increasing operational costs.

Furthermore, the produced ammonia gas can be toxic when released into the atmosphere if it reacts with sulphur dioxide. Electrochemical advanced oxidation processes and photocatalytic processes can also be employed to decompose ammonia; however, they require energy to break down ammonia leading to an increase in cost. Furthermore, the technology can form nitrite and nitrate as by-products, and these determinants harm the health of the end users. In addition to other developed technologies, membrane filtration, adsorption, and ion exchange are promising technologies with high removal efficiencies and have gained international attention. However, the cost of regenerating the absorbent in adsorption and ion exchange is high and results in contamination of the drinking water with salt during the regeneration process, which might give taste to water. These technologies foster secondary pollution from the regenerates, and very little has been entertained in exploring the viability of valorising the regenerates and benefiting from them. This will suffice and advocate for the concept of a circular economy and sustainable development phenomenon. On the other hand, membrane filtration requires sophisticated redesigning for retrofitting, and it has high energy demand; furthermore, membrane fouling and low production rates will result in high operational costs. As an issue of grave concern, the production of brine as the RO rejects from the filtration technique requires proper handling and disposal, thus making this technology unfavourable.

Due to stringent waste management and handling regulations, the environmental footprints associated with brine crystallisation render the technology undesirable. Traditionally, precipitation has been widely used for drinking water purification purposes. Mainly, the use of lime has been utilised for pH control and metal attenuation. This has been classified as a promising technology that can be introduced into conventional drinking water processes. The twilight of magnesium application in removing pollutants such as ammonia and phosphate has gained paramount attention in recent decades. This is attributed to their strong affinity to ammonia and phosphates, which results in the formation of hexa-hydrated-magnesium-ammonia-phosphate. However, a study by Shu et al. (2019) reported low ammonia removal efficiency by the chemical precipitation of between 20 and 30 %. In the study, sulphide precipitation was conducted using sodium sulphide, hydroxide precipitation using sodium hydroxide and carbonate precipitation using sodium carbonate. Struvite precipitation has ammonia a removal efficiency between 80 and 95% when using magnesium chloride as a magnesium source, and it involves an equimolar ratio between $Mg^{2+}: NH_4^+: PO_4^{3-}$.

From this review, it is notable that ammonia has never been removed from drinking water systems. An innovative approach is required to unpack the hampering factors and identify viable research avenues for ammonia removal in drinking water. In light of that and from the identified research gaps, magnesium and phosphates will be added to allow for struvite to form before coagulation and flocculation. Canal water abstracted for drinking water systems has low magnesium and phosphate concentrations. As such, removing ammonia as struvite will require the addition of magnesium and phosphates. A low-cost magnesium source, calcined magnesite (MgO), can be used to minimise the operational cost, increasing the overall costs, and sensitivity analysis will have to be pursued to identify feasible business opportunities and avenues. MgO has an added advantage as it oxidises manganese efficiently and has antimicrobial properties, thus enabling it to reduce the chlorine demand of the water. This study has not been conducted in drinking water sources, primarily due to the projected increased cost of introducing new chemicals or the potential to scale the pipeline and up-take fears.

2.6 Conclusions and recommendations

Ammonia removal technologies were primarily developed to remove ammonia in aqueous wastewater solutions with high ammonia concentrations. BNR, Air/Steam stripping, and chemical precipitation removal efficacies are satisfactory when technologies are operated efficiently. However, population growth, poor designs and mechanical breakdowns of available technologies have resulted in surface water contamination with ammonia. The impact of chlorination due to the interaction between chlorine and ammonia gives water an acceptable taste and smell. Additionally, the oxidation potential of ammonia to nitrite poses an acute health risk to consumers. Ion exchange/adsorption, advanced oxidation, biological air filters and membrane filtration have been earmarked as potential technologies to incorporate in DWTP. Drawbacks such as pollution risks associated with BNR, cost of regeneration, replacement of ion exchange/adsorption reagents, and membrane fouling hinder these technologies. Furthermore, these technologies are mostly in the research stage. Struvite precipitation provides an alternative due to its efficacy in removing ammonia, and manganese. This technology has only been applied in high ammonia concentration aqueous solutions like wastewater and landfill leachate and has yet to be tested in DWTP. Investigating ammonia removal with struvite precipitation and comparing the cost of ammonia removal with other technologies provides an opportunity to save operational costs and implement a technology that will assist in dealing with the ever-worsening situation with regard to surface water nutrient contamination.

References

Abel-Denee, M., Abbott, T., Eskicioglu, C., 2018. Using mass struvite precipitation to remove recalcitrant nutrients and micropollutants from anaerobic digestion dewatering centrate. Water Research 132, 292-300.

Abu Hasan, H., Sheikh Abdullah, S.R., Kamarudin, S.K., Tan Kofli, N., Anuar, N., 2014. Kinetic evaluation of simultaneous COD, ammonia and manganese removal from drinking water using a biological aerated filter system. Separation and Purification Technology 130, 56-64.

Adam, M.R., Othman, M.H.D., Abu Samah, R., Puteh, M.H., Ismail, A.F., Mustafa, A., A. Rahman, M., Jaafar, J., 2019. Current trends and future prospects of ammonia removal in wastewater: A comprehensive review on adsorptive membrane development. Separation and Purification Technology 213, 114-132.

Alshameri, A., Ibrahim, A., Assabri, A.M., Lei, X., Wang, H., Yan, C., 2014. The investigation into the ammonium removal performance of Yemeni natural zeolite: Modification, ion exchange mechanism, and thermodynamics. Powder Technology 258, 20-31.

Altomare, M., Selli, E., 2013. Effects of metal nanoparticles deposition on the photocatalytic oxidation of ammonia in TiO2 aqueous suspensions. Catalysis Today 209, 127-133.

Ansari, A.J., Hai, F.I., Price, W.E., Drewes, J.E., Nghiem, L.D., 2017. Forward osmosis as a platform for resource recovery from municipal wastewater - A critical assessment of the literature. Journal of Membrane Science 529, 195-206.

Arslan, A., Veli, S., 2012. Zeolite 13X for adsorption of ammonium ions from aqueous solutions and hen slaughterhouse wastewaters. Journal of the Taiwan Institute of Chemical Engineers 43, 393-398.

Astals, S., Martínez-Martorell, M., Huete-Hernández, S., Aguilar-Pozo, V.B., Dosta, J., Chimenos, J.M., 2021. Nitrogen recovery from pig slurry by struvite precipitation using a low-cost magnesium oxide. Science of The Total Environment 768, 144284.

Bernardi, F., Zadinelo, I.V., Alves, H.J., Meurer, F., dos Santos, L.D., 2018. Chitins and chitosans for the removal of total ammonia of aquaculture effluents. Aquaculture 483, 203-212.

Bock, G., 2016. Removal of High and Low Levels of Ammonium from Industrial Wastewaters.

Bonmatí, A., Flotats, X., 2003. Air stripping of ammonia from pig slurry: characterisation and feasibility as a pre- or post-treatment to mesophilic anaerobic digestion. Waste Management 23, 261-272.

Booker, N.A., Cooney, E.L., Priestley, A.J., 1996. Ammonia removal from sewage using natural Australian zeolite. Water Science and Technology 34, 17-24.

Capodaglio, A.G., Hlavínek, P., Raboni, M., 2015. Physico-chemical technologies for nitrogen removal from wastewaters: a review %J Revista Ambiente & Água. 10, 481-498.

Çelik, M.S., Özdemir, B., Turan, M., Koyuncu, I., Atesok, G., Sarikaya, H.Z., 2001. Removal of ammonia by natural clay minerals using fixed and fluidised bed column reactors. Water Supply 1, 81-88.

Chai, L.-y., Peng, C., Min, X.-b., Tang, C.-j., Song, Y.-x., Zhang, Y., Zhang, J., Ali, M., 2017. Two-sectional struvite formation process for enhanced treatment of copper–ammonia complex wastewater. Transactions of Nonferrous Metals Society of China 27, 457-466.

Chen, L., Zhou, C.H., Zhang, H., Tong, D.S., Yu, W.H., Yang, H.M., Chu, M.Q., 2017. Capture and recycling of ammonium by dolomite-aided struvite precipitation and thermolysis. Chemosphere 187, 302-310.

Cheng, H., Zhu, Q., Xing, Z., 2019. Adsorption of ammonia nitrogen in low temperature domestic wastewater by modification bentonite. Journal of Cleaner Production 233, 720-730.

Cheremisinoff, N.P., 2002a. Chapter 9 - Membrane Separation Technologies, in: Cheremisinoff, N.P. (Ed.), Handbook of Water and Wastewater Treatment Technologies. Butterworth-Heinemann, Woburn, pp. 335-371.

Cheremisinoff, N.P., 2002b. Chapter 10 - Ion exchange and carbon adsorption, in: Cheremisinoff, N.P. (Ed.), Handbook of Water and Wastewater Treatment Technologies. Butterworth-Heinemann, Woburn, pp. 372-445.

Chuang, Y.-H., Szczuka, A., Shabani, F., Munoz, J., Aflaki, R., Hammond, S.D., Mitch, W.A., 2019. Pilot-scale comparison of microfiltration/reverse osmosis and ozone/biological activated carbon with UV/hydrogen peroxide or UV/free chlorine AOP treatment for controlling disinfection byproducts during wastewater reuse. Water Research 152, 215-225.

Dalanta, F., Kusworo, T.D., 2022. Synergistic adsorption and photocatalytic properties of AC/TiO2/CeO2 composite for phenol and ammonia–nitrogen compound degradations from petroleum refinery wastewater. Chemical Engineering Journal 434, 134687.

Darwish, M., Aris, A., Puteh, M.H., Jusoh, M.N.H., Abdul Kadir, A., 2017. Waste bones ash as an alternative source of P for struvite precipitation. J Environ Manage 203, 861-866.

Department of Water Affairs and Forestry, 1996. South African Water Quality Guidelines (first edition), Field Guide. Department of Water Affairs and Forestry Volume 8.

Dey, S., Basha, S.R., Babu, G.V., Nagendra, T., 2021. Characteristic and biosorption capacities of orange peels biosorbents for removal of ammonia and nitrate from contaminated water. Cleaner Materials 1, 100001.

Ding, Y., Sartaj, M., 2016. Optimization of ammonia removal by ion-exchange resin using response surface methodology. International Journal of Environmental Science and Technology 13, 985-994.

Du, T., Zhang, G., Zou, J., 2022. Coupling photocatalytic and electrocatalytic oxidation towards simultaneous removal of humic acid and ammonia−nitrogen in landscape water. Chemosphere 286, 131717.

Ekama, G.A., 2011. 4.14 - Biological Nutrient Removal A2 - Wilderer, Peter, Treatise on Water Science. Elsevier, Oxford, pp. 409-526.

Eskicioglu, C., Galvagno, G., Cimon, C., 2018. Approaches and processes for ammonia removal from side-streams of municipal effluent treatment plants. Bioresource Technology 268, 797-810.

Feng, J., Zhang, X., Zhang, G., Li, J., Song, W., Xu, Z., 2021. Improved photocatalytic conversion of high-concentration ammonia in water by low-cost Cu/TiO(2) and its mechanism study. Chemosphere 274, 129689.

Galbraith, S.C., Schneider, P.A., Flood, A.E., 2014. Model-driven experimental evaluation of struvite nucleation, growth and aggregation kinetics. Water Research 56, 122-132.

Guaya, D., Valderrama, C., Farran, A., Armijos, C., Cortina, J.L., 2015. Simultaneous phosphate and ammonium removal from aqueous solution by a hydrated aluminium oxide modified natural zeolite. Chemical Engineering Journal 271, 204-213.

Guštin, S., Marinšek-Logar, R., 2011. Effect of pH, temperature and air flow rate on the continuous ammonia stripping of the anaerobic digestion effluent. Process Safety and Environmental Protection 89, 61-66.

Hakimi, M.H., Jegatheesan, V., Navaratna, D., 2020. The potential of adopting struvite precipitation as a strategy for the removal of nutrients from pre-AnMBR treated abattoir wastewater. J Environ Manage 259, 109783.

Han, M., Zhao, Z.-w., Gao, W., Cui, F.-y., 2013. Study on the factors affecting simultaneous removal of ammonia and manganese by pilot-scale biological aerated filter (BAF) for drinking water pre-treatment. Bioresource Technology 145, 17-24.

Hu, L., Yu, J., Luo, H., Wang, H., Xu, P., Zhang, Y., 2020. Simultaneous recovery of ammonium, potassium and magnesium from produced water by struvite precipitation. Chemical Engineering Journal 382, 123001.

Huang, H., Huang, L., Zhang, Q., Jiang, Y., Ding, L., 2015. Chlorination decomposition of struvite and recycling of its product for the removal of ammonium-nitrogen from landfill leachate. Chemosphere 136, 289-296.

Huang, H., Li, B., Dai, J., Wang, W., Zhang, M., Ou, Y., 2021. Ammonia nitrogen removal from coking wastewater and high quality gypsum recovery by struvite recycling by using calcium hydroxide as decomposer. J Environ Manage 292, 112712.

Huang, H., Xiao, D., Zhang, Q., Ding, L., 2014. Removal of ammonia from landfill leachate by struvite precipitation with the use of low-cost phosphate and magnesium sources. Journal of Environmental Management 145, 191-198.

Huang, H., Zhang, P., Zhang, Z., Liu, J., Xiao, J., Gao, F., 2016. Simultaneous removal of ammonia nitrogen and recovery of phosphate from swine wastewater by struvite electrochemical precipitation and recycling technology. Journal of Cleaner Production 127, 302-310.

Huang, J., Kankanamge, N.R., Chow, C., Welsh, D.T., Li, T., Teasdale, P.R., 2018. Removing ammonium from water and wastewater using cost-effective adsorbents: A review. Journal of Environmental Sciences 63, 174-197.

Hube, S., Eskafi, M., Hrafnkelsdóttir, K.F., Bjarnadóttir, B., Bjarnadóttir, M.Á., Axelsdóttir, S., Wu, B., 2020. Direct membrane filtration for wastewater treatment and resource recovery: A review. Science of The Total Environment 710, 136375.

Ji, Y., Bai, J., Li, J., Luo, T., Qiao, L., Zeng, Q., Zhou, B., 2017. Highly selective transformation of ammonia nitrogen to N2 based on a novel solar-driven photoelectrocatalytic-chlorine radical reactions system. Water Research 125, 512-519.

Joseph, J., Sajeesh, A.K., Nagashri, K., Edinsha Gladis, E.H., Sharmila, T.M., Justin Dhanaraj, C., 2021. Determination of ammonia content in various drinking water sources in Malappuram District, Kerala and its removal by adsorption using agricultural waste materials. Materials Today: Proceedings 45, 811-819.

Kabdaşlı, N., Tunay, O., 2018. Nutrient recovery by struvite precipitation, ion exchange and adsorption from source-separated human urine – a review. Environmental Technology Reviews 7, 106-138.

Karri, R.R., Sahu, J.N., Chimmiri, V., 2018. Critical review of abatement of ammonia from wastewater. Journal of Molecular Liquids 261, 21-31.

Kinidi, L., Tan, I.A.W., Abdul Wahab, N., Tamrin, K., Nolasco-Hipolito, C., Salleh, S., 2018. Recent Development in Ammonia Stripping Process for Industrial Wastewater Treatment. International Journal of Chemical Engineering 2018, 1-14.

Kropp, R., Tompkins, D., Barry, T., Zeltner, W., Pepping, G., Anderson, M., Barry, T., 2009. A device that converts aqueous ammonia into nitrogen gas. Aquacultural Engineering 41, 28-34.

Laureni, M., Palatsi, J., Llovera, M., Bonmatí, A., 2013. Influence of pig slurry characteristics on ammonia stripping efficiencies and quality of the recovered ammonium-sulfate solution. Journal of Chemical Technology & Biotechnology 88, 1654.

Li, H., Cao, Y., Liu, P., Li, Y., Zhou, A., Ye, F., Xue, S., Yue, X., 2022. Ammonia-nitrogen removal from water with gC3N4-rGO-TiO2 Z-scheme system via photocatalytic nitrification-denitrification process. Environmental Research 205, 112434.

Li, M., Zhu, X., Zhu, F., Ren, G., Cao, G., Lin, S., 2011. Application of modified zeolite for ammonium removal from drinking water. Desalination 271, 295-300.

Li, Z., Ren, X., Zuo, J.-e., Liu, Y., Duan, E., Yang, J., Chen, P., Wang, Y., 2012. Struvite Precipitation for Ammonia Nitrogen Removal in 7-Aminocephalosporanic Acid Wastewater. Molecules (Basel, Switzerland) 17, 2126-2139.

Liu, H., Zhu, L., Tian, X., Yin, Y., 2017. Seasonal variation of bacterial community in biological aerated filter for ammonia removal in drinking water treatment. Water Research 123, 668-677.

Loganathan, P., Vigneswaran, S., Kandasamy, J., 2013. Enhanced removal of nitrate from water using surface modification of adsorbents – A review. Journal of Environmental Management 131, 363-374.

Masindi, V., Gitari, W.M., Pindihama, K.G., 2016. Adsorption of phosphate from municipal effluents using cryptocrystalline magnesite: complementing laboratory results with geochemical modelling. Desalination and Water Treatment 57, 20957-20969.

Mavhungu, A., Mbaya, R., Masindi, V., Foteinis, S., Muedi, K.L., Kortidis, I., Chatzisymeon, E., 2019. Wastewater treatment valorisation by simultaneously removing and recovering phosphate and ammonia from municipal effluents using a mechano-thermo activated magnesite technology. Journal of Environmental Management 250, 109493.

Mehta, C.M., Batstone, D.J., 2013. Nucleation and growth kinetics of struvite crystallisation. Water Research 47, 2890-2900.

Morari, F., Dal Ferro, N., Cocco, E., 2015. Municipal wastewater treatment with Phragmites australis L. and Typha latifolia L. for irrigation reuse. Boron and heavy metals. Water, Air, and Soil Pollution 226.

O'Farrell, T.P., Frauson, F.P., Cassel, A.F., Bishop, D.F., 1972. Nitrogen Removal by Ammonia Stripping. Journal (Water Pollution Control Federation) 44, 1527-1535.

Owusu-Agyeman, I., Malovanyy, A., Plaza, E., 2015. Pre-concentration of ammonium to enhance treatment of wastewater using the partial nitritation/anammox process. Environ Technol 36, 1256-1264.

Peng, L., Dai, H., Wu, Y., Peng, Y., Lu, X., 2018. A comprehensive review of phosphorus recovery from wastewater by crystallisation processes. Chemosphere 197, 768-781.

Peng, X., Wang, M., Hu, F., Qiu, F., Dai, H., Cao, Z., 2019. Facile fabrication of hollow biochar carbon-doped TiO2/CuO composites for the photocatalytic degradation of ammonia nitrogen from aqueous solution. Journal of Alloys and Compounds 770, 1055-1063.

Pressley, T.A., Bishop, D.F., Roan, S.G., 1972. Ammonia-nitrogen removal by breakpoint chlorination. Environmental Science & Technology 6, 622-628.

Puyen, Z.M., Villagrasa, E., Maldonado, J., Diestra, E., Esteve, I., Solé, A., 2012. Biosorption of lead and copper by heavy-metal tolerant Micrococcus luteus DE2008. Bioresource Technology 126, 233-237.

Raboni, M., Torretta, V., Viotti, P., Urbini, G., 2013. Experimental plant for the physical-chemical treatment of groundwater polluted by Municipal Solid Waste (MSW) leachate, with ammonia recovery.

Rahman, M.M., Salleh, M.A.M., Rashid, U., Ahsan, A., Hossain, M.M., Ra, C.S., 2014. Production of slow release crystal fertiliser from wastewaters through struvite crystallisation – A review. Arabian Journal of Chemistry 7, 139-155.

Rajasekhar, B., Venkateshwaran, U., Durairaj, N., Divyapriya, G., Nambi, I.M., Joseph, A., 2020. Comprehensive treatment of urban wastewaters using electrochemical advanced oxidation process. Journal of Environmental Management 266, 110469.

Ren, H.-T., Liang, Y., Han, X., Liu, Y., Wu, S.-H., Bai, H., Jia, S.-Y., 2020. Photocatalytic oxidation of aqueous ammonia by Ag2O/TiO2 (P25): New insights into selectivity and contributions of different oxidative species. Applied Surface Science 504, 144433.

Romero-Güiza, M.S., Tait, S., Astals, S., del Valle-Zermeño, R., Martínez, M., Mata-Alvarez, J., Chimenos, J.M., 2015. Reagent use efficiency with removal of nitrogen from pig slurry via struvite: A study on magnesium oxide and related by-products. Water Research 84, 286-294.

Ronteltap, M., Maurer, M., Hausherr, R., Gujer, W., 2010. Struvite precipitation from urine – Influencing factors on particle size. Water Research 44, 2038-2046.

Ruiz-Beviá, F., Fernández-Torres, M.J., 2019. Effective catalytic removal of nitrates from drinking water: An unresolved problem? Journal of Cleaner Production 217, 398-408.

Ryu, H.-D., Lee, S.-I., 2010. Application of struvite precipitation as a pretreatment in treating swine wastewater. Process Biochemistry 45, 563-572.

Selcuk, H., Anderson, M.A., 2005. Effect of pH, charge separation and oxygen concentration in photoelectrocatalytic systems: active chlorine production and chlorate formation. Desalination 176, 219-227.

Shavisi, Y., Sharifnia, S., Hosseini, S.N., Khadivi, M.A., 2014. Application of TiO2/perlite photocatalysis for degradation of ammonia in wastewater. Journal of Industrial and Engineering Chemistry 20, 278-283.

Shavisi, Y., Sharifnia, S., Mohamadi, Z., 2016. Solar-light-harvesting degradation of aqueous ammonia by CuO/ZnO immobilized on pottery plate: Linear kinetic modelling for adsorption and photocatalysis process. Journal of Environmental Chemical Engineering 4, 2736-2744.

Shoda, M.E., Sprague, L.A., Murphy, J.C., Riskin, M.L., 2019. Water-quality trends in U.S. rivers, 2002 to 2012: Relations to levels of concern. Science of The Total Environment 650, 2314-2324.

Shu, J., Wu, H., Chen, M., Peng, H., Li, B., Liu, R., Liu, Z., Wang, B., Huang, T., Hu, Z., 2019. Fractional removal of manganese and ammonia nitrogen from electrolytic metal manganese residue leachate using carbonate and struvite precipitation. Water Research 153, 229-238.

Sirés, I., Brillas, E., Oturan, M.A., Rodrigo, M.A., Panizza, M., 2014. Electrochemical advanced oxidation processes: today and tomorrow. A review. Environmental Science and Pollution Research 21, 8336-8367.

Song, Y.-H., Qian, F., Gao, Y., Huang, X., Wu, J., Yu, H., 2015. PHREEQC program-based simulation of magnesium phosphates crystallisation for phosphorus recovery. Environmental Earth Sciences 73, 5075-5084.

Sun, D., Sun, W., Yang, W., Li, Q., Shang, J.K., 2015. Efficient photocatalytic removal of aqueous NH4+–NH3 by palladium-modified nitrogen-doped titanium oxide nanoparticles under visible light illumination, even in weak alkaline solutions. Chemical Engineering Journal 264, 728-734.

Sun, J., Huang, Y., Li, H., Qiu, Y., Zhang, J., Hu, K., Li, J., Ding, Y., 2021. Silver nanoparticle-loaded graphitic carbon nitride/multiwall carbon nanotube composite with improved denitrification to nitrogen gas for the photocatalytic removal of aqueous ammonia nitrogen. Environmental Technology & Innovation 24, 101815.

Takó, S., 2012. Ammonium removal from drinking water–Comparison of the breakpoint chlorination and the biological technology, Conference of Junior Researchers in Civil Engineering, pp. 248-254.

US:EPA, 2019. Drinking water treatability database, Chloramine.

Vareda, J.P., Valente, A.J.M., Durães, L., 2019. Assessment of heavy metal pollution from anthropogenic activities and remediation strategies: A review. Journal of Environmental Management 246, 101-118.

Vocciante, M., De Folly D'Auris, A., Finocchi, A., Tagliabue, M., Bellettato, M., Ferrucci, A., Reverberi, A.P., Ferro, S., 2018. Adsorption of ammonium on clinoptilolite in presence of competing cations: Investigation on groundwater remediation. Journal of Cleaner Production 198, 480-487.

Wang, H., Su, Y., Zhao, H., Yu, H., Chen, S., Zhang, Y., Quan, X., 2014a. Photocatalytic Oxidation of Aqueous Ammonia Using Atomic Single Layer Graphitic-C3N4. Environmental Science & Technology 48, 11984-11990.

Wang, H., Zhang, X., Su, Y., Yu, H., Chen, S., Quan, X., Yang, F., 2014b. Photoelectrocatalytic oxidation of aqueous ammonia using TiO2 nanotube arrays. Applied Surface Science 311, 851-857.

Warmadewanthi, Rodlia, A., Ikhlas, N., Pandebesie, E.S., Bagastyo, A.Y., Herumurti, W., 2020. The Effect of Mixing Rate on Struvite Recovery from The Fertiliser Industry. IOP Conference Series: Earth and Environmental Science 506, 012013.

Wen, G., Hu, Z., Liu, X., Huang, L., 2018. Improvement of the quality of struvite crystals recovered from a mixture of human urine and municipal sewage via a novel two-step precipitation method. Environmental Technology & Innovation 12, 80-90.

Wongcharee, S., Aravinthan, V., Erdei, L., 2020. Removal of natural organic matter and ammonia from dam water by enhanced coagulation combined with adsorption on powdered composite nano-adsorbent. Environmental Technology & Innovation 17, 100557.

World Health, O., 2011. Guidelines for drinking-water quality, 4th ed ed. World Health Organization, Geneva.

World Health, O., 2017. Guidelines for drinking-water quality: fourth edition incorporating first addendum, 4th ed + 1st add ed. World Health Organization, Geneva.

Xi, H., Zhang, X., Hua Zhang, A., Guo, F., Yang, Y., Lu, Z., Ying, G., Zhang, J., 2022. Concurrent removal of phosphate and ammonium from wastewater for utilization using Mg-doped biochar/bentonite composite beads. Separation and Purification Technology 285, 120399.

Xiao, D., Huang, H., Zhang, P., Gao, Z., Zhao, N., 2018. Utilizing the supernatant of waste sulfuric acid after dolomite neutralization to recover nutrients from swine wastewater. Chemical Engineering Journal 337, 265-274.

Xiao, S., Wan, D., Zhang, K., Qu, H., Peng, J., 2016. Enhanced photoelectrocatalytic degradation of ammonia by in situ photoelectrogenerated active chlorine on TiO2 nanotube electrodes. Journal of Environmental Sciences 50, 103-108.

Xue, R., Donovan, A., Zhang, H., Ma, Y., Adams, C., Yang, J., Hua, B., Inniss, E., Eichholz, T., Shi, H., 2018. Simultaneous removal of ammonia and N-nitrosamine precursors from high ammonia water by zeolite and powdered activated carbon. Journal of Environmental Sciences 64, 82-91.

Yan, H., Shih, K., 2016. Effects of calcium and ferric ions on struvite precipitation: A new assessment based on quantitative X-ray diffraction analysis. Water Research 95, 310-318.

Yao, F., Fu, W., Ge, X., Wang, L., Wang, J., Zhong, W., 2020. Preparation and characterisation of a copper phosphotungstate/titanium dioxide (Cu-

H3PW12O40/TiO2) composite and the photocatalytic oxidation of high-concentration ammonia nitrogen. Science of The Total Environment 727, 138425.

Yao, J., Mei, Y., Xia, G., Lu, Y., Xu, D., Sun, N., Wang, J., Chen, J., 2019. Process Optimization of Electrochemical Oxidation of Ammonia to Nitrogen for Actual Dyeing Wastewater Treatment. International Journal of Environmental Research and Public Health 16, 2931.

Ye, Z.-L., Chen, S.-H., Lu, M., Shi, J.-W., Lin, L.-F., Wang, S.-M., 2011. Recovering phosphorus as struvite from the digested swine manure with bittern as a magnesium source. Water science and technology: a journal of the International Association on Water Pollution Research 64, 334-340.

Yun, L., Yu, Z., Li, Y., Luo, P., Jiang, X., Tian, Y., Ding, X., 2019. Ammonia nitrogen and nitrite removal by a heterotrophic Sphingomonas sp. strain LPN080 and its potential application in aquaculture. Aquaculture 500, 477-484.

Zaini, N.S.M., Lenggoro, I.W., Naim, M.N., Yoshida, N., Man, H.C., Bakar, N.F.A., Puasa, S.W., 2021. Adsorptive capacity of spray-dried pH-treated bentonite and kaolin powders for ammonium removal. Advanced Powder Technology 32, 1833-1843.

Zhang, C., He, D., Ma, J., Waite, T.D., 2018. Active chlorine mediated ammonia oxidation revisited: Reaction mechanism, kinetic modelling and implications. Water Research 145, 220-230.

Zhang, X.-n., Guo, Q.-p., Shen, X.-x., Yu, S.-w., Qiu, G.-y., 2015. Water quality, agriculture and food safety in China: Current situation, trends, interdependencies, and management. Journal of Integrative Agriculture 14, 2365-2379.

Zöllig, H., Fritzsche, C., Morgenroth, E., Udert, K.M., 2015. Direct electrochemical oxidation of ammonia on graphite as a treatment option for stored source-separated urine. Water Research 69, 284-294.

CHAPTER THREE

Effective removal of ammonia from aqueous solution using a combination of precipitation and breakpoint chlorination

This chapter is devoted to addressing the following objectives:

- To investigate the Physico-chemical and microbial properties of raw water at the Wallmannsthal water treatment plant (WTP).
- To determine conditions suitable for the removal of ammonia and other contaminants from Wallmannsthal WTP raw and point out the underpinning chemistry.
- To characterise the feed product sludge during the synthesis of struvite using activate magnesite.

Abstract

The ever-growing surface water contamination by various catchment activities poses threats to water treatment entities (facilities). Specifically, the presence of ammonia, microbial contaminants, organic matter, and heavy metals has been an issue of paramount concern to water treatment entities. Herein, a hybrid approach that integrates struvite crystallisation (precipitation) and breakpoint chlorination (stripping) on the removal of ammonia from an aqueous solution was evaluated. Batch experimental studies were used to fulfil the goals of this study, specifically making use of the one-factor-at-a-time approach. The fate of chemical species was underpinned using state-of-the-art analytical instruments and accredited methods. Magnesium oxide nanoparticles (MgO-NPs) were used as the magnesium source, while the high-test hypochlorite (HTH) was based on the hypochlorite activities. Optimum conditions were: Stage 1, 110 mg/L of Mg and P dosage (concentration), 150 rpm of mixing speed, 60 minutes of contact time, and lastly, 120 minutes of sedimentation, while the optimum condition for the breakpoint chlorination (Stage 2) was achieved at 30 minutes of mixing and 8:1 Cl_2:NH3 stoichiometric ratio. In Stage 1, i.e. MgO-NPs, the pH increased from 6.7 to ≥ 9.6, while the turbidity was reduced from 9.1 to ≤ 1.3 NTU. Manganese removal efficacy attained ≥ 97% (174µg/L to 4 µg/L) while Iron was completely removed (11 mg/L to ≤ 0.37 mg/L). Elevated pH also led to the deactivation of bacteria. In Stage 2, i.e. breakpoint chlorination, the product water was further polished by eliminating residual ammonia and TPC at an 8:1 Cl_2-NH_3 weight ratio. Ammonia was reduced from 7.6 to 2.84 mg/L in Stage 1 (62.63% removal) and then from 2.84 to ≤ 0.009 mg/L post breakpoint chlorination (≥ 99% removal). Lastly, from breakpoint chlorination and beyond, disinfectant by-products (DBPs) formed, with chloroform as the most dominant DBP. Overall, synergistic and complementary effects of integrating struvite synthesis and breakpoint chlorination hold great promise in removing contaminants from surface water.

Keywords: Contamination of surface water; surface water treatment; ammonia and manganese removal; struvite synthesis; breakpoint chlorination; integrated technologies; and microbial deactivation and disinfection by-products.

3.1 Introduction

The alarming contamination of surface water which is exasperated by various catchment activities has been an issue of paramount concern to water treatment entities (facilities). In particular, downstream entities experience challenges from various upstream activities primarily due to introduction of toxic and hazardous substances (Mavhungu et al., 2020, Masindi et al., 2021). These activities include agriculture, municipal wastewater treatment plant, mining operations, construction, industrial processes, urban run-offs, natural weathering and leaching, and precipitation (Sharma et al., 2021). These activities introduce chemical substances that alter the Physico-chemical and microbial characteristics of the receiving environment, making it unsuitable to foster life and render its intrinsic values. Of prime concern is municipal wastewater treatment facilities that discharge effluents that do not comply with the regulatory requirements and specifications. Effluents emanating from poor-performing wastewater treatment facilities enrich surface water with inorganic constituents, organic matter, and microbial loads, including ammonia and phosphate that make the water eutrophic (Adam et al., 2019, Mavhungu et al., 2019). Elevated levels of ammonia in water can potentially deplete oxygen in the water and can also cause eutrophication which in turn poses damage to aquatic life, amongst others (Hu et al., 2020, Chen et al., 2022). In South Africa, Roodeplaat, Bronkhorstspruit, and Hartbeespoort dams have experienced eutrophication, which has increased algae levels and hyacinths in the catchment.

Furthermore, ammonia has the potency to pose harm to human health upon exposure. Excess ammonia concentration in the drinking water system might be oxidised, thus producing nitrite in distribution systems. Nitrite can cause blue baby syndrome (Methemoglobinemia) (Capodaglio et al., 2015). In addition, excessive ammonia levels have been reported to cause numerous health effects upon exposure. Specifically, it can cause cancer of the stomach, oesophagus and pharynx (Chen et al., 2022). In water treatment plants, ammonia has a high affinity for chlorine, which negatively hinders the oxidation of manganese, thus producing brownish water enriched with a metallic taste (Adam et al., 2019). Compounding to these challenges, the consumer also loses confidence in the water produced by any given entity as a result of the colour of the water despite its non-observable effects and health risk (WHO, 2017).

The prevalence of these contaminants has reportedly forced drinking water treatment plants to periodically stop production due to the ineffectiveness of conventional treatment systems (coagulation and flocculation, sedimentation, filtration, and disinfection processes) in removing ammonia and manganese (Abu Hasan et al., 2014). However, attempts to remove these contaminants in conventional water treatment plants (WTPs) are mainly achieved at the expense of chemicals and secondary pollution as a trade-off. Consequently, this has led to water shortages in the respective supply area. The phenomenon of periodic plant shutdown has already started in South Africa, with media reports detailing challenges experienced in the Northern side of Pretoria (Etheridge, 2019). As such, removal of ammonia in water is imperative, and this will ensure that residents and end-users are supplied with safe water for human consumption.

Various technologies have been developed, piloted and employed to remove ammonia from wastewater. These technologies include the following:

- biological nutrients removal (BNR) (Ekama, 2011);
- breakpoint chlorination (Sharma et al., 2021);
- chemical precipitation (Warmadewanthi et al., 2020);
- ion exchange (Ding and Sartaj, 2016);
- adsorption (Vocciante et al., 2018, Wongcharee et al., 2020);
- electrochemical oxidation technologies like photocatalytic oxidation (Altomare and Selli, 2013, Wang et al., 2014);
- electrochemical oxidation (Zhang et al., 2015, Zöllig et al., 2015); and
- photo-electrochemical oxidation (Kropp et al., 2009, Tang et al., 2020).

Amongst these technologies, the biological nutrient removal (BNR) method is the most common method employed to breakdown ammonia in wastewater, and this is ideal for municipal wastewater (MWW) and packaged sanitation plants such as the moving bed bioreactors (MBBR) but not suitable for drinking water since MWW rely on microbial communities. In contrast, drinking water relies on chemical processes (Chen et al., 2022). Furthermore, the limiting factors for alternative technologies are high energy and operational cost, demands for structural amendment, poor performance, incompatibility with real-scale applications, and premature emerging technologies. However, chemical precipitation through struvite synthesis and breakpoint chlorination has emerged as the best and most promising technologies after the BNR system (Chen et al., 2022).

Specifically, chemical precipitation, on the other hand, is one of the most stable and efficient ammonia removal technologies that can be easily incorporated into an existing system and has recorded high ammonia removal efficiencies (Chen et al., 2022) with the end product struvite being a slow release fertiliser which can be sold for agricultural purposes (Mavhungu et al., 2019). In light of the basic chemistry, surface water has a low magnesium and phosphate concentration. Higher magnesium and phosphate concentrations are required for efficient removal of ammonia, which will increase the treatment cost and deter the widespread application of struvite technology (Huang et al., 2014). To counter high costs, research has focused on using a low-cost magnesium source such as MgO by-products (tailings), magnesite mineral, bittern, and seawater, yielding similar removal rates as recorded when using pure magnesium salts (Huang et al., 2014). Li et al. (2022) reduced ammonium concentration from 140 mg/L to 2.5mg/L using low spent refractory brick leaching effluent as the magnesium source. Mavhungu et al. (2019) used low-cost calcined magnesite as a magnesium source and removed 75% ammonium from wastewater with an initial concentration of 123 mg/L. Those technologies struggle to attain 100% ammonia removal, and regulatory frameworks require an ammonia concentration of ≤1.5 mg/L N (American Public Health et al., 1998, SABS, 2015, WHO, 2017).

Similarly, breakpoint chlorination is one of the proven technologies to eliminate ammonia from drinking water. The most effective stoichiometry of chlorine to ammonia was reported to be 7.6:1 (Pressley et al., 1972). However, the potential for the formation of chlorine by-products after the reaction of chlorine with natural organic matter hinders the use of this technology (Capodaglio et al., 2015, Sharma et al., 2021). Be that it may, notable strides have been made in terms of by-products management. For instance, the combination of chlorination and adsorption with PAC and zeolite reduced ammonia by 67%, while the disinfection by-products, i.e., dimethylammonium iodide (DMAI) and dimethyl aminopyridine (DMAP), were reduced by 73% and 40%, respectively (Abu Hasan et al., 2014).

Considering the advantages of individual technologies, leveraging their weaknesses and creating synergy toward their enhanced performance is viable. This could be achieved by integrating these two technologies in a stepwise fashion, with chemical precipitation using struvite as pre-treatment (Stage 1) and breakpoint chlorination as a polishing stage (Stage 2) for the complete removal of ammonia. Similar attempts have been made, but there were areas of deficiencies that require attention. In particular, Chen et al. (2022) conducted a study on the simultaneous removal of manganese and ammonia from an aqueous solution via the incorporation of metal hydroxide precipitation, struvite synthesis, breakpoint chlorination, and coagulation with ferric salts. Although the technology was proven effective, the precursors needed to fulfil the project's goals deemed the study unattractive due to high costs and sophisticated processes. Furthermore, their study did not address the potential by-products expected from the high chlorine dosages; hence it was perceived as the pitfall of the study since by-products are toxic and carcinogenic.

According to the authors, this will be the first study in design and execution to explicitly integrate struvite synthesis and breakpoint chlorination to remove ammonia and manganese from surface water (canal water). Furthermore, the formation of potential by-products will meticulously be evaluated, and a safe approach to the required limit will be adopted. This study will go a long way in curtailing the challenges faced by drinking water utilities.

3.2 Materials and methods

3.2.1 Procurement of chemicals and acquisition of raw water

All chemicals used in this study were of analytical grade. Potassium dihydrogen phosphate (KH_2PO_4) was procured from Aqualytic solution limited (Pty). Activated magnesite was procured from Sterkfontein carbonates (Ltd) Pty. Raw water was collected from a canal system which receives water from the Roodeplaat dam, Pretoria, Gauteng province, South Africa. The raw water was collected on 21 June 2021.

3.2.2 Preparation of the stock solution

The stock solution for struvite synthesis was prepared using calcined magnesite (MgO-NPs) and potassium dihydrogen phosphates as magnesium and phosphates sources, respectively. Serial dilutions were done to acquire the required working solution of 1 g/L. Mg and P stock solution dilution involved weighing 1.65 g of MgO-NPs and 1.43 g of potassium dihydrogen phosphate. The desired working solutions were prepared according to the planned experiments. Chlorine stock solution was prepared using calcium hypochlorite (HTH). A mass of 1.42 g of calcium hypochlorite was added to 1 L with ultrapure water.

3.2.3 Optimization studies

This study was stratified into two sections; section one consisted of the removal of ammonia by struvite precipitation, while in section two, the breakpoint chlorination was carried out as a secondary treatment. A Phipps and Bird Jar stirrer with adjustable speed (Variable speed drive: VSD) was employed to conduct the laboratory experiments.

3.2.3.1 Struvite synthesis laboratory

Factors influencing the removal of ammonia as struvite included mixing time, molar ratio and mixing speed. The study was performed using the one-factor-at-a-time (OFAAT), and the main essence was to create an optimal condition suitable for the highest ammonia removal (struvite yield).

3.2.3.1.1 The influence of mixing time on the removal of ammonia

Firstly, the influence of contact time on the removal of pollutants was explicitly determined. The graded beakers were filled with 1L of canal water (comprising approximately 6.51 mg/L of ammonia concentration) (Table 1). Thereafter, the prepared working solution, which comprised the known magnesium and phosphate concentrations (Section 3.2.2), was added to each beaker (Mg and P dosages of 40 mg/L each). The mixtures were equilibrated for 15, 30, 60, 90, 120 and 240 minutes at 200 rpm using the Phipps and Bird jar stirrer. After mixing, the contents were allowed to settle for 2 hours (sedimentation), and the supernatants were filtered using a Whatman 1 filter paper. Lastly, the filtered effluent was analyzed for ammonia, phosphate, calcium, magnesium, turbidity, pH, manganese, *E.* coli, and total coliform. Optimum conditions from this experiment were used in the subsequent experiment.

3.2.3.1.2 The influence of Mg and P dosages on the removal of ammonia

The effects of the Mg and P dosage on the removal of the pollutants were studied on different Mg and P equi-dosages (10, 30, 50, 70, 90 and 110 mg/L). While the Mg and P dosages were varied, the optimal contact time from Section 3.2.3.1.1 (60 minutes), mixing speed (200 rpm) and sedimentation time (2 hrs) were kept constant. After each experiment, the supernatant effluent was filtered with a Whatman 1 filter paper (MN 615.Ǿ 185 mm – Macherey-Nagel (MN)$^{@TM}$) and then collected for physicochemical and microbiological characterisation as stipulated in Section 3.2.3.1.1.

3.2.3.1.3 The influence of mixing speed on the removal of ammonia

The influence of mixing speed and dosage were evaluated using optimal conditions from Sections 3.2.3.1.1 and 3.2.3.1.2, respectively. To determine the influence of the mixing speed, the experiments were performed at varying mixing speeds ranging from 50, 100, 150, 200 and 250 rpm. During each experiment, both Mg and P dosages were kept at 110 mg/L (optimal as determined from Section 3.2.3.1.2), and the mixing time was fixed at 60 min (an optimal condition from Section 3.2.3.1.1). The sedimentation time (2hrs) was kept constant. After each experiment, the supernatant effluent was filtered with a Whatman 1 filter paper (MN 615.Ǿ 185 mm – Macherey-Nagel (MN)$^{@TM}$) and then collected for physicochemical and microbiological characterisation as stipulated in 3.2.3.1.1.

3.2.3.1.4 Treatment of canal raw water at optimal conditions.

Sections 3.2.3.1.1 to 3.2.3.1.3 determined the optimum mixing time, dosage, and mixing speed. Henceforth, raw water from the canal (river) was treated under optimal conditions. The graded beakers were filled with 1L of ammonia-rich raw water, and experiments were conducted at Mg and P dosages of 110 mg/L, mixing speed of 150 rpm, contact time of 60 minutes, and the contents were allowed to settle for 2 hrs. After each experiment, the supernatant effluent was filtered with a Whatman 1 filter paper (MN 615.Ǿ 185 mm – Macherey-Nagel (MN)$^{@TM}$), and then the aliquots were collected for physicochemical and microbiological characterisation as stipulated in Section 3.2.3.1.1.

3.2.3.2 Breakpoint chlorination

The product water from the struvite synthesis stage was taken to a polishing step, i.e. breakpoint chlorination. The main attempt was to fully decompose residual ammonia and make the product water suitable for drinking or any other defined use as stipulated in different regulatory frameworks and structures (national and international).

3.2.3.2.1 Effect of chlorine dosage on the removal of residual ammonia

The influence of the chlorine dosage on the removal of ammonia was evaluated following what has been reported by (Devi and Dalai, 2021). A Phipps and Bird Jar stirrer with adjustable speed (Variable speed drive: VSD) was employed to fulfil the goals of this experiment. Each beaker was filled with 1L of product water from the struvite synthesis experiment. Varying dosages of chlorine to ammonia ratio (0-14) of hypochlorite solution prepared as described in Section 3.2.2 were added into graded beakers and followed the adopted procedure described by (Devi and Dalai, 2021). After that, the solutions were mixed for 30 minutes, congruent with what was reported by (Charrois and Hrudey, 2007). The mixing speed was at 200 rpm, which was solely selected in line with the water treatment plant's flow rate (hydraulics). As a quality control initiative, the experiments were conducted in triplicate, and the acquired outcomes were reported as averages (mean values) with standard deviation (SDV). Lastly, the product water (aliquots) from individual beakers were collected and immediately characterised for total and residual chlorine, *E. coli*, total coliform, ammonia, nitrite, nitrate, natural organic matter (TOC), trihalomethanes (THMs), pH, and conductivity.

3.2.4 Characterisation

3.2.4.1 Characterisation of aqueous samples

Ammonia, nitrite and nitrate were measured using a Gallery Plus analyser (Thermo Fischer Scientific Brand, USA). The conductivity and pH of the solution were measured using an HQ40d multi-meter pH meter (Hach Company, Loveland, USA), which was calibrated using standard buffer solutions. Iron and manganese were measured using an Inductively Plasma Optical Emission Spectrometer (ICP-OES), Agilent (Agilent, Santa Clara, CA, USA). Phosphate concentrations were quantified using the molybdenum–antimony visible light-based spectrophotometric method (SEPA, 2002). The turbidity was measured using a HACH 2100 AN turbid meter Total, free chlorine and monochloramine were analysed using a MISP-REM-HAH-DR3900 colourimeter (Hach Company, Loveland, USA). Trihalomethanes were measured using a Gas Chromatography-Mass Spectrometry (GC-MS) (Agilent technologies 5975 C, CA, USA), which is connected to a purge and trap (OI Analytical Eclipse 4660 Purge and Trap Sample Concentrator) instrument. Standard methods were used to analyse the samples (Rice et al., 2012). International standards of organization 17025 (ISO 17025), accredited laboratories and National Institution of Standard Technology (NIST) standards were considered for sample analysis.

3.2.4.2 Solid Characterisation

The mineralogical constituents of both feed material and produced (resultant sludge) were quantified using an X-ray diffraction identifier (Phillip PW 1710 diffractometer model). Chemical bonds were identified with an FT-IR Tensor 27 instrument, while the morphology of the solid structure was measured by SEM-EDS, Hitachi, and JOEL JSM-840 equipment. XRD analyses were conducted at the University of Pretoria in South Africa.

3.3 Results and discussions

3.3.1 Physicochemical and microbial properties of raw water

The raw water's physical, chemical and microbial properties were considered against the South African drinking water quality standard (SANS 241), as shown in **Table 3.1**.

Table 3.1: The raw water's physical, chemical and microbial properties against the South African drinking water quality standard.

Parameter	Units	SANS Limit	Concentration
E. coli	MPN/100 mL	≤ 0	167
Coliform	MPN/100 mL	≤ 10	2420
Total plate count	MPN/1mL	≤ 1000	29600
Ammonia	mg/L N	≤ 1.5	6.51
TOC	mg/L C	≤ 1.5	7.62
Phosphate $^{-}$	mg/L	≤ 1.5	0.72
Magnesium	mg/L	≤ 1.5	1.1
Turbidity	NTU	≤ 1	9.1
Iron (Fe)	µg/L	≤ 400	267
Manganese (Mn)	µg/L	≤ 100	300
Calcium (Ca)	mg/L	≤ 300	22
Potassium (K)	mg/L	≤ 100	5.9
Sodium (Na)	mg/L	≤ 100	22

According to **Table 3.1**, the risk parameters observed in the raw water comprised the microbial community, i.e., *E. coli* (167 MPN/100mL), total coliform (2420 MPN/100mL) and total plate count (29600 MPN/1mL), turbidity (9.1 NTU), ammonia (6.51 mg/L), and manganese (300 µg/L). These parameters were observed to be higher than the minimum allowable limits according to South African National Standards (SANS) for drinking water. Consequently, the parameters must be lowered to ensure compliance with the regulatory bodies. *Escherichia coli* (*E. coli*) is a bacterium used to indicate the presence of faecal coliform and disease-causing organisms such as *Salmonella typhi*. However, the microbial community in the raw water is expected due to the Roodeplaat Dam receiving effluent from wastewater treatment works upstream of the catchment. The aesthetic manganese level in the raw water can oxidise, leading to brownish water with a metallic taste and the potential to taint laundry and scale pipes (Adam et al., 2019). The ammonia in the water provides a serious challenge, mainly the potential formation of nitrite through oxidation, and nitrite can cause methemoglobinemia (Capodaglio et al., 2015, Shu et al., 2019). Furthermore, ammonia hampers manganese removal (Adam et al., 2019), provides nutrients to microorganisms, and subsequently increases chlorine demand. Lastly, as shown in **Table 3.1**, concentrations of magnesium (1.1 mg/L) and phosphate (0.72 mg/L) in the raw water are lower than ammonia. As such, Mg^{2+} and PO_4^{3-} concentrations must be augmented to allow for struvite precipitation with ammonia (Huang et al., 2014, Huang et al., 2016). A similar approach is going to be adopted in this novel study.

3.3.2 Primary stage (Phase 1): Struvite synthesis

3.3.2.1 Effect of contact time

The variation in the percentage removal of inorganic contaminants as a function of contact time is depicted in **Figure 3.1**.

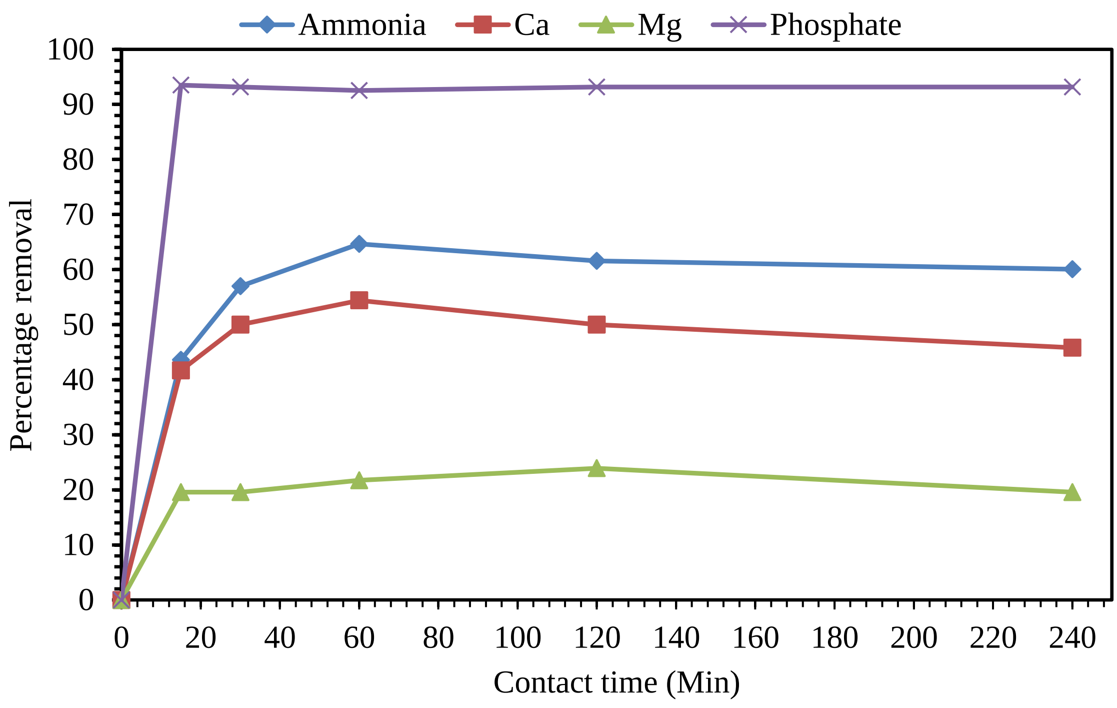

Figure 3.1: Variation in percentage removal of inorganic contaminants as a function of contact time (Experimental conditions: 40 mg/L of Mg, 40 mg/L of P, 7 mg/L of ammonia, 200 rpm mixing speed and ambient temperature).

As shown in **Figure 3.1**, there was an increase in the removal of inorganic contaminants with an increase in the contact time. Specifically, there was a sharp increase in the ammonia percentage removal rate, which was observed from 0 minutes to 60 minutes yielding approximately 64.66% of ammonia removal. Furthermore, increasing the contact time to beyond 60 minutes resulted in a slight or insignificant reduction in ammonia levels. Interestingly, there was a slight reduction in ammonia with a general yield of 60.06% at 240 min. As such, the reduction in the removal efficacy of ammonia after 60 minutes could be attributed to the oversaturation condition of the aqueous system resulting in a breakdown of the precipitate, thus promoting the partial dissolution of ammonia back into water matrices. Other studies observed similar observations (Mavhungu et al., 2019; Warmadewanthi et al., 2020). The raw water is comprised of low levels of magnesium and phosphate^{-}as such, an adequate amount of these elements should be seeded to foster struvite formation (Hakimi et al., 2020). A significant removal in magnesium and phosphate was also observed as a function of contact time, with magnesium reaching 23.17% and phosphate achieving 93.17% within 60 minutes of contact time. This denotes the feasible formation of struvite since there was simultaneous removal of contaminants from the aqua-sphere. Thenceforth, increasing the contact time led to insignificant changes in inorganic contaminants, hence confirming that the system has reached equilibrium. From the obtained results, i.e. ammonia, phosphate and magnesium levels, it can grossly be inferred that these compounds are possibly being removed as struvite. The calcium attained 54% removal efficacy, which could be linked to the formation of calcium phosphate. Hence, the competition between Mg^{2+} and Ca^{2+} ions for PO_4^{3-} ions was postulated as the limiting factor towards the formation of struvite. Albeit, the concentration was very low, leading to quick depletion of calcium from the aqueous system.

The variation in the percentage removal of *E. coli*, turbidity, coliform, Mn, Fe, and total plate count (TPC) as a function of contact time is depicted in **Figure 3.2**.

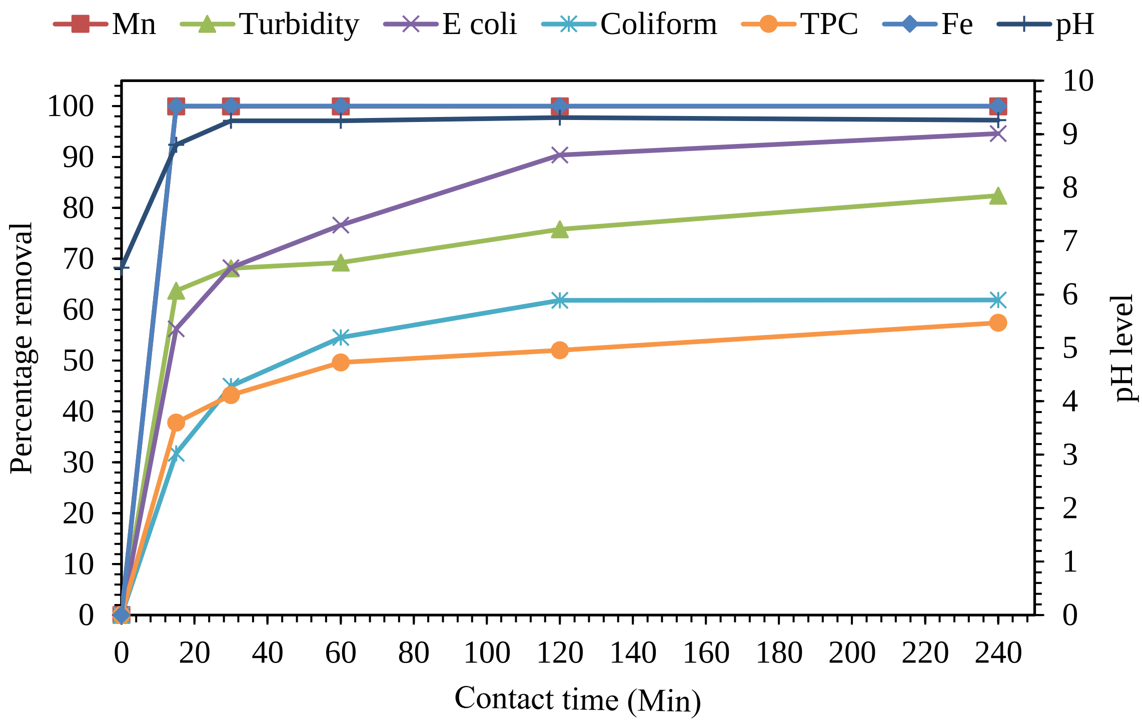

Figure 2.2: Variation of the levels of Mn, Fe, pH, turbidity, TPC, total coliform, and E. coli as a function of contact time (Experimental conditions: 40 mg/L of Mg, 40 mg/L of P, 7 mg/L of ammonia, 200 rpm mixing speed and ambient temperature).

As shown in **Figure 3.2**, the pH was observed to increase with an increase in contact time. A rapid increase was observed in the first 15 minutes, where the pH increased from 6.5 to 8.8. Thereafter, an increase was observed to be proportional to time, reaching 9.25 in 30 minutes. A similar trend was observed for Fe and Mn, with the elements reaching their maximum removal within 15 minutes of contact. This could be explained by the possible precipitation of these elements as the pH increased. Similar observations were reported (Masindi et al., 2018, Shu et al., 2019).

Furthermore, the removal efficacy for *E. coli*, coliform and total plate count was observed to be congruent to contact time. Specifically, within the first 15 minutes, a sharp increase in the removal of *E. coli* (56.23%), coliform (31.81%) and TPC (37.8%) was observed. The trends continue to gradually increase with time, yielding 94.61% for *E. coli*, 61.91% for coliform and 57.42% for TPC after 240 minutes.

Conversely, Huang et al. (2014) have reported a negligible impact of adding magnesium and phosphoric acid on microbial activity. However, Huang et al. (2014) denoted the effect of pH on microbial deactivation, and the authors emphasized that an increase in pH with contact time creates alkaline conditions and these conditions are not suitable for the survival of microorganisms. Thus leading to their reduction. Finally, as shown in **Figure 3.2**, the trend for turbidity attenuation was observed to increase with an increase in contact time. In particular, a sharp increase in turbidity removal (63.73%) was observed within the first 15 minutes, after which a gradual increment in removal rates was observed with the contact time, eventually yielding 82.41% removal after 240 minutes. Lastly, a drastic reduction in NTU could be explained by the mixing duration, which promotes the destabilisation of charged particles leading to the formation of flocs since magnesium can act as a coagulant.

3.3.2.2 Effects of equal dosages of Mg and P

The variation in the percentage removal of inorganic contaminants as a function of dosage is depicted in **Figure 3.3**.

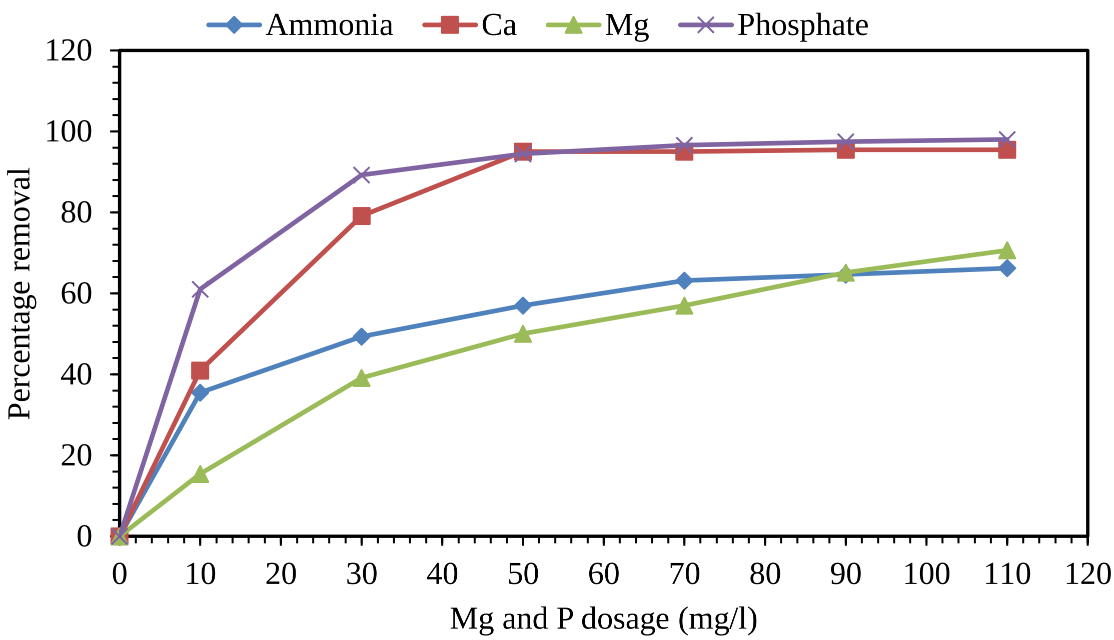

Figure 3.3: Variation in percentage removal of inorganic contaminants as a function of dosage (Fixed experimental conditions: 60 minutes of contact time, 7 mg/L of ammonia, 200 rpm mixing speed and ambient temperature).

As shown in **Figure 3.3**, ammonia recovery is in direct proportion to the equal dosages of Mg and P and 35.43% of ammonia was recovered from the Mg and P dosage of 10 mg/L each. Henceforth, the recovery was directly proportional to the dosage and eventually yielded 66.21% at 110 mg/L (Mg and P). Similar trends were observed in a study conducted by Hu et al. (2020). Moreover, the Mg: N:P ratio and pH were deemed to be the paramount factors in the formation of struvite. This corroborates what has been reported by other authors (Hakimi et al., 2020, Hu et al., 2020).

Furthermore, a sharp increase in calcium removal was observed from 0-70 mg/L, thereafter, the removal efficacy was observed to have flattened out, denoting that equilibrium was reached. Higher removal rates for calcium could be attributed to the adsorption of phosphate leading to the formation of calcium phosphate; hence, the level of phosphate removal was observed to increase in the latter part of the measurements slightly. A similar trend was observed for magnesium, which could explain the possibility of struvite formation. The lower removal rates of ammonia could be attributed to competition for PO_4^{3-} ions between Mg^{2+} and Ca^{2+} ions. These findings are similar to findings from previous studies (Hakimi et al., 2020, Hu et al., 2020, Li et al., 2022). Hu et al. (2020) removed 0.3% to 6.1% of ammonia from water that was treated without calcium pre-treatment, i.e. Mg: N:P ratios (1:1:1 to 1.8:1:1.8). Furthermore, the impact of calcium could be explained by the lower solubility (k_{sp}) of calcium phosphate (2.0 X 10^{-29}) concerning that of magnesium ammonia phosphate (MAP) (2.5 X 10^{-13}) hence confirming higher feasibility of calcium precipitation as compared to MAP (Hu et al., 2020). To offset the high calcium concentration in an aqueous solution, Hu et al. (2020) pre-treated the feed water with sodium carbonate (soda ash) in a quest to form calcium carbonate as a trade for Ca attenuation. Their study demonstrated a higher removal efficacy (85.9%) as struvite, confirming that calcium is a limiting factor. Similarly, Li et al. (2022) used spent refractory brick gravel as a magnesium source and achieved close to 99.6% and 98.2% removal efficacies for phosphate and ammonia, respectively. Higher removal rates were achieved by first precipitating calcium through leaching of spent refractory brick with sulphate to form gypsum and subsequently using low calcium effluent with higher magnesium levels.

Furthermore, Li et al. (2022) reported that the ammonia concentration was reduced from 140 mg/L N to 2.5 mg/L N at an Mg: N:P ratio of 2:1:2. In this study, increasing magnesium and phosphate dosages provided enough PO_4^{3-} ions to overcome foreign ions, i.e. calcium ions in water, and eventually yielded higher ammonia recovery rates (66.21%) at equal Mg and P dosage of 110 mg/L. Furthermore, as shown in **Figure 3.3**, insignificant increases in magnesium and phosphate levels were observed to increase with dosage, confirming that these elements are reacting to form a by-product, i.e. struvite. From the observed trends **(Figure 3.3),** it can be inferred that ammonia is removed from the aqueous media as Magnesium Ammonia Phosphate (MAP), also known as struvite **(Equation 3.3).**

On the other hand, calcium is removed as calcium phosphate. As reported in the literature, researchers have synthesised struvite at an Mg: N:P ratio of 1:1:1, yielding high ammonia removal (Ryu and Lee, 2010, Li et al., 2012; Darwish et al., 2017). In this study, the lower Mg and P dosage of 10 mg/L resulted in ≤ 34% removal efficacy for ammonia, which could primarily be linked to the raw water concentration of calcium (22 mg/L), as shown in **Table 3.1**. Thenceforth, it is evident that calcium competes for phosphate ions due to the formation of calcium phosphate, thus depleting the available phosphate. This will then hinder the precipitation of MAP, popularly known as struvite (Equation 3.1-3.3):

$$5Ca^{+} + 3HPO_4^{2-} + H_2O \rightarrow Ca_5(PO_4)_3(OH)\downarrow + 4H^{+} \tag{3.1}$$

$$3Ca^{2+} + 2HPO_4^{2-} \rightarrow Ca_3(PO_4)_2\downarrow + 2H^{+} \tag{3.2}$$

$$Mg^{2+} + NH_4^{+} + H_nPO_{4n}^{3-} + 6H_2O \rightarrow MgNH_4PO_4.6H_2O + nH^{+} \tag{3.3}$$

The variation in the percentage removal of *E. coli*, turbidity, coliform, Mn, Fe, and total plate count (TPC) as a function of dosage is depicted in **Figure 3.4**.

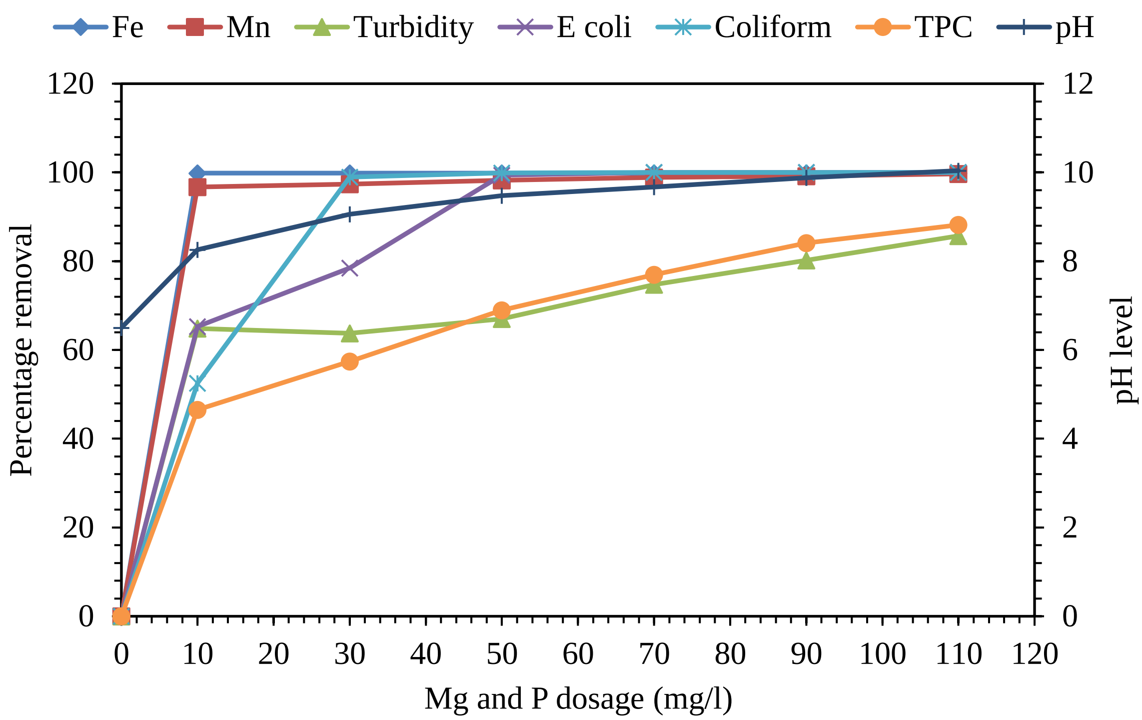

Figure 3.4: Variation of the levels of Mn, Fe, pH, turbidity, TPC, total coliform, and *E. coli* as a function of dosage (Experimental conditions: 60 minutes of contact time, 200 rpm of mixing speed and ambient temperature).

As shown in **Figure 3.4**, there was an increase in pH with an increase in dosage. Specifically, the pH increased from 6.5 to 8.26 when the equal Mg and P dosages were 10 mg/L and then ≥10.04 when the dosages were 110 mg/L. Results are consistent with what was reported in Mavhungu et al. (2019) and Masindi et al. (2017). An increase in pH is attributed to the dissolution of the mother material, i.e. calcined magnesite (MgO-NPs), hence leading to the addition of alkalinity (Masindi et al., 2017).

As shown in **Figure 3.4,** there was an increase in the removal efficacy of Fe and Mn with an increase in the feedstock dosage. A rapid increase was observed from 0-30 mg/L dosages. Thereafter, the trends were flattened, hence denoting that Fe and Mn were depleted from the aqueous system. This could be attributed to a higher pH (≥9.1) that is conducive for the precipitation of those chemical species. The findings are similar to studies conducted by Guan et al. (2021) where they recovered 98.8% Fe as precipitate using $MgCl_2$ at pH of 9. Masindi et al. (2018) reported that Fe precipitated at pH ranges from 3-3.5 while Mn precipitated when the pH was ≥ 8.5- 9.5, which explicitly supports this study's findings. Shu et al. (2019) study yielded 99% manganese removal when the pH was 8 during the removal of ammonia as struvite. As such, results from this study corroborate what has been reported in the literature. Furthermore, there was a direct proportion between dosage and turbidity (NTU - Nephelometric Turbidity unit). In essence, higher dosages (110 mg/L) resulted in an 85.71% reduction in initial turbidity. These results signify that the feedstock elements are acting as coagulants, hence scavenging colloids and dissolved substances.

Finally, the *E. coli*, coliform and total plate count were also removed with an increase in pH and alkalinity resulting from an increase in calcined magnesite dosage. The microbial load, TPC, coliform and *E. coli* followed a similar trend. As shown in **Figure 3.4**, microbial deactivation sharply increased at Mg and P dosages of 10 mg/L and pH of 8.26 (65.27% *E. coli*, 52.03% coliform and 46.55% plate count) and the deactivation rates increased with dosage and pH. At pH (9.67) and higher, *E. coli* and coliform bacteria were completely deactivated with TPC, eventually reduced by 88.15% when the pH was 10.04, and Mg:P was 110 mg/L. From the observation in **Figure 3.4,** it can be deduced that the non-detection in the final water suggests that higher pH or alkaline conditions are not suitable for the survival of the bacterial community. The optimal pH for incubating microbial community ranges from 6 to 8 (Navab-Daneshmand et al., 2022); hence they were seen to die in higher pH environments. A previous study reported that the microbial community during struvite formation is inhibited only when sodium dihydrogen phosphate (NaH_2PO_4) or sodium hydrogen phosphate ($NaHPO_4$) as phosphate source was used since it increases salt loads, which deactivates microbes (Huang et al., 2014). Furthermore, the authors concluded that combining MgO and phosphoric acid would negligibly affect the microbial community (Huang et al., 2014). In this study, the deactivation can be attributed to the increase in pH (≥ 9.6), leading to conditions which are not conducive to microbial growth. The survival of microorganisms in Huang et al. (2014) can be attributed to lower pH of 8, which was insufficient for their deactivation. In addition, magnesium ^{in} wastewater has been reported to be beneficial for microbial growth (Ahring et al., 1991).

3.3.2.3 Effects of mixing speed

The variation in the percentage removal of inorganic contaminants as a function of mixing speed is depicted in **Figure 3.5**.

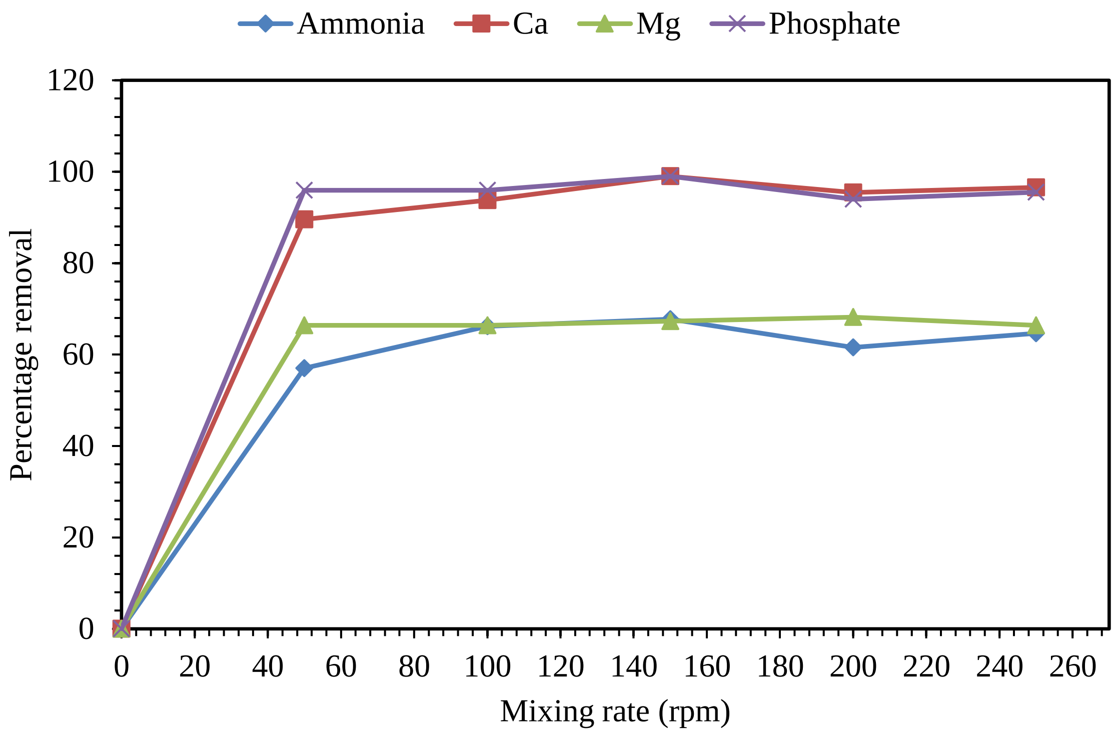

Figure 3.5: Variation in percentage removal of inorganic contaminants as a function of mixing speed (Experimental conditions: 110 mg/L of Mg, 110 mg/L of P, 7 mg/L of ammonia, 60 minutes contact time and ambient temperature).

As shown in **Figure 3.5**, the mixing speed was observed to influence the percentage removal of contaminants. Specifically, ammonia removal was observed to increase with an increase in mixing speed initially. A lower mixing rate (50 rpm) yielded 56.99% ammonia removal; a similar trend was observed until 150 rpm (67.74 % removal). After that, the removal rates reduced beyond 150 rpm (61.60%), i.e. 200 rpm, and it ultimately reached 64.46. % at 250 rpm. Interestingly, the levels of phosphate and magnesium removal rates were initially observed to increase with mixing speed, eventually yielding 99% of phosphate and 67.27% of magnesium at 150 rpm mixing speed. Worryingly, however, is the slight reduction in magnesium and phosphate removal rates when the mixing speed increased to 200 rpm and afield, hence confirming the possibility of struvite destruction at high mixing speed. Findings from this study corroborate what has been reported by Warmadewanthi et al. (2020). The authors attained a maximum mixing speed at 157 rpm and compromised efficacy beyond 200 rpm. Similar removal rates were observed by Kim et al. (2009). Interestingly, a rapid increase in removal rate was observed in the calcium trend at lower mixing rates (89.58% calcium removal) at 50 rpm and continued to increase, eventually yielding 96.55% calcium removal at the highest mixing rates.

The variation in the percentage removal of *E. coli*, turbidity, coliform, Mn, Fe, and total plate count (TPC) as a function of mixing speed is depicted in **Figure 3.6**.

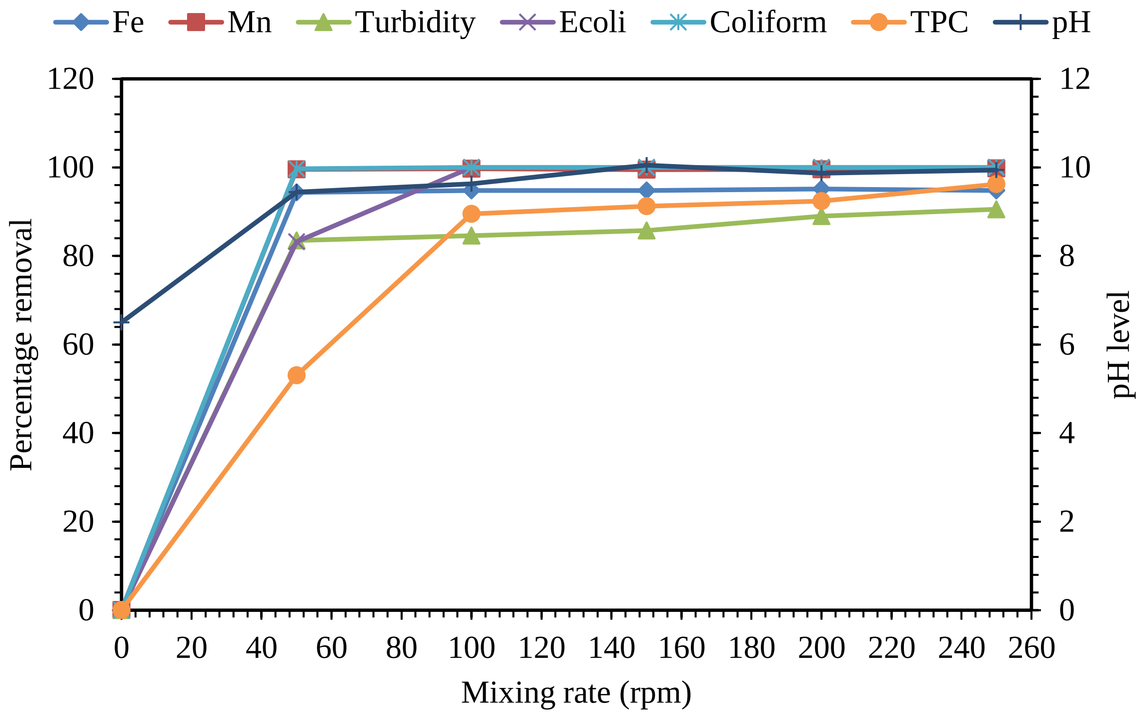

Figure 3.6: Variation of the levels of Mn, Fe, pH, turbidity, TPC, total coliform, and *E. coli* as a function of dosage (Experimental conditions: 110 mg/L of Mg, 110 mg/L of P, 7 mg/L of ammonia, 60 minutes contact time and ambient temperature).

As shown in **Figure 3.6**, there was an increase in the pH with an increase in mixing speed. A high mixing speed enhances the feedstock's agitation, leading to rapid dissolution and subsequently an increase in pH. Similarly, the Fe and Mn removal levels were also observed to have attained a maximum at 50 rpm. However, this is proportional to the pH. Similar observations were reported in previous studies (Masindi et al., 2018, Shu et al., 2019, Guan et al., 2021). A similar trend was observed for turbidity, which yielded 83.52% efficacy and eventually reached 90.55% at 250 rpm. In essence, the higher mixing intensity enhances the distribution of dissolved coagulant and destabilisation of the same charge particulates in the water, leading to the formation of larger flocs which easily settle out of the solution, resulting in clear product water. Carolina González (2019) evaluated the impact of mixing energy and observed an increase in particle size of the precipitate with an increase in mixing energy, leading to the formation of larger crystals which resulted in a higher concentration of ammonia accumulating or binding to the crystal, thus reducing the concentration of ammonia from the surface water. Finally, the microbial deactivation rates, *E. coli*, Coliform and TPC trends were observed to sharply increase with mixing intensity, primarily due to the increment in pH. Interestingly, the complete deactivation of *E. coli* and Coliform bacteria was achieved at pH ≥ 9. However, the TPC bacteria showed some resistance as compared to *E. coli* and Coliform bacteria, but higher pH values denoted higher efficacy, i.e. 91.25% at pH 10.05.

3.3.2.4 Solid characterisation

The composition of the feed and product sludge was evaluated in this section. The main quest was to determine the fate of inorganic contaminants after the interaction of MgO-NPs and rich water contaminants. Specifically, this section will succinctly unpack the mineralogical and morphological properties and other chemical properties as confirmed by different analytical techniques.

3.3.2.4.1 Mineralogical characterisation

The mineralogical properties of activated magnesite (MgO-NPs) and product sludge were evaluated using X-ray diffraction (XRD), and the results are presented in **Figure 3.7**.

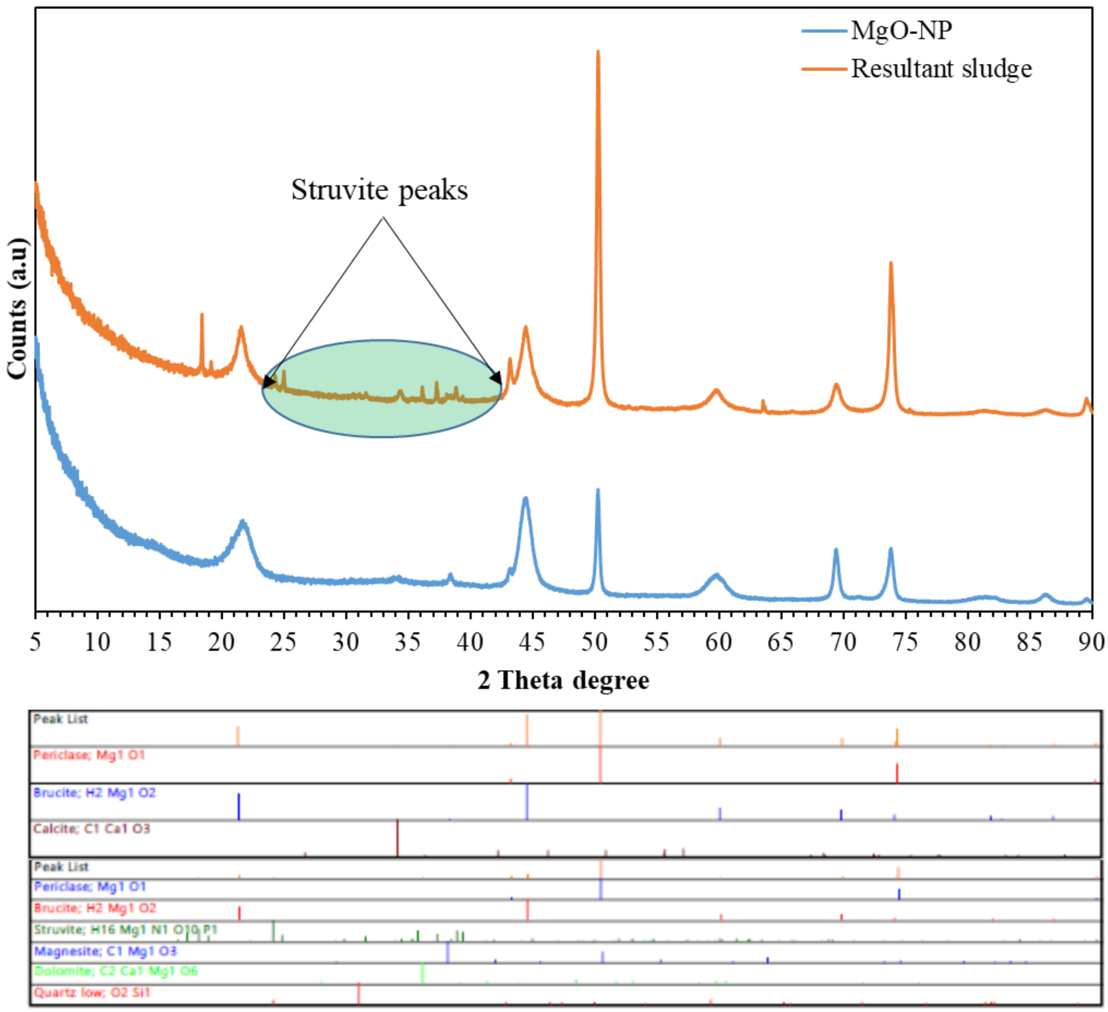

Figure 3.7: The mineralogical properties of Activated magnesite (MgO-NPs) and product sludge (struvite).

As shown in **Figure 3.7**, the activated magnesite (MgO-NPs) comprises periclase, brucite and calcite. Other studies reported similar results (Masindi et al., 2018; Mavhungu et al., 2019). Of importance is the presence of calcite and brucite found in the feed product, which will contribute to the introduction of calcium and magnesium. The magnesium will react with ammonia found in canal water and phosphate to form the struvite **(Equation 3.3)**. Furthermore, the dissolution of Mg and Ca will also increase the pH value **(Equation 3.4-3.5)**. The resultant higher pH is responsible for the oxidation of metals and deactivation of the microbial load found in water, which explains the reduction in concentration from effluent water.

$$\mathrm{MgO + H_2O \rightarrow Mg^{2+} + 2OH^-} \quad (3.4)$$

$$\mathrm{CaO + H_2O \rightarrow Ca^{2+} + 2OH^-} \quad (3.5)$$

Figure 3.7 shows the observed peaks of periclase, calcite, struvite, magnesite, dolomite and quartz in the product sludge. More importantly, the observed struvite peaks in the product sludge further substantiate the reduction of ammonia in surface water through the reaction of magnesium, phosphate, and ammonia, forming struvite, also known as MAP.

3.3.2.4.2 Morphological properties

The morphological properties of the activated magnesite (MgO-NP) and product sludge were evaluated using a high-resolution (HR) Focused Ion Beam (FIB) Scanning Electron Microscope (SEM) (HR-FIB-SEM), and the results are presented in **Figure 3.8**.

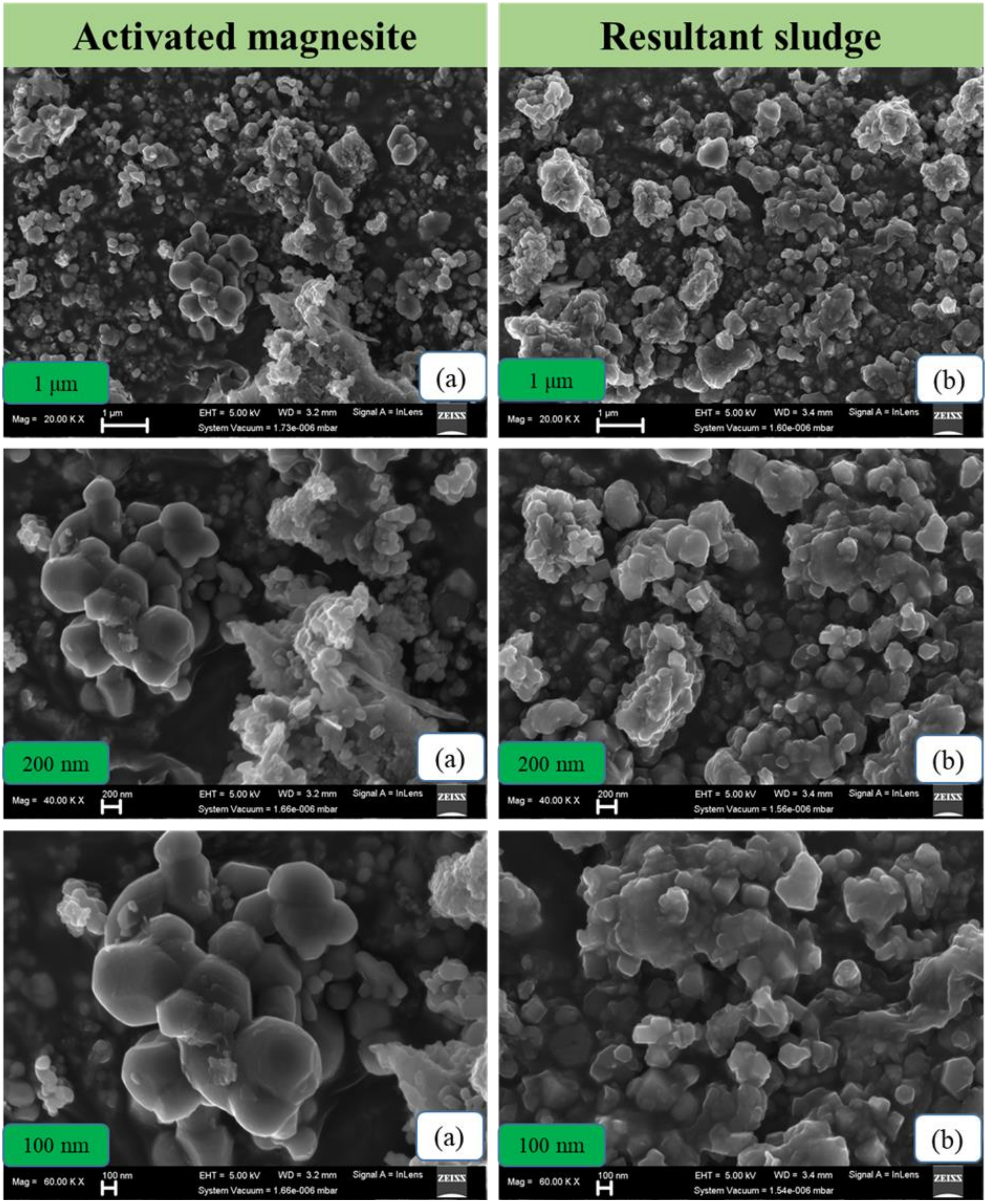

Figure 3.8(a-b): The morphological properties of activated magnesite (a) and product sludge (b) obtained by FESEM at 1 µm, 100 nm, and 200 nm.

Figure 3.8 (a) shows that the activated magnesite (MgO-NP) had nano-sheet-like structures with hexagonal structures distributed across the surface. A similar observation was observed in previous studies (Masindi et al., 2018, Mavhungu et al., 2019). Furthermore, **Figure 3.8(b)** shows changes in the morphological characteristics of the feed material, hence suggesting dissolution and possible deposition of new chemical phases. In **Figure 3.8(b)**, the formed structures in the product sludge are observed to be constituted of both irregular and orthorhombic shaped structures, and similar structures were observed in previous studies (Li et al., 2012, Alemu et al., 2020, Chen et al., 2022). Previous research studies have reported that struvite crystals have varying shapes, which can include a needle-like shape (Huang et al., 2014), coffin shape (Prywer et al., 2012) and feather shape (Liu et al., 2013), amongst others. Heraldy et al. (2017) and Ronteltap et al. (2010), after evaluating the varying shapes, concluded that shape is primarily dependent on formation conditions. Furthermore, Masindi et al. (2018) further expanded on the influence of struvite's shape and reported that the feed material's purity and constituents influenced the produced struvite morphology.

3.3.2.4.3 Chemical Species-functional group using FTIR

The Fourier transform infrared spectroscopy FTIR was considered for the evaluation of the inner structure of the feed material (MgO-NP) and produced sludge, and the results are presented in **Figure 3.9**.

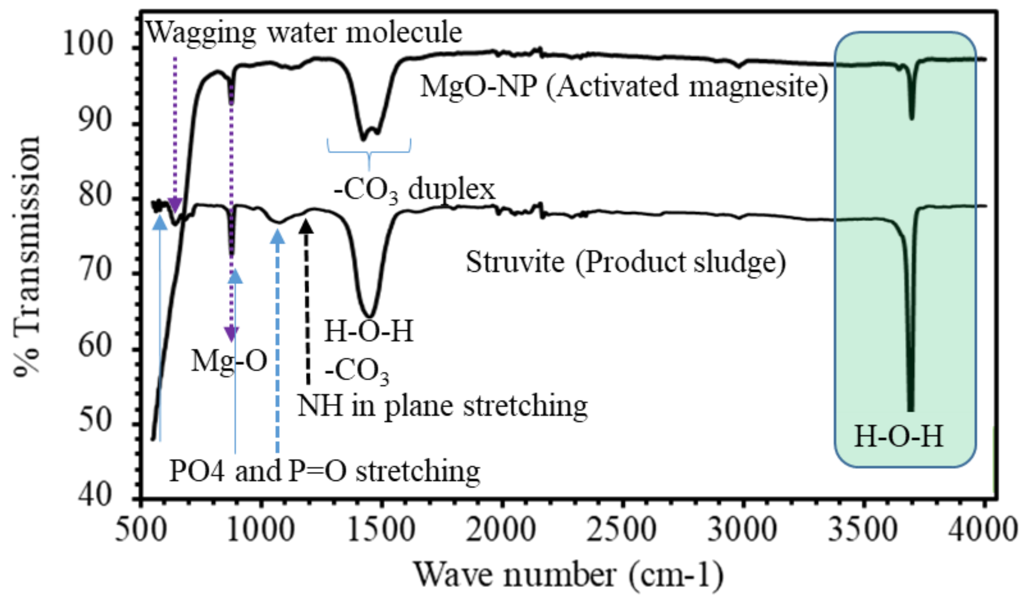

Figure 3.9: The functional groups of activated magnesite (MgO-NP) and product sludge.

Struvite in water comprises phosphate, ammonia, and magnesium ions (MAP). As such, for the FTIR characterisation, the focus is on identifying those primary elements. **Figure 3.9** shows the results of the activated magnesite and product sludge. As shown in **Figure 3.9**, the feed product, activated magnesite functional groups included Mg-O metal-oxygen bond, carbonates duplexes and water hydration (hydroxyl groups). The presence of a water group within the feed product indicates the likelihood of finding brucite in the feed product. These results corroborate with the results presented in Section 3.3.2.4.1 (XRD results). Previous studies observed similar peaks (Masindi et al., 2018; Mavhungu et al., 2019). More importantly, the FTIR results of the product sludge exhibit Mg-O metal-oxygen bond, N-H bond in-plane stretching and PO_4 and P=O stretching. These results confirm that magnesium, phosphate, and ammonia formed the struvite. The observed wavenumbers of peaks on the product sludge were in good agreement with other studies (Heraldy et al., 2017, Masindi et al., 2018, Mavhungu et al., 2019, Chen et al., 2022) and supported the XRD and water analysis results.

3.3.3 Secondary stage (Phase 2): Breakpoint chlorination

3.3.3.1 Effects of molar ratios on breakpoint chlorination

The effect of the initial chlorine dosages on the removal of residual ammonia from the product water is shown in **Figure 3.10**.

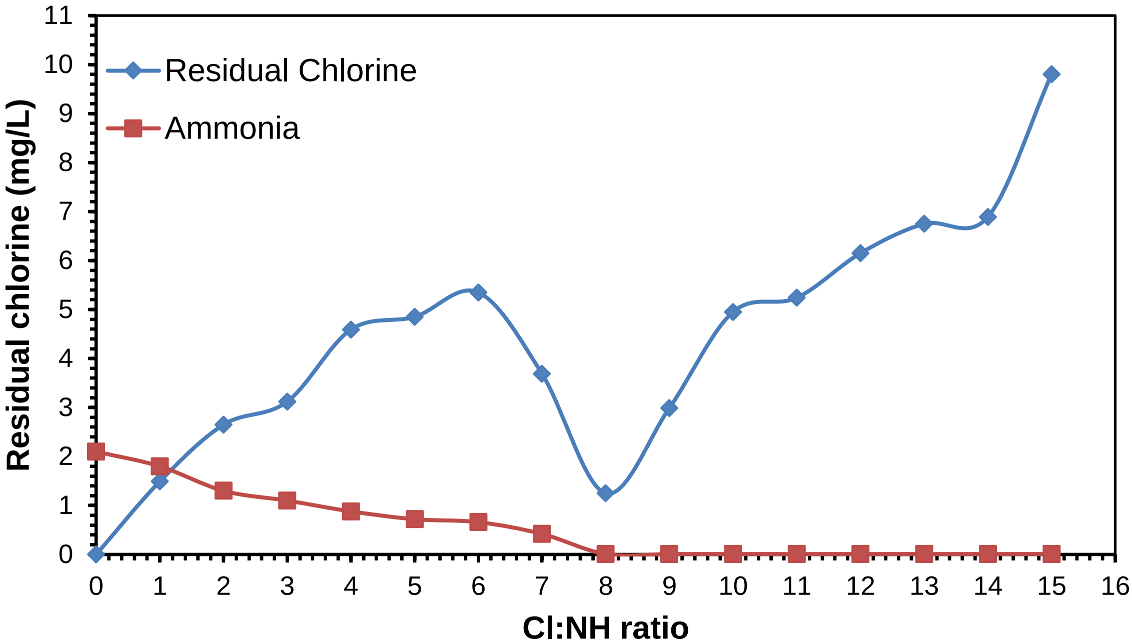

Figure 3.10: The effect of initial chlorine dosages on removing residual ammonia from the product water (Experimental conditions: 2.1 mg/L N of ammonia, 200 rpm mixing speed, 30 minutes contact time and ambient temperature).

The breakpoint chlorination curve, shown in **Figure 3.10**, displays a typical curved shape, as was also demonstrated by other researchers (Yang et al., 2005, Zhang et al., 2011, Stefán et al., 2019). As shown in **Figure 3.10**, the ammonia concentration decreased with increased chlorine. The complete removal of ammonia was achieved at a Cl_2:NH_3 weight ratio of 8:1. At a Cl_2:NH_3 weight ratio of 8:1, the residual ammonia was observed to decline to ≤0.009 mg/L N. Stoichiometrically, complete de-ammonification can be achieved by a Cl_2:NH_3 weight ratio of 7.6:1 (Pressley et al., 1972, Chen et al., 2022). However, water intermediaries can lead to chlorine competition (Pressley et al., 1972, Takó, 2012, Sharma et al., 2021), necessitating a higher dose of hypochlorite (chlorine) for the complete de-ammonification process. Furthermore, monochloramine and hypochlorous (HOCl) side reactions can potentially increase the need for hypochlorite (Fang et al., 2018), leading to higher dosages. Increasing the Cl_2:NH_3 ratio beyond the breakpoint did not significantly improve ammonia removal (**Figure 3.10**). The mechanism for breakpoint chlorination is explained using **Equation (3.6-3.9)** (Takó, 2012, Capodaglio et al., 2015, Adam et al., 2019):

$$\mathrm{Ca(ClO)_2 + 2H_2O \rightarrow 2HOCl + Ca^{2+} + 2OH^-} \quad (3.6)$$
$$\mathrm{NH_4^+ + HOCl \rightarrow NHCl + H_20 + \ H^+} \quad (3.7)$$
$$\mathrm{NH_4^+ + HOCl \rightarrow NH_2Cl + H_20 + \ H^+} \quad (3.8)$$
$$\mathrm{2NH_2Cl + HOCl \rightarrow N_2 \uparrow +3HCl + H_2O} \quad (3.9)$$

Initially, calcium hypochlorite converts to HOCl in water **(Equation 3.6),** which then reacts with ammonia to form monochloramine **(Equation 3.7)**. Continuous addition of chlorine converts the monochloramine to dichloramine **(Equation 3.8)** and then to nitrogen gas which escapes to the atmosphere leading to complete de-ammonification of ammonia in water **(Equation 3.9)**. Many studies reported a stoichiometric weight ratio of 7.6:1 of Cl_2:NH_3 as suitable for complete oxidation of ammonia to nitrogen gas, provided that ammonia is the only dominant demand species in the water (Pressley et al., 1972, Capodaglio et al., 2015, Stefán et al., 2019). However, studies have shown that the theoretical ratio is accurate only in synthetic water (ideal system). Higher ratios were reported when the technology was applied to natural water sources with constituents such as natural organic matter (NOM). Pressley et al. (1972) predicted that a Cl_2:NH_3 weight ratio of 8:1 in a system with ammonia, the chlorine demand will be able to remove ammonia as nitrogen. Takó (2012) reported on a study conducted by Laky et al. (2010), who decomposed ammonia to nitrogen at a Cl_2:NH_3 ratio of 8.6:1. Specifically, Takó (2012) argued that if the water contains natural organic matter (NOM) and iron (Fe), the chlorine demand will increase leading to higher chlorine dosages required to decompose ammonia.

3.3.3.2 Trihalomethanes (THMs) formation and speciation

Trihalomethanes (THMs) are chemicals mainly found in water after treatment with chlorine. The concentrations of THMs in water is dependent on concentration of organic material, chlorine dosage and the water temperature. Four THMs are formed, namely bromoform, chloroform, bromodichloromethane, and dibromochloromethane. Long term exposure to THMs exceeding drinking water limits can be carcinogenic. The potential formation of trihalomethane (THM) and its speciation with varying chlorine dosages are presented in

Figure 3.11.

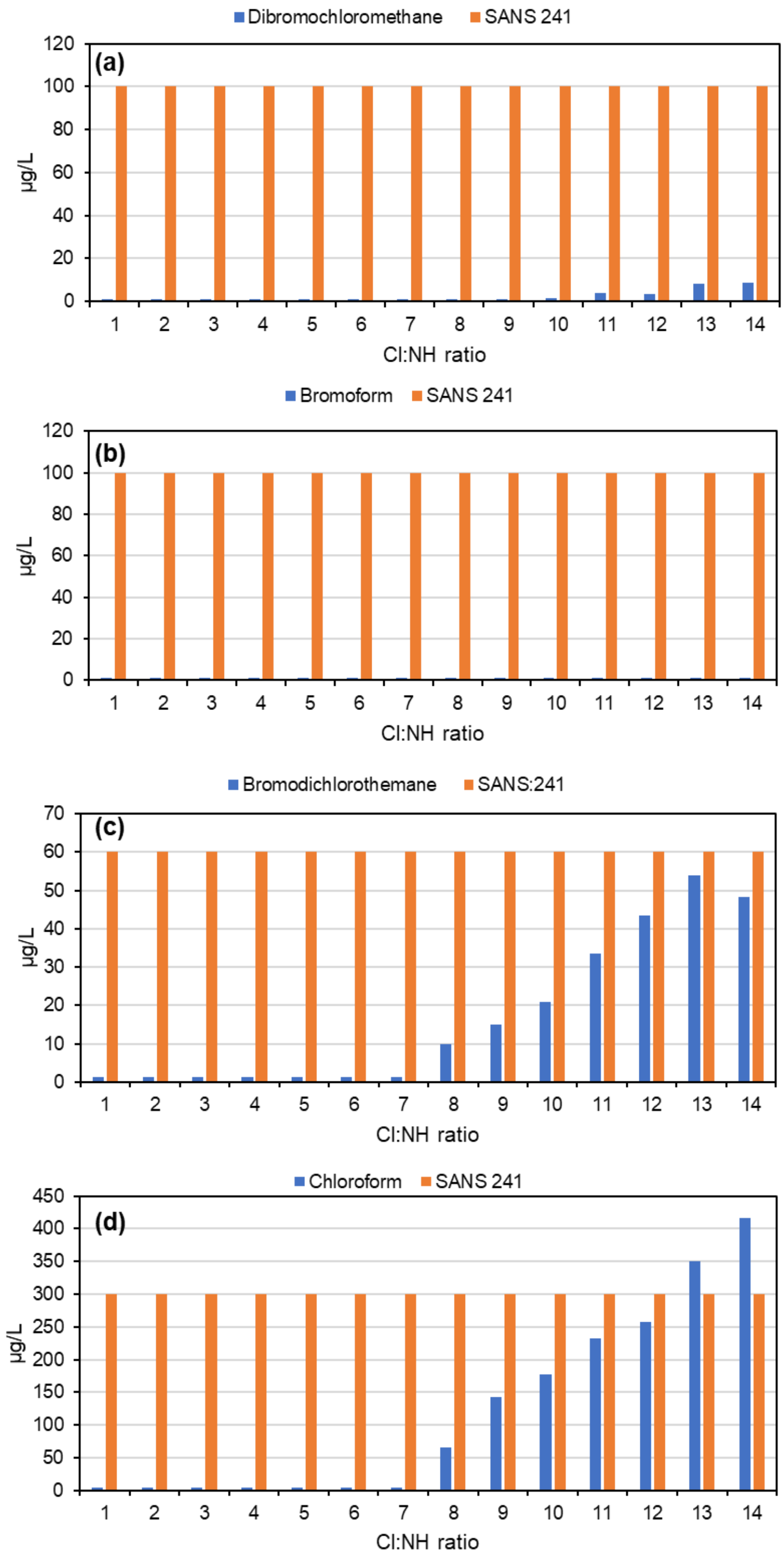

Figure 3.11: The potential formation of trihalomethane (THM) and its speciation with varying chlorine dosage (Experimental conditions: 2.1 mg/L N of ammonia, 200 rpm mixing speed, 30

minutes contact time and ambient temperature) (a) Dibromochloromethane (b) Bromoform (c) Bromodichloromethane (d) Chloroform.

As shown in **Figure 3.11 (a-d)**, the formation of four trihalomethanes, i.e., dibromochloromethane, bromoform, bromodichloromethane, and chloroform, were observed, and this was proportional to an increase in chlorine dosage. In particular, no change in trihalomethane concentrations was observed until the chlorine to ammonia ratio increased to 8:1, and this is a point where complete de-ammonization of effluent was achieved (Breakpoint). **Figure 3.11 (c)** and **Figure 3.11(d)** show that as the chlorine to ammonia weight ratio increased to 8:1 and beyond, there was a spike in bromodichloromethane and chloroform was observed**.** Essentially, the concentration of both chloroform and bromodichloromethane increased with increasing chlorine dosage. The most abundant species was observed to be chloroform. As shown in **Figure 3.11(d)**, chloroform spiked significantly after breakpoint chlorination reaching 416 µg/L at a Cl_2:NH_3 weight ratio of 14:1, while bromodichloromethane reached 53 µg/L at the same ratio. Insignificant dibromochloromethane concentration increases were observed, reaching 8.2 µg/L at a Cl_2:NH_3 weight ratio of 14:1, as shown in **Figure 3.11(a)**.

Regarding bromoform, as evident from **Figure 3.12(b)**, increasing the Cl_2:NH_3 weight ratio had little or no significant impact on bromoform. From the observations in **Figure 3.11**, it can be inferred that chlorine reacts with ammonia first and then reacts with natural organic matter, which could be explained by lower-than-expected trihalomethane formation before breakpoint chlorination. Similar observations were reported in Stefán et al. (2019), where the formation of DBPs was driven by temperature and chlorine dosage and not so much by organic matter as was expected. Furthermore, the authors elucidated that the reaction of chlorine with natural organic matter results after complete de-ammonification.

In addition, the potential risk associated with THMs can be elaborated using the combined toxicity of all THMs. Combined toxicity of all THMs is calculated by dividing the individual concentrations of each THMs by its guideline value and summing up the division. Variation of the combined toxicity of all THMs as a function of chlorine to ammonia ratio are shown in **Figure 3.12**.

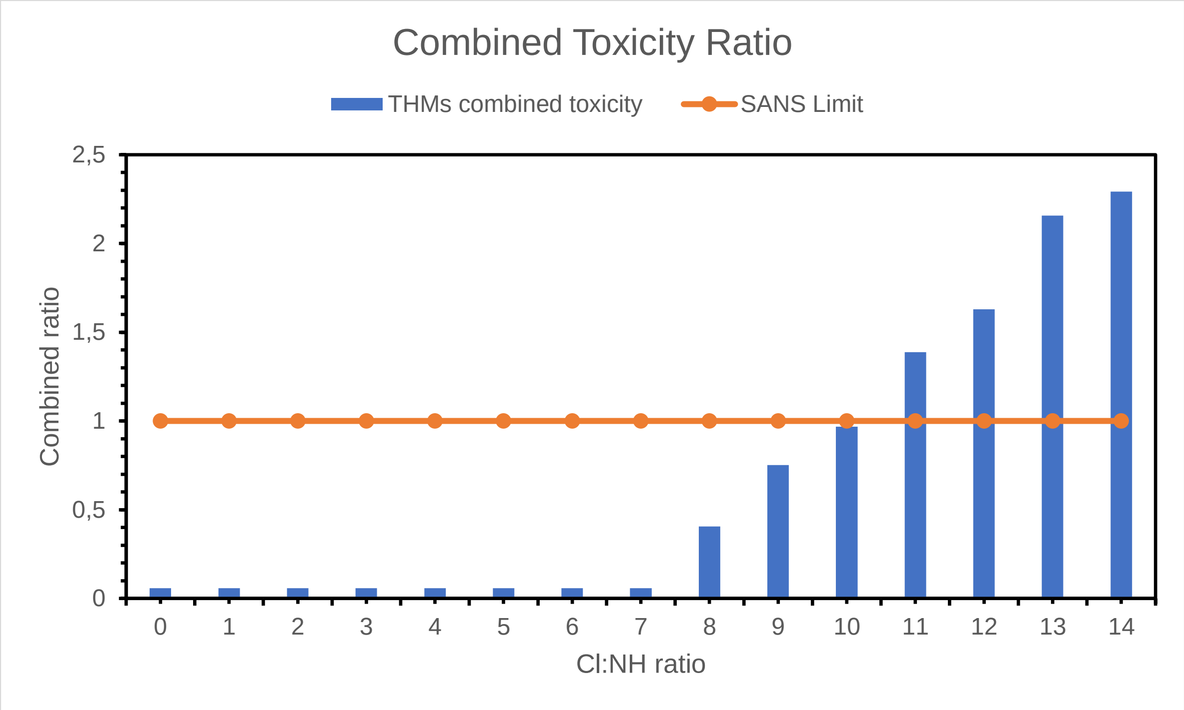

Figure 3.12: Variations in the combined toxicity of all THMs as a function of chlorine to ammonia ratio (Experimental conditions: 2.1 mg/L N of ammonia, 200 rpm mixing speed, 30 minutes contact time and ambient temperature).

As shown in **Figure 3.12**, the combined toxicity of all THMs notably increased after the breakpoint chlorination. Specifically, the combined toxicity increased from 0.056 when the Cl_2:NH_3 weight ratio was 7:1 to 0.405 at a Cl_2:NH_3 ratio of 8:1. The combined toxicity of all THMs continued to increase with increase in Cl_2:NH_3 ratio, eventually exceeding the WHO and SANS allowable limit of ≤1 at chlorine to ammonia weight ratio of 11:1 (Combined toxicity was 1.387). The trend continued an upward trajectory reaching a combined toxicity of 2.292 when the Cl_2:NH_3 weight ratio was 14:1. The potential increment in combined toxicity of all THMs after breakpoint emphasizes the need for closely monitoring breakpoint ratios to ensure compliance to South African national standards (SANS) for drinking water and WHO allowable regulated drinking water limits. To counter the potential for the formation of disinfection byproducts, potential polishing treatment, such as adsorption with powder-activated carbon (PAC), could be added after breakpoint chlorination to ensure compliance with disinfection by-products. Post disinfection with chlorine dioxide is another technology being extensively researched which can be incorporated to maintain residual in the distribution provided that pretreatment with chlorine is optimized to a breakpoint to avoid the formation of THMs.

3.4 Treatment of surface water at optimum conditions.

The microbiological, physical, and chemical characterisation of the raw and treated water after the two-stage treatment process, i.e., struvite treated (Stage 1) and breakpoint chlorination (Stage 2), at optimum condition are shown in **Table 3.2**.

Table 3.2: The microbiological, physical, and chemical characterisation of the raw and treated water after the two-stage treatment process, i.e., struvite treated (Stage 1) and breakpoint chlorination (Stage 2), at optimum condition.

Determinants	Units	SANS	Raw	Struvite (Stage 1)	Breakpoint (Stage 2)
E. coli	MPN/100 mL	ND	4800	ND	ND
Total coliform	MPN/100 mL	≤11	8700	57	ND
Total plate count	CFU/1 mL	≤1000	51385	6700	2
Nitrate	mg/L N	≤11	3.8	3.9	3.2
Nitrite	mg/L N	≤0.9	0.87	0.68	0.04
TOC	mg/L C	≤10	7.12	7.04	5.94
Iron	µg/L	≤400	11	≤ 0.37	≤ 0.37
Manganese	µg/L	≤100	174	4	≤ 0.09
pH @ 25°c	pH units	≤5.00 to ≤ 9.70	6.7	9.6	8.9
Turbidity	NTU	≤1	9.1	1.3	1.66
Ammonia	mg/L N	≤1.5	7.60	2.84	≤ 0.009
Phosphate	mg/L	≤ 10	0.66	0.11	0.12
Calcium	mg/L	≤ 300	31	12	19
Magnesium	mg/L	≤ 100	2.1	40	44
Chloroform	µg/L	≤ 300	3.35	3.35	145
Bromoform	µg/L	≤ 100	1.34	1.34	1.34
Dibromochloromethane	µg/L	≤ 100	1.24	1.24	3.45
Bromodichloromethane	µg/L	≤ 60	1.24	1.24	9.33

Finally, raw canal water was firstly treated under optimum conditions as identified in Sections 3.3.2.1.1 - 3.3.2.1.1 (mixing duration; 60 min, Mg:P dosage 110 mg/L, ambient temperature, and mixing speed of 150 rpm) with the effluent from Stage 1 undergoing a polishing stage with breakpoint chlorination at chlorine to ammonia weight ratio of 8:1 as the second stage of the treatment process. Raw water, struvite treated canal water (Stage 1), and breakpoint chlorination results are reported in **Table 3.2**. Raw water comprised elevated levels of organic, microbial, and inorganic contaminants. These parameters were identified to be above the prescribed limits stipulated in SANS 241 and WHO specifications. From the results in **Table 3.2**, it can be deduced that the optimal struvite precipitation conditions (Stage 1) can effectively remove or reduce the identified risk pollutants. Interestingly, the addition of calcined magnesite (MgO-NP) increased the pH from 6.7 to 9.6, thus creating conducive conditions for oxidation metals iron and manganese. Specifically, iron and manganese removal rates were ≥ 99%, respectively. More importantly, the main pollutant, ammonia, as shown in **Table 3.2**, was reduced to 2.84 mg/L from an initial concentration of 7.60 mg/L (62.63% ammonia removal). Henceforth, the residual concentration of ammonia was still higher than the SANS 241 and WHO limit (≤1.5 mg/L N), needing further treatment to lower ammonia concentration to drinking water standards. The introduction and observed reduction of magnesium and phosphate with ammonia (**Table 3.2**) in the final effluent coupled with an increment in pH from 6.7 to 9.6, is a clear indication that a reaction is occurring leading to the attenuation of these compounds and the formation of magnesium ammonia phosphate (MAP), or struvite. In addition, water treatment under optimal conditions was observed to be effective in dealing with microbial species in water, as shown in **Table 3.2**. The *E. coli* was completely removed from the canal water from an initial concentration of 4800 MPN/100mL, while coliform and TPC were reduced from 8700 MPN/100mL and 51835 CFU/1mL to 57 MPN/100mL and 6700 CFU/1mL, respectively in stage 1. The non-detection of *E. coli*, ≥ 99% reduction in coliform bacteria and ≥ 87% reduction in TPC bacteria in the final water suggests that higher pH or alkaline conditions are not suitable for the survival of the bacterial community. The optimal pH for incubating microbial community ranges from 6 to 8 (Navab-Daneshmand et al., 2022). The secondary treatment effluent results are shown in Stage 2 in **Table 3.2**. The secondary treatment conditions were at a mixing rate of 200 rpm and a contact time of 30 minutes with chlorine added to make a Cl_2:NH_3 ratio of 8:1. With raw water containing 7.12 mg/L of organic carbon (TOC), insignificant changes were observed in the effluent of Stage 1. However, the level reduced to 5.94 mg/L C after Stage 2. This, in turn, emphasizes that the reaction between chlorine and the natural matter is an adverse reaction only occurring after the complete breakdown of ammonia. As shown in **Table 3.2**, at breakpoint chlorination, TPC was reduced by ≥ 99% while coliform bacteria completely deactivated, and a complete breakdown of ammonia was achieved (≤ 0.009 mg/L N) while THM formation was limited to the reaction of

TOC with chlorine and with increments in chloroform (145µg/L) and bromodichloromethane (9.33µg/L) observed after ammonia was completely removed. breakpoint. However, the THMs concentrations were lower than the SANS 241 limits. Notable Ca increases (19 mg/L) in Stage 2 effluent were observed after calcium hypochlorite was added as a chlorine source. Furthermore, the Stage 2 effluent turbidity increased to 1.66 NTU because of oxidation reactions. The integrated technology (based on **Table 3.2**) effectively removed the identified pollutants except for turbidity, which exceeded the SANS 241 limit. The potential benefits of the integrated technology consist of lowering the operational cost. The calcined magnesite dosage increased the pH of water, eliminating the need for calcium hydroxide, but only a slight coagulant dosage will be required to lower the turbidity to the required standards as recommended by SANS 241 (≤1 NTU) (SABS, 2015).

3.5 Conclusions

This study successfully proved the effectiveness of integrating struvite synthesis and breakpoint chlorination. An integrated and hybrid technology, which employed struvite precipitation as pre-treatment and breakpoint chlorination as the polishing stage, was found to be effective in removing ammonia, microbial species (*E. coli,* total coliform and TPC) and iron and manganese to levels below the SANS 241 limit. The optimum conditions were Stage 1, 110 mg/L of Mg and P dosage (concentration), 150 rpm of mixing speed, 60 minutes of contact time, and lastly, 120 minutes of sedimentation, while optimum conditions for the breakpoint chlorination (Stage 2) were achieved at 30 minutes of mixing and a Cl_2:NH_3 weight ratio of 8:1. In Stage 1, i.e., for the MgO-NPs, the pH increased from 6.7 to ≥ 9.6, while the turbidity was reduced from 9.1 to ≤ 1.3 NTU. Iron (Fe) was removed entirely (11 mg/L to ≤ 0.37 mg/L), and Manganese (Mn) attained ≥ 97% removal efficacy (174 µg/L to ≤ 4 µg/L. Elevated pH levels also led to the deactivation of *E. coli*, while total coliform and TPC bacteria were reduced by ≥ 99% and ≥ 87%, respectively. In Stage 2, i.e., breakpoint chlorination, the product water was further polished through the elimination of residual ammonia at a Cl_2:NH_3 weight ratio of 8:1. Ammonia was reduced from 7.6 to 2.84 mg/L in Stage 1 (62.63% removal) and then from 2.84 to ≤0.009 mg/L post breakpoint chlorination (≥ 99% ammonia removal). Furthermore, the introduction of chlorine deactivated residual coliform and TPC bacteria. Lastly, from breakpoint chlorination and beyond, disinfectants by-products (DBPs) formed, with chloroform as the most dominant DBP. However, the DBPs were lower than regulated standards at breakpoint chlorination. Overall, the synergistic and complementary effects of integrating struvite synthesis and breakpoint chlorination hold great promise for the removal of contaminants from surface water.

References

Abu Hasan, H., Sheikh Abdullah, S. R., Kamarudin, S. K., Tan Kofli, N. & Anuar, N. 2014. Kinetic evaluation of simultaneous COD, ammonia and manganese removal from drinking water using a biological aerated filter system. Separation and Purification Technology, 130, 56-64.

Adam, M. R., Othman, M. H. D., Abu Samah, R., Puteh, M. H., Ismail, A. F., Mustafa, A., A. Rahman, M. & Jaafar, J. 2019. Current trends and future prospects of ammonia removal in wastewater: A comprehensive review on adsorptive membrane development. Separation and Purification Technology, 213, 114-132.

Ahring, B. K., Alatriste-Mondragon, F., Westermann, P. & Mah, R. A. 1991. Effects of cations on Methanosarcina thermophila TM-1 growing on moderate concentrations of acetate: production of single cells. Applied Microbiology and Biotechnology, 35, 686-689.

Alemu, A., Fanta, A., Liu, W., Dessie, A., Hao, X. & Wang, A. 2020. Rift Valley Lake as a potential magnesium source to recover phosphorus from urine. Environmental Research, 184, 109363.

Altomare, M. & Selli, E. 2013. Effects of metal nanoparticles deposition on the photocatalytic oxidation of ammonia in TiO2 aqueous suspensions. Catalysis Today, 209, 127-133.

American Public Health, A., American Water Works, A. & Water Environment, F. 1998. Standard methods for the examination of water and wastewater, Washington, D.C., APHA-AWWA-WEF.

Capodaglio, A. G., Hlavínek, P. & Raboni, M. 2015. Physico-chemical technologies for nitrogen removal from wastewaters: a review %J Revista Ambiente & Água. 10, 481-498.

Carolina González, M. 2019. Effect of the stirring speed on the struvite formation using the centrate from a WWTP. Revista Facultad de Ingeniería.

Charrois, J. & Hrudey, S. 2007. Breakpoint chlorination and free-chlorine contact time: Implications for drinking water N-nitrosodimethylamine concentrations. Water Research, 41, 674-82.

Chen, Y., Long, J., Chen, S., Xie, Y., Xu, Z., Ning, Z., Zhang, G., Xiao, T., Yu, M., Ke, Y., Peng, L. & Li, H. 2022. Multi-step purification of electrolytic manganese residue leachate using hydroxide sedimentation, struvite precipitation, chlorination and coagulation: Advanced removal of manganese, ammonium, and phosphate. Science of The Total Environment, 805, 150237.

Chowdhury, S. 2013. Trihalomethanes in drinking water: Effect of natural organic matter distribution. Water S.A, 39, 1-17.

Darwish, M., Aris, A., Puteh, M. H., Jusoh, M. N. H. & Abdul Kadir, A. 2017. Waste bones ash as an alternative source of P for struvite precipitation. J Environ Manage, 203, 861-866.

Devi, P. & Dalai, A. K. 2021. Implications of breakpoint chlorination on chloramines decay and disinfection by-products formation in brine solution. Desalination, 504, 114961.

Ding, Y. & Sartaj, M. 2016. Optimization of ammonia removal by ion-exchange resin using response surface methodology. International Journal of Environmental Science and Technology, 13, 985-994.

Ekama, G. A. 2011. 4.14 - Biological Nutrient Removal A2 - Wilderer, Peter. Treatise on Water Science. Oxford: Elsevier.

Etheridge, J. 2019. Water in Hammanskraal not fit for human consumption - SAHRC [Online]. News 24. [Accessed 23/12/2019 2019].

Guan, Q., Zeng, G., Gong, B., Li, Y., Ji, H., Zhang, J., Song, J., Liu, C., Wang, Z. & Deng, C. 2021. Phosphorus recovery and iron, copper precipitation from swine wastewater via struvite crystallisation using various magnesium compounds. Journal of Cleaner Production, 328, 129588.

Hakimi, M. H., Jegatheesan, V. & Navaratna, D. 2020. The potential of adopting struvite precipitation as a strategy for the removal of nutrients from pre-AnMBR treated abattoir wastewater. J Environ Manage, 259, 109783.

Heraldy, E., Rahmawati, F., Heriyanto, H. & Putra, D. 2017. Preparation of struvite from desalination waste. Journal of Environmental Chemical Engineering, 5.

Hu, L., Yu, J., Luo, H., Wang, H., Xu, P. & Zhang, Y. 2020. Simultaneous recovery of ammonium, potassium and magnesium from produced water by struvite precipitation. Chemical Engineering Journal, 382, 123001.

Huang, H., Liu, J., Wang, S., Jiang, Y., Xiao, D., Ding, L. & Gao, F. 2016. Nutrients removal from swine wastewater by struvite precipitation recycling technology with the use of Mg3(PO4)2 as active component. Ecological Engineering, 92, 111-118.

Huang, H., Xiao, D., Zhang, Q. & Ding, L. 2014. Removal of ammonia from landfill leachate by struvite precipitation with the use of low-cost phosphate and magnesium sources. Journal of Environmental Management, 145, 191-198.

Kim, D., Kim, J., Ryu, H.-D. & Lee, S.-I. 2009. Effect of mixing on spontaneous struvite precipitation from semiconductor wastewater. Bioresource Technology, 100, 74-78.

Kropp, R., Tompkins, D., Barry, T., Zeltner, W., Pepping, G., Anderson, M. & Barry, T. 2009. A device that converts aqueous ammonia into nitrogen gas. Aquacultural Engineering, 41, 28-34.

Li, D. Y., Cho, Y. C., Hsu, M. H. & Lin, Y. P. 2022. Recovery of phosphate and ammonia from wastewater via struvite precipitation using spent refractory brick gravel from steel industry. J Environ Manage, 302, 114110.

Li, Z., Ren, X., Zuo, J.-E., Liu, Y., Duan, E., Yang, J., Chen, P. & Wang, Y. 2012. Struvite Precipitation for Ammonia Nitrogen Removal in 7-Aminocephalosporanic Acid Wastewater. Molecules (Basel, Switzerland), 17, 2126-39.

Liu, B., Giannis, A., Zhang, J., Chang, V. W. & Wang, J. Y. 2013. characterisation of induced struvite formation from source-separated urine using seawater and brine as magnesium sources. Chemosphere, 93, 2738-47.

Marais, S. S., Ncube, E. J., Msagati, T. a. M., Mamba, B. B. & Nkambule, T. T. I. 2019. Assessment of trihalomethane (THM) precursors using specific ultraviolet absorbance (SUVA) and molecular size distribution (MSD). Journal of Water Process Engineering, 27, 143-151.

Masindi, V., Foteinis, S., Nduli, K. & Akinwekomi, V. 2021. Systematic assessment of SARS-CoV-2 virus in wastewater, rivers and drinking water – A catchment-wide appraisal. Science of The Total Environment, 149298.

Masindi, V., Gitari, M. W., Tutu, H. & Debeer, M. 2017. Synthesis of cryptocrystalline magnesite–bentonite clay composite and its application for neutralization and attenuation of inorganic contaminants in acidic and metalliferous mine drainage. Journal of Water Process Engineering, 15, 2-17.

Masindi, V., Ndiritu, J. G. & Maree, J. P. 2018. Fractional and step-wise recovery of chemical species from acid mine drainage using calcined cryptocrystalline magnesite nano-sheets: An experimental and geochemical modelling approach. Journal of Environmental Chemical Engineering, 6, 1634-1650.

Mavhungu, A., Masindi, V., Foteinis, S., Mbaya, R., Tekere, M., Kortidis, I. & Chatzisymeon, E. 2020. Advocating circular economy in wastewater treatment: Struvite formation and drinking water reclamation from real municipal effluents. Journal of Environmental Chemical Engineering, 8, 103957.

Mavhungu, A., Mbaya, R., Masindi, V., Foteinis, S., Muedi, K. L., Kortidis, I. & Chatzisymeon, E. 2019. Wastewater treatment valorisation by simultaneously removing and recovering phosphate and ammonia from municipal effluents using a mechano-thermo activated magnesite technology. Journal of Environmental Management, 250, 109493.

Navab-Daneshmand, T., Guo, B., Gehr, R. & Frigon, D. 2022. Impact of pH and removed filtrate on E. coli regrowth and microbial community during storage of electro-dewatered biosolids. Science of The Total Environment, 814, 152544.

O'driscoll, C., Sheahan, J., Renou-Wilson, F., Croot, P., Pilla, F., Misstear, B. & Xiao, L. 2018. National scale assessment of total trihalomethanes in Irish drinking water. J Environ Manage, 212, 131-141.

Pressley, T. A., Bishop, D. F. & Roan, S. G. 1972. Ammonia-nitrogen removal by breakpoint chlorination. Environmental Science & Technology, 6, 622-628.

Prywer, J., Torzewska, A. & Płociński, T. 2012. Unique Surface and Internal Structure of Struvite Crystals Formed by Proteus mirabilis. Urological research, 40.

Rice, E. W., Bridgewater, L., Association, A. P. H., Association, A. W. W. & Federation, W. E. 2012. Standard Methods for the Examination of Water and Wastewater, American Public Health Association.

Ronteltap, M., Maurer, M., Hausherr, R. & Gujer, W. 2010. Struvite precipitation from urine – Influencing factors on particle size. Water Research, 44, 2038-2046.

Ryu, H.-D. & Lee, S.-I. 2010. Application of struvite precipitation as a pretreatment in treating swine wastewater. Process Biochemistry, 45, 563-572.

SABS 2015. South African National Standard (SANS 241-1:2015) Drinking Water. Part 1: Microbiological, Physical, Aesthetic and Chemical Determinants. In: (SABS), S. D. O. T. S. A. B. O. S. (ed.). Pretoria, South Africa.

Sharma, N., Mohapatra, S., Padhye, L. P. & Mukherji, S. 2021. Role of precursors in the formation of trihalomethanes during chlorination of drinking water and wastewater effluents from a metropolitan region in western India. Journal of Water Process Engineering, 40, 101928.

Shu, J., Wu, H., Chen, M., Peng, H., Li, B., Liu, R., Liu, Z., Wang, B., Huang, T. & Hu, Z. 2019. Fractional removal of manganese and ammonia nitrogen from electrolytic metal manganese residue leachate using carbonate and struvite precipitation. Water Research, 153, 229-238.

Stefán, D., Erdélyi, N., Izsák, B., Záray, G. & Vargha, M. 2019. Formation of chlorination by-products in drinking water treatment plants using breakpoint chlorination. Microchemical Journal, 149, 104008.

Takó, S. Ammonium removal from drinking water–Comparison of the breakpoint chlorination and the biological technology. Conference of Junior Researchers in Civil Engineering, 2012. 248-254.

Tang, W., Zhang, Y., Bai, J., Li, J., Wang, J., Li, L., Zhou, T., Chen, S., Rahim, M. & Zhou, B. 2020. Efficient denitrification and removal of natural organic matter, emerging pollutants simultaneously for RO concentrate based on photoelectrocatalytic radical reaction. Separation and Purification Technology, 234, 116032.

US: EPA. 2019. Drinking water treatability database, Chloramine [Online]. Available: iuspub.epa.gov/tdb/pages/treatment [Accessed December 23, 2019 2019].

Vocciante, M., De Folly D'auris, A., Finocchi, A., Tagliabue, M., Bellettato, M., Ferrucci, A., Reverberi, A. P. & Ferro, S. 2018. Adsorption of ammonium on clinoptilolite in presence of competing cations: Investigation on groundwater remediation. Journal of Cleaner Production, 198**,** 480-487.

Wang, H., Su, Y., Zhao, H., Yu, H., Chen, S., Zhang, Y. & Quan, X. 2014. Photocatalytic Oxidation of Aqueous Ammonia Using Atomic Single Layer Graphitic-C3N4. Environmental Science & Technology, 48**,** 11984-11990.

Warmadewanthi, Rodlia, A., Ikhlas, N., Pandebesie, E. S., Bagastyo, A. Y. & Herumurti, W. 2020. The Effect of Mixing Rate on Struvite Recovery from The Fertiliser Industry. IOP Conference Series: Earth and Environmental Science, 506**,** 012013.

WHO 2017. Guidelines for drinking-water quality: fourth edition incorporating first addendum, Geneva, World Health Organization.

Wongcharee, S., Aravinthan, V. & Erdei, L. 2020. Removal of natural organic matter and ammonia from dam water by enhanced coagulation combined with adsorption on powdered composite nano-adsorbent. Environmental Technology & Innovation, 17**,** 100557.

Yang, X., Shang, C. & Huang, J.-C. 2005. DBP formation in breakpoint chlorination of wastewater. Water Research, 39**,** 4755-4767.

Zhang, H., Liu, H., Zhao, X., Qu, J. & Fan, M. 2011. Formation of disinfection by-products in the chlorination of ammonia-containing effluents: significance of Cl2/N ratios and the DOM fractions. J Hazard Mater, 190**,** 645-51.

Zhang, X., Li, W., Blatchley, E. R., Wang, X. & Ren, P. 2015. UV/chlorine process for ammonia removal and disinfection by-product reduction: Comparison with chlorination. Water Research, 68**,** 804-811.

Zöllig, H., Fritzsche, C., Morgenroth, E. & Udert, K. M. 2015. Direct electrochemical oxidation of ammonia on graphite as a treatment option for stored source-separated urine. Water Research, 69**,** 284-294.

CHAPTER FOUR

A pilot study on the removal of ammonia from river water using the integration of struvite synthesis and breakpoint chlorination

This chapter is devoted to addressing the following objectives:

- To perform a cost analysis of the chemicals used in the developed technology denoting the proposed system's viability.
- To compare the quality of product water with different water quality regulatory frameworks,

Abstract

The presence of ammonia in aqueous environments and solutions has been a topical issue of prime concern. Levels that exceed ≈1.5 mg/L in final water lead to the formation of nitrite, which has the potential to bind haemoglobin hence limiting the capacity of red blood cells to carry oxygen leading to myriads of health issues, including cyanosis, shortness of breath, nausea, headache, and dizziness. In addition, ammonia in drinking water hinders the oxidation of manganese while providing nutrients for bacterial growth, massively increases the operational cost, and in worst cases, leads to temporary plant shutdowns due to elevated levels of ammonia. In the present investigation, a pilot study for removing ammonia using the integration of struvite precipitation and breakpoint chlorination is reported. A 1000 litres (1 m^3) per run (LPR) pilot plant was utilised to fulfil the goals of this study. In particular, this novel techno-economic study adopted optimum conditions from laboratory assays, and they comprise 110 mg/L of Mg and P dosage (concentration), 150 rpm of mixing speed, 60 minutes of contact time, and lastly, 120 minutes of sedimentation (Stage 1) while the optimum condition for the breakpoint chlorination was 30 minutes of mixing and 8:1 Cl_2:NH_3 weight ratio (Stage 2). Results from this study demonstrated techno-viable synergistic and complementary effects, with, i.e., Stage 1 having an increase in pH from 8.15 to 10.16 and a steep reduction in manganese (≥99.0%) and iron (≥99%) concentrations, respectively. *E. coli* and coliform bacteria were completely deactivated, while TPC bacteria was reduced by 91%. The attenuation of ammonia was in the range of 6.73 mg/L to 2.40 mg/L-N (64.34% removal efficacy) was observed. In Stage 2, i.e. breakpoint chlorination, ammonia was reduced from 2.40 mg/L to ≤ 0.009 mg/L-N after the interaction of water with chlorine whilst the micro-organisms were completely removed. Lastly, but not least, economic evaluation amounted to **R4.85/kl (\$0.31/m^3**) chemical costs. However, there is a massive potential for cost savings (53.2%) by replacing Kh_2PO_4 with waste phosphoric acid. Finally, the techno-economic evaluation study's results showed great potential compared to similar studies. This will be a game-change and it will play a notable role in managing elevated levels of ammonia and other contaminants, specifically for low- and middle-income countries (LMIC), and further afield.

Keywords: Economic analysis; hybrid approach; struvite synthesis; breakpoint chlorination; ammonia removal; calcium hypochlorite (HTH); and real surface water treatment.

4.1 Introduction

Due to rapid population growth, various catchment activities, and industrialisation, surface water quality is continually deteriorating, which is attributed to notorious contaminants embedded therein. In particular, agricultural practices, mining activities, and municipal wastewater treatment plants have been identified as the main culprits impacting raw water quality for various uses. Of main concern is the concentration of ammonia, turbidity, iron (Fe), manganese (Mn), and microbial load; i.e., *E. coli,* faecal coliform, and total plate count, which perpetually increase hence aggravating the typical physicochemical and microbial state of raw water and its treatability index (Masindi, 2020). Water treatment entities abstract water from the river and underground reserves for purification purposes and distribute the cleaned water to different end-users. Most drinking water treatment systems follow a conventional treatment process chain, which comprises pre-oxidation, coagulation and flocculation, sedimentation, filtration, and post disinfection, and the main quest is to ensure that the end-product complies with the drinking water standards, specifications, and guidelines (Marais et al., 2019).

Worryingly, the continued deterioration of raw water quality, which concomitantly increases the treatment demand, has proportionally increased the treatment costs (Masindi, 2020). Drinking water treatment technologies have shown great efficiencies in dealing with turbidity, microbial load, Fe, and Mn, amongst other contaminants. However, the presence of ammonia constitutes a different challenge, and it seems very challenging and exorbitant to address such an issue in drinking water treatment plants. The maximum allowable limit for ammonia in drinking water is ≤ 1.5 mg/L N (SABS, 2015, WHO, 2017) and it is often above the limits, specifically for low- and middle-income countries (LMIC) with dilapidated, under-designed, and poorly maintained wastewater treatment infrastructure.

Specifically, ammonia in drinking water, can cause both operational and health challenges. Excess ammonia is known to cause blue baby syndrome and cancer of the stomach, pharynx and oesophagus (Chen et al., 2022). Furthermore, the ammonia affinity to chlorine hampers the oxidation of manganese in water, affecting the water treatment efficacy (Adam et al., 2019). Furthermore, manganese has the potential to affect water aesthetically at final water levels ≥ 100μg/L, tainting laundry and giving the water a metallic taste (WHO, 2017), while levels ≥ 400 μg/L affect the health of consumers, potentially leading to neurological disorders and induced mental illnesses (Chen et al., 2022). Regarding the environment, excess ammonia levels have led to depletion of oxygen in water, eutrophication and, most troubling, toxicity for fish, affecting aquaculture (Tekerlekopoulou and Vayenas, 2008, Bernardi et al., 2018). Taking into consideration both health and environmental effects of ammonia, its recovery and removal is imperative for sustainability and safety of potable water. Fortunately, numerous technologies have proven to be efficient for the removal of ammonia, especially in wastewater treatment works, albeit its excruciating and indispensable dependence on biological treatment processes.

Technologies that have been employed for the removal of ammonia rely on different mechanisms, which include, adsorption, precipitations, ion exchange, filtration, bio-sorption, bio (phyto)remediation, crystallisation, volatilization, and distillation (Tekerlekopoulou and Vayenas, 2008, Masindi and Foteinis, 2021, Masindi et al., 2022a). These technologies have advantages and disadvantages, but the preference for technology is chiefly based on cost-effectiveness, sustainability, efficacy, and sludge production. However, biological nutrient removal (BNR) technology is the most preferred technology due to its simplicity and effectiveness (Adam et al., 2019, Hakimi et al., 2020). However, the bacteria responsible for ammonia are sensitive to cold, i.e., winter conditions, hence hindering their efficacy and performance in cold conditions. Adsorption limits quick saturation and poor performance in concentrated solutions, while filtration and ion exchange generate brine and require exorbitant amounts of energy. On the other hand, chlorination technology is available in both the water and wastewater treatment process. However, high operational costs and the formation of carcinogenic by-products limit the application of this technology (Tekerlekopoulou and Vayenas, 2008). Struvite precipitation is the most sustainable and stable technology with the least environmental constraints, and it produces beneficial by-products that could beneficially be used as slow-release fertiliser hence fostering the concept of sustainability, circular economy, and valorisation of waste materials specifically when viewed under the recovery, recycle and re-use paradigm for wastewater beneficiation (Chen et al., 2022, Masindi et al., 2022b).

Struvite precipitation, even with high ammonia recovery yields, in most cases produces effluent with ammonia concentration higher than the ones required for drinking water limits, being ≥1.5 mg/L. Li et al. (2022) employed struvite precipitation using spent refractory brick gravel from the steel industry as magnesium recovers 99.6% phosphate and 98.2% ammonia. In their study, ammonia concentration was lowered from an initial concentration of 140 mg/L to 2.5 mg/L N, which is higher than the drinking water standards. The affluent will require polishing to reduce ammonia to required drinking water quality to comply with drinking water standards. Researchers are opting to integrate different treatment technologies and the main quest is to acquire the synergetic effects emanating from different techniques assembled to it to enhance the contaminants removal efficacy (Masindi et al., 2019). However, most studies are still in the early stages of development, with their efficacies evaluated on a laboratory scale. In light of that, the pre-treatment of ammonia-rich water via struvite precipitation to reduce ammonia as an initial stage of treatment attenuate ammonia to lower levels hence making it viable to introduce breakpoint chlorination as a polishing stage.

Recently, Chen et al. (2022) employed a treatment chain that included hydroxide precipitation, struvite precipitation, breakpoint chlorination and ferric coagulation to remove Mn and ammonia from Mn residue by the electrolyte. This has demonstrated the feasibility and effectiveness of integrating different technologies. Congruent to these findings, our laboratory studies successfully demonstrated the feasibility of integrating struvite precipitation as a pre-treatment step and breakpoint chlorination as a polishing stage. The study attained excellent results in terms of ammonia removal. Albeit, there was a dire need to upscale the technology and demonstrated it on a pilot scale, hence the main quest to determine the robustness of the technology in real settings. In light of that, this study, therefore, seeks to perform the cost analysis of the removal of ammonia from an aqueous environment using the integration of struvite synthesis and breakpoint chlorination.

4.2 Materials and Methods

4.2.1 Acquisition of the samples

Ammonia-rich raw water was collected from the canal system, which receives water from the Roodeplaat dam, Gauteng province, South Africa (25.62083°S 28.37138°E). The raw water was collected on 16 May 2022. Specifically, common catchment activities are wastewater treatment facilities and agricultural practices that are located upstream of the catchment. These activities, although not to the only sources, significantly contribute to introducing contaminants to the catchment. Thermo-chemically activated cryptocrystalline magnesite was procured from the Sterkfontein Carbonates (Pty) Ltd Company. A salt of 500 g of pure potassium dihydrogen phosphate was procured from Aqualytic™ (Pty) Ltd. Essentially, activated cryptocrystalline magnesite and the potassium dihydrogen phosphate salts were employed as fundamental sources of Mg^{2+} and PO_4^{3-}, respectively, for struvite synthesis. The ambient ammonia concentration in real river (canal) water was used as a seeding concentration, and the stoichiometry was cognizant of its respective levels. Finally, the calcium hypochlorite (High Test Hypochlorite - HTH) grains, ±70% of available chlorine, were supplied by Protea chemicals (Pty) Ltd, and this was effectively employed for the breakpoint chlorination experiments.

4.2.2 Description of the unit processes

The schematic illustration of the unit processes used for the integrated treatment of real river water for the removal of ammonia is shown in **Figure 4.1**. The system comprises two phases: phase 1 is struvite synthesis, and phase 2 is breakpoint chlorination.

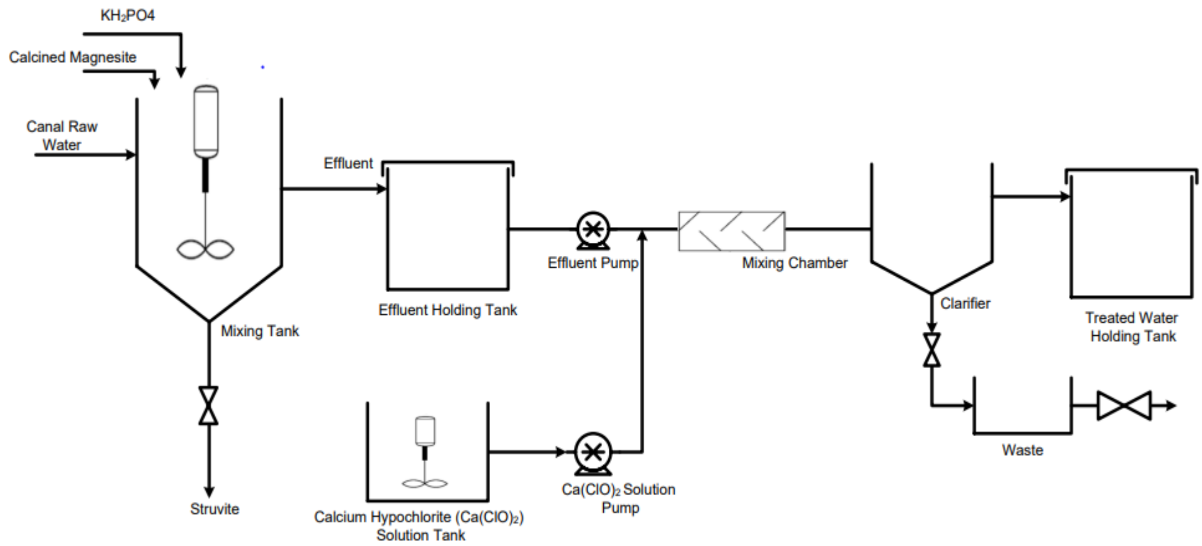

Figure 4.1: The schematic illustration of the unit processes used for the integrated treatment of real river water for the removal of ammonia.

4.2.2.1 Struvite synthesis (Stage 1)

In this stage, struvite precipitation was fulfilled as a first step towards attenuating ammonia from the real river water. Specifically, the thermo-mechano-chemically activated cryptocrystalline magnesite and potassium hydrogen phosphate (KH_2PO_4) were seeded in canal water to attain the required stoichiometry and facilitate the chemical reaction. The chief attempt was to remove aqueous ammonia as struvite through the combination of Magnesium Ammonia Phosphate (MAP), popularly known as struvite. The adopted optimum conditions were 110 mg/L of Mg and P dosage, mixing at 150 rpm of mixing speed, 60 minutes of contact time, and 120 minutes of sedimentation. After the experiments, the supernatant was transferred to a 1 m^3 reactor for the breakpoint experiment. In addition, the supernatant was also collected from this reactor, and it was analyzed for ammonia, phosphate, calcium, magnesium, pH, manganese, *E* coli, total coliform, free chlorine, nitrite, nitrate, calcium, total organic carbon (TOC), trihalomethanes (THMs) and pH. This was done to ascertain the performance of this system on a pilot scale and determine its relativity to the results obtained from the laboratory assays. Experiments were repeated three times, and the results were reported as mean values. This was done to determine the trustworthiness of the pilot scale (1000 L) results.

4.2.2.2 Breakpoint chlorination (Stage 2)

In Stage 2 of this study, the 1000 L/hr pilot plant was used for breakpoint chlorination studies. Specifically, the Ebara CDX-90/10, 0.75kW feed pump regulated flow to 2 L/s in a continuous flow reactor. The Seko TPR603 ORP pump dosed hypochlorite at chlorine to ammonia ratio of 8:1, which was optimal from the laboratory studies. The treated water (product water) was collected at the product water tank after 30 minutes. Thereafter, the supernatants were characterized for ammonia, phosphate, calcium, magnesium, turbidity, pH, manganese*, E* coli, total coliform, calcium, TOC, trihalomethanes (THMs) and pH. As demonstrated in section 4.2.2.1, the experiments were repeated 3 times and the results were reported as mean values. This was done to demonstrate the robustness of the system and its ability to give consistent results at various experimental runs.

4.2.3 Characterisation

4.2.3.1 Characterisation of aqueous samples

Ammonia was quantified using the Gallery Plus analyser (Anotec) (Discreet Analyser). Disinfection by-products, i.e., THMs, were analysed with the Agilent Chromatography Mass Spectrometry (GC-MS) (Agilent technologies 5975 C, CA, USA), which is connected to a purge and trap sample concentrator (OI Analytical Eclipse 4660 Purge and Trap Sample Concentrator). The pH and electrical conductivity were determined using an HQ40d multimeter probe. The turbidity was ascertained using the HACH 2100 AN turbidity meter. The Hach equipment was procured from the Hach Company (Pty) Ltd (Colorado, Loveland, USA). The metal concentrations of Fe and Mn were evaluated using an Inductively Coupled Plasma Optical Emission Spectrometer (ICP-OES) (Agilent, Santa Clara, CA, USA). The total organic carbon (TOC) was ascertained using a Shimadzu model TOC-L CPH analyser (Shimadzu Corporation, Japan). The *E. coli* and total coliform were determined using the Colilert method. Specifically, the Colilert method employs a substrate technology wherein the coliforms metabolise nutrient indicators ONPG (detection of β-galactosidase activity) and *E. coli* metabolises the MUG substrate (detection of β-D-glucuronidase activity). Lastly, the pour plate method was employed for levels of plate count (TPC).

Furthermore, standard methods were followed in analysing the samples (Rice et al., 2012). In addition, sample analyses were conducted in an ISO 17025 accredited laboratory. The National Institute of Standards and Technology (NIST) standards and inter-laboratory analyses were performed to corroborate the results.

4.2.3.2 Characterisation of feed and product solids

Different analytical and state-of-the-art analytical instruments were used to understand the fate of ammonia in the struvite synthesis reactor. Specifically, the An Auriga Cobra FIB FESEM, Carl Zeiss supplied, Sigma VP FE-SEM, and HR-SEM coupled with EDS sputter technology, were utilised to ascertain microstructural properties and elemental composition of the feed and product sludge.

4.2.4 Economic Evaluation

The economic evaluation of the developed process was also performed. Specifically, the developed hybrid technology, i.e., struvite synthesis and breakpoint chlorination, demonstrated good performance in the laboratory scale experiments and similar results were acquired at a pilot scale. As such, the cost factor was observed to be the fundamental factor that could influence the implementation of this technology. This study systematically focused on the comparison of breakpoint chlorination alone and the hybrid system. The quest was to demonstrate the effect of synergy on the costs and efficacy. To quantify the cost of treating surface water contaminated with ammonia, prices were acquired from the catalogue of different suppliers that prominently supply different water treatment plants in South Africa. The economic evaluation meticulously focused on chemicals. However, this assessment did not include costs related to civil, equipment, maintenance, electrical and labour. This could be attributed to the fact that there is no intention to change those functionalities except for the chemicals used to remove and decompose ammonia from an aqueous solution fully.

4.3 Results and discussions

4.3.1 Water quality results

The current study meticulously employed the hybrid approach to effectively remove ammonia from aqueous environments using a combination of struvite precipitation and breakpoint chlorination in a step-wise fashion. Specifically, the first stage, i.e., struvite precipitation, incorporated the use of calcined (activated) magnesite and potassium dihydrogen phosphate as magnesium and phosphate sources, whereas the second stage, comprising the polishing of ammonia from the product water (supernatant) emanating from the struvite reactor using breakpoint chlorination. The results depicting the performance of the hybrid approach on the removal of ammonia and other water quality risk parameters at optimal conditions as determined in our previous study are shown in **Table 4.1.**

Table 4.1: Feed water's microbiological, physical, and chemical properties before and after the removal of ammonia via struvite precipitation and breakpoint chlorination.

Determinants	**Units**	**WHO Limits**	**SANS Limits**	**Feed**	**Stage 1**	**Stage 2**
E. coli	MPN/100 mL	ND	ND	270	ND	ND
Total coliform	MPN/100 mL	ND	≤11	3, 600	ND	ND
Total plate count	CFU/1 mL	≤500	≤1000	26000	2340	4
TOC	mg/L C	-	≤10	7.81	7.26	4.58
Turbidity	NTU	≤5	≤1.5	5.21	1.71	2.36
Iron	µg/L	≤100	≤400	23	≤0.37	≤0.37
Manganese	µg/L	≤50	≤100	102	≤0.09	≤0.09
pH @ 25℃	pH units	6.5-8.8	≤5≤ 9.7	8.15	10.16	9.11
Ammonia	mg/L N	≤1.5	≤1.5	6.73	2.40	≤0.009
Phosphate	mg/L	-	≤ 10	6	0.25	0.55
Calcium	mg/L	-	≤ 300	36	8	30
Magnesium	mg/L	-	≤ 100	2.1	40	41
Chloroform	µg/L	≤ 300	≤ 300	3.35	3.35	206
Bromoform	µg/L	≤ 100	≤ 100	1.34	1.34	1.34
Dibromochloromethane	µg/L	≤ 100	≤ 100	1.24	1.24	4.99
Bromodichloromethane	µg/L	≤ 60	≤ 60	1.24	1.24	24.8

As shown in **Table 4.1**, the obtained results were congruent with the results obtained in our previous study. Specifically, microbial and inorganic contaminants were significantly removed from the aqueous solution. Furthermore, *E. coli*, total coliform, iron, and manganese were significantly removed in stage one of the chemical reaction. In addition, Table 4.1 shows a significant reduction in ammonia and TPC in the final water in Stage 1 of the treatment process. However, the effluent concentrations of 2.40 mg/L of ammonia and 2340 CFU/1mL of TPC were non-compliant with the world health organization (WHO) and SANS 241 allowable limits of ≤1.5 mg/L N for ammonia, ≤ 500 CFU/1mL and ≤1000 CFU/1mL for TPC respectively.

Furthermore, the pH increased significantly in Stage 1 of the treatment process and reached pH ≥10**.** An increase in pH was primarily due to the dissolution of activated cryptocrystalline magnesite. Furthermore, calcined (activated) magnesite comprised trivial amounts of calcite and brucite (periclase) and their dissolution contributed to the introduction of calcium and magnesium to the waterbodies (Masindi et al., 2018, Mavhungu et al., 2019). Thenceforth, an increase in pH agrees with results from our laboratory scale studies and other studies reported in the literature (Masindi et al., 2017, Mavhungu et al., 2019, Mavhungu et al., 2021). Furthermore, the dissolution of magnesium and calcium also contributes to an increase in pH, as illustrated by **Equations 4.1 and 4.2**.

$$\mathrm{MgO + H_2O \rightarrow Mg^{2+} + 2OH^-} \quad (4.1)$$

$$\mathrm{CaO + \ H_2O \rightarrow Ca^{2+} + \ 2OH^-} \quad (4.2)$$

The alkaline conditions with pH ≥ 10, created after the dissolution of the activated magnesite or MgO-NPs, could possibly hinder the growth of bacteria, leading to their complete deactivation, with *E. coli* and coliform bacteria reaching ≈99.9% reduction, whilst TPC reached 91% reduction. In addition, the higher pH, i.e., pH ≥ 9, led to the removal of Mn, as illustrated by **Equation 4.3**.

$$\mathrm{Mn^{2+} + nOH^- \rightarrow Mn(OH)_2} \quad (4.3)$$

More importantly, from **Table 4.1**, the results show a reduction in ammonia and calcium levels in the product water from **Stage 1**, while magnesium levels notably increased. As expected, magnesium increased from the dissolution of periclase and brucite. However, the magnesium will react with phosphate and ammonia in Stage 1 to form a combination of magnesium ammonia phosphate (MAP), popularly known as struvite which explains the reduction of ammonia from surface water as illustrated by **Equation 4.4**.

$$\mathrm{Mg^{2+} \ + \ NH_4^+ + H_nPO_{4n}^{3-} + 6H_2O \rightarrow MgNH_4PO_4.6H_2O + nH^+} \quad (4.4)$$

The reduction of calcium level from 36 mg/L to 8 mg/L could also be attributed to the dissolution of the potassium dihydrogen phosphate (KH_2PO_4). Optimal conditions involved dosages of 110 mg/L for both magnesium and phosphate$^-$ and residual levels of magnesium and phosphate of 40 mg/L and 0.25 mg/L, respectively, confirming reactions amongst ions in solution during struvite synthesis (Stage 1). The reduction of calcium results from a reaction with PO_4^{3-} forming calcium phosphate, as presented in **Equation 4.5**.

$$3Ca^{2+} + 2HPO_4^{2-} \rightarrow Ca_3(PO_4)_2 \downarrow + 2H^+ \quad (4.5)$$

In addition, the reduction of phosphate concentration to 0.25 mg/L in Stage 1 further shows phosphate as the limiting reagent with its high affinity to calcium, limiting the phosphate reaction with magnesium and ammonia, thus hindering the phosphate reaction with magnesium and ammonia and the formation of struvite. The obtained results are similar and congruent to what has been reported in the literature (Hu et al., 2020, Li et al., 2022). This will then require higher dosages of phosphate to overcome its demand and the effect of competing ions. Breakpoint chlorination was employed to polish the water to the required standard further, as stipulated in WHO and SANS-241 standards. Specifically, product water from Stage 1 comprised ammonia and TPC levels, i.e., 2.40 mg/L and 2340 CFU/1mL, respectively, that exceed the WHO and SANS 241 allowed limits. However, chlorination technology is primarily employed for deactivating bacteria and viruses (Adam et al., 2019, Sharma et al., 2021). In this phase of the study, hypochlorite was added for the removal of residual TPC (≈4 CFU/1mL), which became compliant with regulated limits of ≤ 500 CFU/1mL and ≤ 1000 CFU/1mL in WHO and SANS-241 standards, respectively (WHO, 2011, SABS, 2015). The interaction of hypochlorite and water is illustrated in **Equation 4.6**.

$$Ca(ClO)_2 + 2H_2O \rightarrow 2HOCl + Ca^{2+} + 2OH^- \quad (4.6)$$

As shown in **Equation 4.6**, the addition of high-test hypochlorite (HTH) introduces calcium into the solution. This further explains an increase in calcium level (30 mg/L) after product water treatment with hypochlorite, as shown in **Table 4.1**. Furthermore, the formed hypochlorous product is responsible for the deactivation of microorganisms. Its formation led to a reduction of the pH from 10.16 to 9.11 in Stage 2. More importantly, the optimal chlorination dosage of 8:1 to weight ratio of effluent ammonia was adequate to overcome the demand in the water, and it eventually led to the reduction of ammonia from 2.40 mg/L to ≤ 0.009 mg/L within 30 minutes of contact time, as shown in **Equation 4.7**.

$$NH_4^+ + 1.5\,HOCl \rightarrow 0.5N_2 \uparrow + 1.5\,H_2O + 2.5\,H^+ + 1.5\,Cl^- \quad (4.7)$$

Finally, adding chlorine also contributed to the formation of disinfection by-products (Marais et al., 2019, Stefán et al., 2019, Sharma et al., 2021). As such, an increment in the levels of THMs was observed after the interaction of chlorine with product water, as shown in **Table 4.1.** Specifically, chloroform (206 µg/L) and bromodichloromethane (24.8 µg/L) were the most prevalent THMs. This finding is similar to the results by Marais et al. (2019). Furthermore, in **Table 4.1,** the TOC concentration reduced from 7.26 mg/L to 4.58 mg/L after adding chlorine, hence inciting the formation of THMs, since an adverse reaction occurs after the removal of ammonia. This finding is similar to findings reported in other studies (Takó, 2012, Stefán et al., 2019, Sharma et al., 2021). Turbidity increased from 1.71 NTU in stage 1 to 2.36 NTU after stage 2 due to oxidation reaction after the addition of chlorine. Lastly, although there was the formation of THMs, the levels were still below the drinking water standard. Finally, the combined technology proved to have significant potential in ensuring compliance with potable water standards.

4.3.2 Solids characterisation

This section shows insights into the fate of chemical species after the removal of ammonia from an aqueous solution as struvite.

4.3.2.1 Elemental composition from EDX

The elemental composition of feed and product minerals after the removal of ammonia from an aqueous solution using MgO-NPs is shown in **Figure 4.2(a-b).**

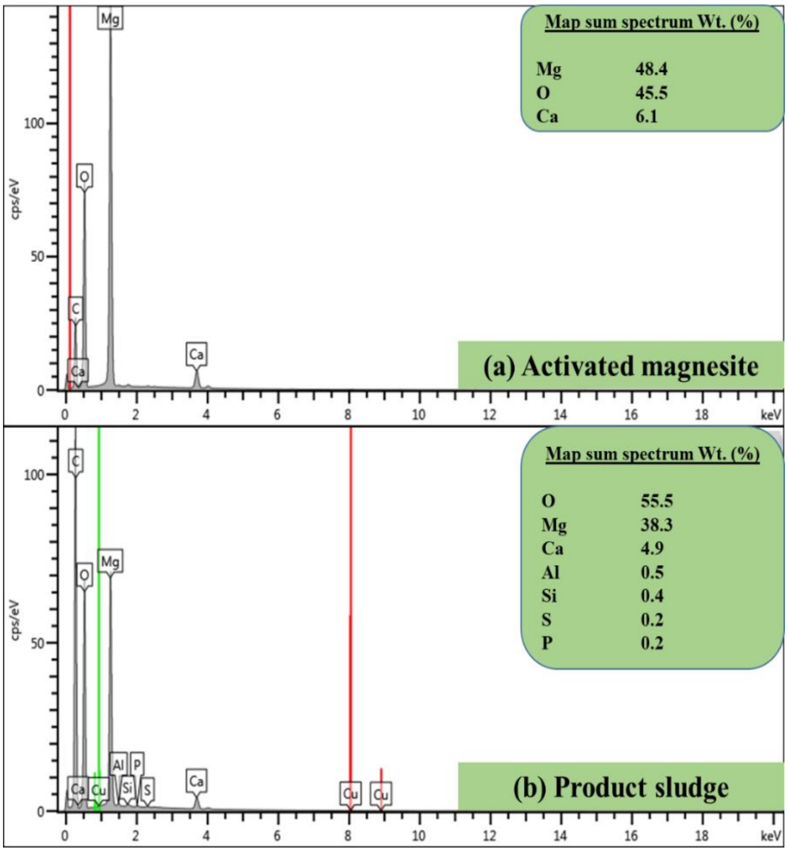

Figure 4.2(a-b): Elemental composition of feed and product minerals after the removal of ammonia from aqueous solution using MgO-NPs.

As shown in **Figure 4.2a**, calcined magnesite or MgO-NPs are made up of Mg, O, and Ca. The predominant elements were the Mg and O, hence denoting that the feed mineral is periclase (MgO). The presence of magnesium within the feed product is imperative for reaction with ammonia and phosphate, forming Magnesium Ammonia Phosphate (MAP). Furthermore, **Figure 4.2b** shows the elemental composition of the resultant (product) sludge after removing ammonia as struvite. As shown in **Figure 4.2b**, new elements were observed in the product water after reacting with the natural canal water. Specifically, Al, Si, S and P, were identified as additional elements in the product sludge. The presence of new elements in the product sludge confirms the reaction of chemical species in water and MgO-NPs. The identified elements are similar to the ones of struvite, as Masindi et al. (2022a) reported.

4.3.2.2 Elemental mapping from EDX

The elemental mapping of MgO-NPs and resultant sludge during the removal of ammonia from an aqueous solution are shown in **Figure 4.3(a-b)**.

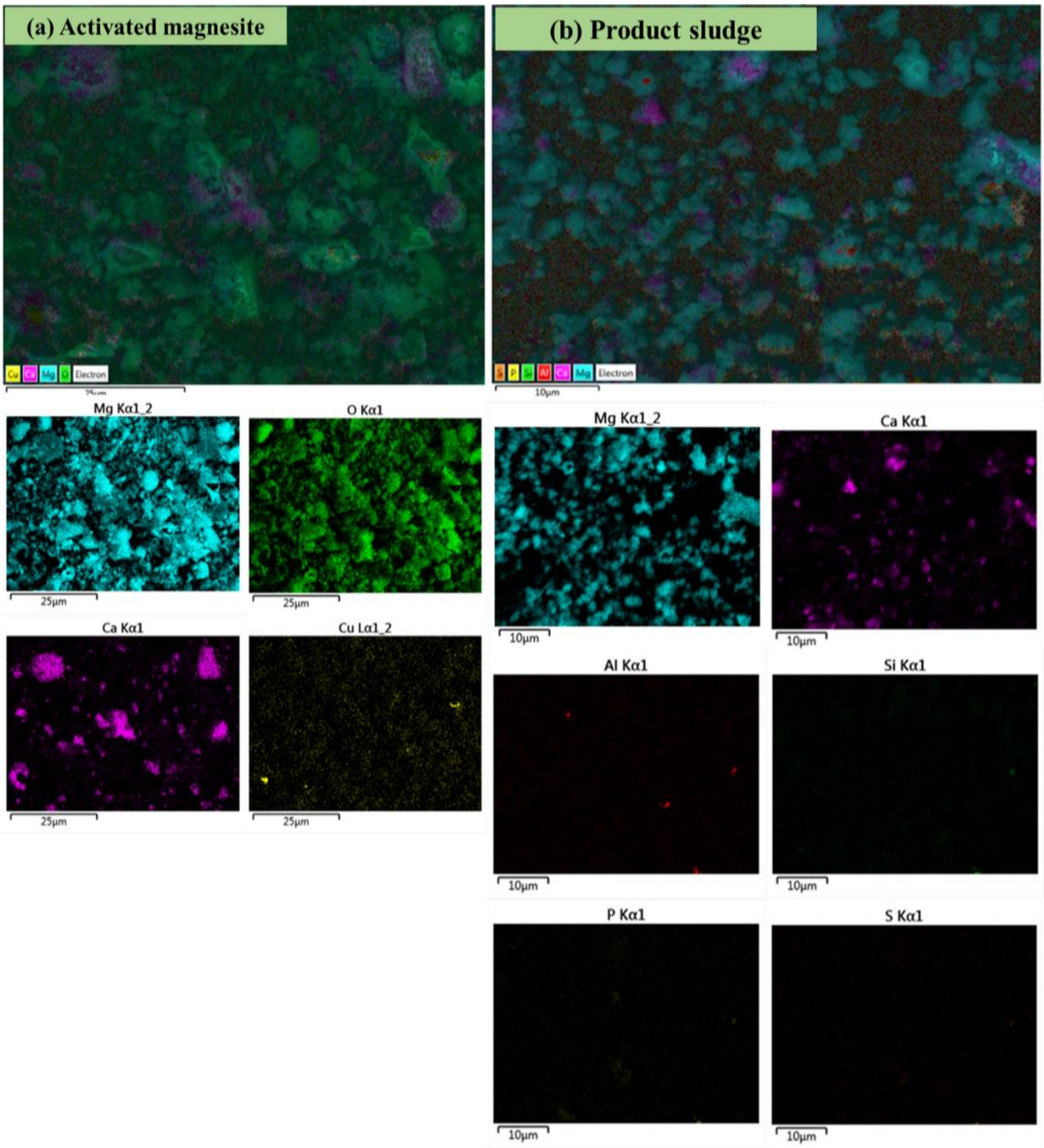

Figure 4.3(a-b): The elemental mapping of MgO-NPs and resultant sludge during the removal of ammonia from an aqueous solution.

As shown in **Figure 4.3a**, the elemental analysis showed that the feed material was concentrated with Mg, O, and some Ca. The results agree with the map spectrum results from the preceding section. Elevated levels of Mg and O denote that the material is periclase (MgO-NPs). Finally, the results for the elemental composition of the resultant sludge, as shown in **Figure 4.3b**, comprises Mg, Ca Al, S, Si, and P. More importantly, the observed concentration of phosphate and magnesium within the resultant sludge, coupled with the reduction of magnesium and phosphate $^-$ in surface water, confirms that struvite precipitation is more probable.

4.4 Economics analysis

In this section, the process of removing ammonia from an aqueous solution was examined from an economic point of view. The economic evaluation was estimated based on the current chemical costs from recent marketing catalogues. Specifically, the primary consideration for economic evaluation strictly focused on chemical reagents. Other possible costs, such as workforce, design and electricity cost, were not considered in this instance. Results for the economic evaluation of the removal of ammonia using breakpoint chlorination and a combination of breakpoint chlorination and struvite synthesis are shown in **Table 4.2**.

Table 4.2: Results for the economic evaluation of ammonia removal using breakpoint chlorination and a combination of breakpoint chlorination and struvite synthesis.

Hybrid Technology			
Chemicals	**Cost per KG**	**Dosage (kg)**	**Cost**
Calcined Magnesite or Activated MgO	2,5	0,07	0,175
Potassium dihydrogen Phosphate	10,21	0,02	0,2042
Calcium hypochlorite	34.56	0,00306	0,105759
Lime	4		
Coagulant	14,52		
Cost ®/1OOL			**0.485**
Cost c/Kl			**R4,85 per Kl**
Breakpoint Chlorination			
Chemicals	**Price per Kg**	**Dosage**	**Cost**
Calcined Magnesite			
Potassium dihydrogen Phosphate			
Calcium hypochlorite	34.56	0,022	0.76032
Lime	4	0,0019	0,0076
Coagulant	14,52	0,0008	0,011616
Cost ®/100L			**0.780**
Cost R/Kl			**R7.80 per kl**

As shown in **Table 4.2**, the overall cost to break down ammonia from an aqueous solution amounted to **R 4.85/kl** for the hybrid process. The hybrid process was conducted using pure chemicals, i.e., potassium dihydrogen phosphate and HTH, contributing to 61.6% of the overall cost. In **Table 4.3**, the overall treatment cost, after the potential replacement of potassium dihydrogen phosphate with the readily available waste phosphoric acid as phosphate source, could culminate in better and cheaper technology, with an estimated cost of **R 0.82/kg**, coupled with replacement of high-test hypochlorite with liquid chlorine, with the current cost of R 11.92/kg. Replacement of the chemicals can reduce the overall operational cost to R 2.27/kl (Table 4.3), equating to a 53.2% cost savings. A study by Huang et al. (2015) achieved savings in chemicals of **68%** when they replaced pure chemicals with calcined magnesite and phosphoric acid. More importantly, even with the potential to save costs when replacing pure chemicals, this technology emerges above the rest compared to technologies piloted to treat different water sources to potable water standards. In general, breakpoint chlorination was expensive compared to the integration of struvite synthesis and breakpoint chlorination hence denoting that the synergy between two technologies offers the cheapest and most effective and ecologically friendly technology that water treatment entities can employ.

Table 4.3: Estimated operational costs of the hybrid technology with liquid chlorine and waste phosphoric acid as the primary reagents.

Hybrid Technology with Ferric and Liquid chlorine			
Chemicals	**Price per Kg**	**Dosage**	**Cost ®**
Calcined Magnesite	2,5	0,07	0,175
Waste Phosphoric	0,82	0,02	0,0164
Liquid Chlorine	11,92	0,00306	0,0364752
Lime	4		
Coagulant	14,52		
Cost ®			**0,2278752**
Cost R/Kl			**R2,27 per Kl**

Numerous processes have been employed for the removal of ammonia from aqueous solutions. In particular, Mavhungu et al. (2020) employed the synthesis of struvite and drinking water reclamation from wastewater using reverse osmosis. The cost of the authors' technology amounted to **\$ 0.8/m^3**, equivalent to **R 12.584/kl (\$0.8/m^3),** considering the current exchange rate for the US dollar to Rand of **R 15.73**. Masindi et al. (2019) valorized acid mine drainage for drinking water reclamation using a battery of technologies, which comprise metals precipitation, gypsum synthesis, and reverse osmosis (RO). In their study, the overall treatment cost amounted to **R 56.60/kl ($ 3.59/m^3).**

Furthermore, as presented in **Table 4.2,** chlorine technology requires additional steps, such as stabilization with calcium hydroxide and coagulation with a polymer, which eventually increases the chemical cost to **R 7.80/kl ($ 0.50/m^3)**. The potential to reduce the operational cost of the hybrid approach, struvite synthesis and chlorination to **R 2.27/kl ($ 0.14/m^3)** when replacing pure chemicals substantiates the feasibility and economic sustainability of the hybrid process. In addition, the potential for beneficiating from the formed struvite as slow-release fertiliser will be a magnificent trade-off since it has the retail price of **R 4 321.4/ton ($ 274.7/ton)** as reported in Mavhungu et al. (2021). The ecological and economic trade-off will also contribute to the reduction of costs, but more importantly, a reduced environmental impact of the produced sludge, which becomes a resource as compared to current classification systems for generated waste.

4.5 Conclusions and recommendations

The cost analysis of the removal of ammonia from an aqueous environment, using the integration of struvite synthesis and breakpoint chlorination was successfully evaluated at a pilot scale. A 1000 litres (1 m^3) per run (LPR) pilot plant was utilised to fulfil the goals of this study. Specifically, this novel economic study adopted optimum conditions from the laboratory assays, and they comprise 110 mg/L of Mg and P dosage (concentration), 150 rpm of mixing speed, 60 minutes of contact time, and lastly, 120 minutes of sedimentation (Stage 1) while optimum conditions for the breakpoint chlorination were 30 minutes of mixing and 8:1 Cl_2:NH_3 weight ratio (Stage 2) and duly verified them. Results from this study demonstrated the techno-viable synergistic and complementary effects, with, i.e., Stage 1 having an increase in pH from 8.15 to 10.16 and a steep reduction in manganese (≥99.0%) and iron (≥99.6%) concentrations, respectively. *E. coli* and coliform bacteria were completely deactivated (≥99% removal), while TPC was reduced by 91%. The attenuation of ammonia ranged from 6.73 mg/L to 2.40 mg/L-N (64.34 % removal efficacy). In Stage 2, i.e., breakpoint chlorination, ammonia was reduced from 2.40 mg/L to ≤0.009 mg/L-N after water interaction with chlorine, whilst the micro-organisms were removed entirely. Lastly but not least, the techno-economic evaluation established chemical costs of **R 4.85/kl ($ 0.31/m^3)**. However, there is a massive potential for cost savings (53.2%) by replacing KH_2PO_4 with waste phosphoric acid. Finally, results from the cost analysis evaluation study showed great potential when compared to similar studies.

References

Adam, M. R., Othman, M. H. D., Abu Samah, R., Puteh, M. H., Ismail, A. F., Mustafa, A., A. Rahman, M. & Jaafar, J. 2019. Current trends and future prospects of ammonia removal in wastewater: A comprehensive review on adsorptive membrane development. Separation and Purification Technology, 213, 114-132.

Bernardi, F., Zadinelo, I. V., Alves, H. J., Meurer, F. & Dos Santos, L. D. 2018. Chitins and chitosans for the removal of total ammonia of aquaculture effluents. Aquaculture, 483, 203-212.

Chen, Y., Long, J., Chen, S., Xie, Y., Xu, Z., Ning, Z., Zhang, G., Xiao, T., Yu, M., Ke, Y., Peng, L. & Li, H. 2022. Multi-step purification of electrolytic manganese residue leachate using hydroxide sedimentation, struvite precipitation, chlorination and coagulation: Advanced removal of manganese, ammonium, and phosphate. Science of The Total Environment, 805, 150237.

Hakimi, M. H., Jegatheesan, V. & Navaratna, D. 2020. The potential of adopting struvite precipitation as a strategy for the removal of nutrients from pre-AnMBR treated abattoir wastewater. J Environ Manage, 259, 109783.

Hu, L., Yu, J., Luo, H., Wang, H., Xu, P. & Zhang, Y. 2020. Simultaneous recovery of ammonium, potassium and magnesium from produced water by struvite precipitation. Chemical Engineering Journal, 382, 123001.

Huang, H., Huang, L., Zhang, Q., Jiang, Y. & Ding, L. 2015. Chlorination decomposition of struvite and recycling of its product for the removal of ammonium-nitrogen from landfill leachate. Chemosphere, 136, 289-296.

Li, D. Y., Cho, Y. C., Hsu, M. H. & Lin, Y. P. 2022. Recovery of phosphate and ammonia from wastewater via struvite precipitation using spent refractory brick gravel from steel industry. J Environ Manage, 302, 114110.

Marais, S. S., Ncube, E. J., Msagati, T. a. M., Mamba, B. B. & Nkambule, T. T. I. 2019. Assessment of trihalomethane (THM) precursors using specific ultraviolet absorbance (SUVA) and molecular size distribution (MSD). Journal of Water Process Engineering, 27, 143-151.

Masindi, V. 2020. Dataset on physicochemical and microbial properties of raw water in four drinking water treatment plants based in South Africa. Data in Brief, 31, 105822.

Masindi, V., Fosso-Kankeu, E., Mamakoa, E., Nkambule, T. T. I., Mamba, B. B., Naushad, M. & Pandey, S. 2022a. Emerging remediation potentiality of struvite developed from municipal wastewater for the treatment of acid mine drainage. Environmental Research, 210, 112944.

Masindi, V. & Foteinis, S. 2021. Recovery of phosphate from real municipal wastewater and its application for the production of phosphoric acid. Journal of Environmental Chemical Engineering, 9, 106625.

Masindi, V., Foteinis, S. & Chatzisymeon, E. 2022b. Co-treatment of acid mine drainage and municipal wastewater effluents: Emphasis on the fate and partitioning of chemical contaminants. Journal of Hazardous Materials, 421, 126677.

Masindi, V., Gitari, M. W., Tutu, H. & Debeer, M. 2017. Synthesis of cryptocrystalline magnesite–bentonite clay composite and its application for neutralization and attenuation of inorganic contaminants in acidic and metalliferous mine drainage. Journal of Water Process Engineering, 15, 2-17.

Masindi, V., Ndiritu, J. G. & Maree, J. P. 2018. Fractional and step-wise recovery of chemical species from acid mine drainage using calcined cryptocrystalline magnesite nano-sheets: An experimental and geochemical modelling approach. Journal of Environmental Chemical Engineering, 6, 1634-1650.

Masindi, V., Osman, M. S. & Shingwenyana, R. 2019. Valorization of acid mine drainage (AMD): A simplified approach to reclaim drinking water and synthesize valuable minerals – Pilot study. Journal of Environmental Chemical Engineering, 7, 103082.

Mavhungu, A., Foteinis, S., Mbaya, R., Masindi, V., Kortidis, I., Mpenyana-Monyatsi, L. & Chatzisymeon, E. 2021. Environmental sustainability of municipal wastewater treatment through struvite precipitation: Influence of operational parameters. Journal of Cleaner Production, 285, 124856.

Mavhungu, A., Masindi, V., Foteinis, S., Mbaya, R., Tekere, M., Kortidis, I. & Chatzisymeon, E. 2020. Advocating circular economy in wastewater treatment: Struvite formation and drinking water reclamation from real municipal effluents. Journal of Environmental Chemical Engineering, 8, 103957.

Mavhungu, A., Mbaya, R., Masindi, V., Foteinis, S., Muedi, K. L., Kortidis, I. & Chatzisymeon, E. 2019. Wastewater treatment valorisation by simultaneously removing and recovering phosphate and ammonia from municipal effluents using a mechano-thermo activated magnesite technology. Journal of Environmental Management, 250, 109493.

Rice, E. W., Bridgewater, L., Association, A. P. H., Association, A. W. W. & Federation, W. E. 2012. Standard Methods for Examining Water and Wastewater, American Public Health Association.

SABS 2015. South African National Standard (SANS 241-1:2015) Drinking Water. Part 1: Microbiological, Physical, Aesthetic and Chemical Determinants. In: (SABS), S. D. O. T. S. A. B. O. S. (ed.). Pretoria, South Africa.

Sharma, N., Mohapatra, S., Padhye, L. P. & Mukherji, S. 2021. Role of precursors in the formation of trihalomethanes during chlorination of drinking water and wastewater effluents from a metropolitan region in western India. Journal of Water Process Engineering, 40, 101928.

Stefán, D., Erdélyi, N., Izsák, B., Záray, G. & Vargha, M. 2019. Formation of chlorination by-products in drinking water treatment plants using breakpoint chlorination. Microchemical Journal, 149, 104008.

Takó, S. Ammonium removal from drinking water–Comparison of the breakpoint chlorination and the biological technology. Conference of Junior Researchers in Civil Engineering, 2012. 248-254.

Tekerlekopoulou, A. & Vayenas, D. 2008. Simultaneous biological removal of ammonia, iron and manganese from potable water using a trickling filter. Biochemical Engineering Journal - BIOCHEM ENG J, 39, 215-220.

WHO 2011. Guidelines for drinking-water quality. 4th ed ed. Geneva: World Health Organization.

WHO 2017. Guidelines for drinking-water quality: fourth edition incorporating first addendum, Geneva, World Health Organization.

Chapter Five

Conclusions and recommendations

5.1 Conclusions

This study was designed in an attempt to address the following technical objectives:

- To investigate the Physico-chemical and microbial properties of raw water at the Wallmannsthal water treatment plant (WTP).
- To determine conditions suitable for the removal of ammonia and other contaminants from Wallmannsthal WTP raw and point out the underpinning chemistry.
- To characterise the feed and product sludge during the synthesis of struvite using activated magnesite.
- To perform an economic analysis of the chemicals used in the developed technology denoting the proposed system's viability.
- To compare the quality of product water with different water quality regulatory frameworks.

This study sufficiently and explicitly met the set objectives and hypothesis. The gross focus was to explore the integration of struvite synthesis as pre-treatment followed by breakpoint chlorination as polishing technology for the removal of ammonia and other pollutants from surface water, i.e. canal water. Specifically, the water quality analysis of surface water revealed the presence of ≥ 167 MPN/100 mL of *E. coli*, ≥ 2420 MPN/100 mL of faecal coliform, ≥ 26000 CFU/1mL of total plate count (TPC), ≥ 6.51 mg/L of ammonia, and ≥ 100μg/L of manganese as risk parameters requiring treatment. The main quest is to ensure the production of potable water that is suitable for drinking and other defined purposes. The results show that surface water is highly polluted and can potentially cause myriads of health challenges, including watery or bloody diarrhoea, fever, abdominal cramps, nausea, blue baby syndrome, and vomiting if the water is consumed prior treatment.

In this novel study, two treatment chains were integrated to form a hybrid process that comprises two different technologies synergistically combined to yield desired results. In particular, the pre-treatment stage involved the synthesis of struvite using calcined (activated) magnesite followed by breakpoint chlorination using high test hypochlorite (HTH) as the chlorine source. In the first stage, raw water was treated with activated magnesite (MgO-NPs) and sodium dihydrogen phosphate to form struvite. The removal efficiencies for the removal of *E coli*, coliform, and manganese were ≥ 99%, respectively, whilst ammonia and TPC were reduced by 62.63% and 87.07%, respectively. The optimum conditions for the struvite reactor were observed to be 110 mg/L of Mg and P dosage (concentration), 150 rpm of mixing speed, 60 minutes of contact time, and 120 minutes of sedimentation. Under these conditions, the pH increased from 6.7 to 9.6, which is ideal for removing metals and deactivating bacteria. The functional group for activated magnesite included Mg-O metal bond, carbonates duplexes and hydroxyl group as water, whilst the product sludge comprised Mg-O metal-oxygen bond, N-H bond in-plane stretching, and PO_4 and P=O stretching; hence confirming the sinking of P and N as the primary contaminants. Furthermore, the activated magnesite comprised brucite and calcite, whilst the resultant sludge was rich in periclase, calcite, struvite, magnesite, dolomite, and quartz. Both XRD and FTIR results confirm that magnesium, phosphate and ammonia formed the struvite, and these results corroborate with the findings related to aqueous solution characterisation, i.e. ICP-OES findings. In the second stage, stage 1 effluent was treated using HTH as a chlorine source at a chlorine to ammonia (Cl_2:NH_3) weight ratio of 8:1 and 30 minutes of contact time. These conditions reduced TPC and ammonia by ≥ 99%, respectively. However, slight increments in disinfection by-products, mainly chloroform (145 µg/L), were observed after adding chlorine, but concentrations were lower than the regulated drinking water standards of 300 µg/L.

Subsequent to successful laboratory assays, optimum conditions from the laboratory study were used for an up-scaled system, i.e., a pilot study. The main aim was to demonstrate the technology's robustness and feasibility in natural environments. Cost analysis on removing contaminants using the hybrid process was successfully evaluated on a pilot plant. The cost analysis focused on chemical dosages and reagents used during the study. A 1000 litres (1 m^3) per run (LPR) pilot plant was utilised to fulfil the goals of this study. *E coli*, faecal coliform, iron, and manganese were reduced by ≥ 99%, respectively, while TPC and ammonia were reduced by 91% and 64.34%, respectively (stage 1). In stage 2, i.e., the polishing stage, TPC and ammonia were reduced by ≥ 99%, respectively. However, slight increments in disinfection by-products, mainly chloroform (206 µg/L), were observed after adding chlorine, but concentrations were lower than the regulated drinking water standards of 300µg/L. The cost analysis amounted to chemical costs of **R4.85/kl (\$0.31/m^3)**, which was lower than the breakpoint chlorination cost of **R7.80/kl (\$0.50/m^3)** when pursued alone. In addition, there is a massive potential for cost savings (53.2%) by replacing Kh_2PO_4 with waste phosphoric acid, which could reduce the overall cost to **R2.27/kl (\$0.14/m^3)**. Lastly, but not least, results from laboratory assays corroborated results from pilot assays. Overall, the integration of struvite synthesis and breakpoint chlorination resulted in water that met most water quality standards.

5.2 Recommendations

The hybrid process, i.e., integrating struvite synthesis and breakpoint chlorination, resulted in an affluent almost fully compliant with South African drinking water and WHO standard, albeit an increase in turbidity was observed after chlorination. More importantly, the promising results were in laboratory and pilot studies. However, further research avenues need to be explored to enhance the techno-viability further and give the much-needed confidence in larger-scale applications. Future studies and research avenues should focus on the following:

- Coupling polyelectrolyte coagulants and powder-activated carbon (PAC) for removal of turbidity and organic matter including the chlorination by-products. This will go a long way in enhancing the performance of the system.
- Performing experiments using cheaper phosphate sources such as the waste phosphoric acid will significantly reduce the operational costs of the developed technology.
- An in-depth techno-economic evaluation (TIA) should be performed to determine the economic viability of the developed technology and its viability on a larger scale.
- To determine the sustainability and robustness of the technology, this hybrid technology will need to be evaluated over a longer operational period, e.g., 30 days continuously, this will demonstrate some operational challenges and its robustness.
- Performing a life cycle assessment (LCA) of the developed technology will allow researchers to determine the ecological footprints of the developed technology and its sustainability including possible trade-offs.

Appendices

Appendices A: Treatment of real river water at optimum conditions: Laboratory study

Optimal Laboratory Studies											
Parameters	**Units**	**SANS Limits**	**Raw**	**Struv 1**	**Struv 2**	**AV**	**STDEV**	**Break 1**	**Break 2**	**AV**	**STDEV**
E. coli	Counts/ 100 mL	ND	4800	0	0	**0**	**0.000**	0	0	**0**	**0.000**
Total coliform	Counts/ 100 mL	<10	8700	61	53	**57**	**5.657**	0	0	**0**	**0.000**
Total Plate count (TPC)	CFU/ 1mL	<1000	51835	6672	6728	**6700**	**39.60**	1	2	**2**	**0.707**
Chloroform	ug/L	<300	3.35	3.35	3.35	**3.35**	**0.000**	147	143	**145**	**2.828**
Bromoform	ug/L	<100	1.34	1.34	1.34	**1.34**	**0.000**	1.34	1.34	**1.34**	**0.000**
Dibromodichloromethane	ug/L	<100	1.24	1.24	1.24	**1.24**	**0.000**	3.24	3.66	**3.45**	**0.297**
Bromodichloromenthane	ug/L	<60	1.24	1.24	1.24	**1.24**	**0.000**	9.45	9.21	**9.33**	**0.170**
pH	pH units	5,7-9,7	6.7	9.58	9.62	**9.6**	**0.028**	8.86	8.95	**8.91**	**0.064**
Iron (Fe)	ug/L	<100	11	0.37	0.37	**0.37**	**0.000**	0.37	0.37	**0.37**	**0.000**
Ammonia	mg/L	<1,5	7.6	3.03	2.64	**2.84**	**0.276**	0.009	0.009	**0.009**	**0.000**
Manganese(Mn)	ug/L	<100	174	4	4	**4**	**0.000**	0.09	0.09	**0.09**	**0.000**
Phosphate	mg/L	<10	0.18	3.1	3.5	**3.30**	**0.283**	5.7	6.3	**6**	**0.424**
Calcium	mg/L	<300	31	12	12	**12**	**0.000**	17	21	**19**	**2.828**
Magnesium	mg/L	<100	2.1	41	39	**40**	**1.414**	43	44	**44**	**0.707**
Nitrate	mg/L	<11	0.16	2.9	3.5	**3.2**	**0.424**	2.6	3.2	**2.9**	**0.424**
Nitrite	mg/L	<0,9	0.01	0.21	0.34	**0.275**	**0.092**	0.01	0.01	**0.01**	**0.000**
TOC	mg/L	<1,5	7.62	7.55	7.57	**7.56**	**0.014**	6.02	5.86	**5.94**	**0.113**
Turbidity	NTU	<1,5	9.1	1.36	1.3	**1.33**	**0.042**	1.7	1.62	**1.66**	**0.057**

Appendices B: Treatment of real river water at optimum conditions: Pilot study

Parameters	**Units**	**SANS Limits**	**Raw**	**Struv 1**	**Struv 2**	**AV**	**STDEV**	**Break 1**	**Break 2**	**AV**	**STDEV**
E. coli	Counts/ 100 mL	ND	270	0	0	**0.000**	**0.000**	0	0	**0**	**0.000**
Total coliform	Counts/ 100 mL	<10	3600	0	0	**0.000**	**0.000**	0	0	**0**	**0.000**
Total Plate count (TPC)	CFU/ 1mL	<1000	26000	2297	2383	**2340**	**60.81**	0	8	**4**	**5.657**
Chloroform	ug/L	<300	3.35	3.35	3.35	**3.35**	**0.000**	201	211	**206**	**7.071**
Bromoform	ug/L	<100	1.34	1.34	1.34	**1.34**	**0.000**	1.34	1.34	**1.34**	**0.000**
Dibromodichloromethane	ug/L	<100	1.24	1.24	1.24	**1.24**	**0.000**	3.42	6.55	**4.985**	**2.213**
Bromodichloromenthane	ug/L	<60	1.24	1.24	1.24	**1.24**	**0.000**	23.4	26.2	**24.8**	**1.980**
pH	pH units	5,7-9,7	8.15	10.2	10.12	**10.16**	**0.057**	9.05	9.17	**9.11**	**0.085**
Iron (Fe)	ug/L	<100	11	0.37	0.37	**0.37**	**0.000**	0.37	0.37	**0.37**	**0.000**
Ammonia	mg/L	<1,5	6.73	2.57	2.22	**2.395**	**0.247**	0.009	0.009	**0.009**	**0.000**
Manganese(Mn)	ug/L	<100	174	0.09	0.09	**0.09**	**0.000**	0.09	0.09	**0.09**	**0.000**
Phosphate	mg/L	<10	6	0.14	0.36	**0.25**	**0.156**	0.54	0.56	**0.55**	**0.014**
Calcium	mg/L	<300	36	7.9	8.1	**8**	**0.141**	32	28	**30**	**2.828**
Magnesium	mg/L	<100	2.6	39	41	**40**	**1.414**	39	43	**41**	**2.828**
Nitrate	mg/L	<11	5.3	3.6	3.8	**3.7**	**0.141**	3.8	3.6	**3.7**	**0.141**
Nitrite	mg/L	<0,9	1.2	0.27	0.27	**0.27**	**0.000**	0.01	0.01	**0.01**	**0.000**
TOC	mg/L	<10	7.81	7.31	7.25	**7.28**	**0.042**	4.66	4.5	**4.58**	**0.113**
Turbidity	NTU	<1,5	5.21	1.75	1.66	**1.705**	**0.064**	2.32	2.41	**2.365**	**0.064**